

AN ABSTRACT OF THE THESIS OF

Holly C. Garrow for the degree of Master of Science in  
Oceanography presented on June 28, 1984.

Title: Shoreline Rhythmicity On a Natural Beach

Abstract approved: **Redacted for privacy**  
Robert A. Holman

Twenty-four air photo mosaics and a nine month long field study are used to identify and explain the characteristic shoreline morphologies of a 10 km long beach on the Oregon Coast. The study area is between the Siletz River and Government Point. Cuspate topography is common on the northern third of this beach and its development there has been related to major periods of dune erosion.

High water lines, assumed to be lines of constant elevation, were identified and digitized on each of nineteen photo mosaics. From statistical analyses of these records, it is concluded that cusps and embayments do not always form in the same longshore locations, eliminating the simple model for their origin of topographic trapping of a single edge wave. Spectral analyses of the data sets show a consistent longshore wavelength of 800-1000 m when cuspate topography is present.

Bi-weekly surveys were made of an 830 m site, 2-2.8 km south of the Siletz River, from September 1982 to June 1983. Seven storms

with significant wave heights greater than 5 m occurred during the study period. This period of time is especially interesting due to the El Niño phenomenon and its associated anomalous environmental conditions. Eleven profile lines were established at approximately 80 m intervals alongshore. Statistical and R-mode analyses of the survey data indicates a longshore rhythmicity of 800-850 m. A maximum longshore migration rate of 400 m in 50 days was documented for the cusped topography. Regression analysis shows that only 28% of the variance in elevation at a location is explained by frequency and duration of contact with the ocean. Run-up data were also collected using a super-8 movie camera directed alongshore. Spectral analyses of these records revealed a dominance of infragravity motions in the run-up.

Important to the problem of understanding variations in beach morphology is the ability to quantify these variations in simple terms. A successful set of variables is as follows. On/offshore position of the shoreline is best described by the mean offshore distance to a particular contour. The amplitude of the rhythmicity is then just the standard deviation about that distance. The longshore phase of the rhythmicity is best expressed by the first factor scores calculated by R-mode factor analysis on a data set in which each contour is normalized to the same mean and standard deviation.

Regression analysis between these morphology signals and various environmental parameters confirms some well established trends but also provides some surprises. On/offshore position of the shoreline is negatively correlated with mean significant wave height

over the prior two weeks, as expected. More interestingly, the amplitude of the rhythmicity also shows a negative correlation with wave height. This is opposite to the relationship found during major episodes of erosion on Siletz Spit. Consideration of the available data suggests that incident wave characteristics related to the proximity of a storm center are important to the development of rhythmic topography on Siletz Spit.

Some estimates of response time of the beach to changes in wave conditions can be made with this data set, although the bi-weekly sampling precludes comments on very rapid response. In general, the beach response was rather slow, with mean shoreline position changing, at most, 5 m between surveys. Interestingly, the amplitude of the rhythmicity showed larger responses, with up to 10 m change during any two week period.

Models for the development of rhythmic topography are evaluated in light of these analyses. Edge waves are determined to provide a reasonable mechanism, with a model of two topographically constrained edge waves progressing northward from Government Point, accounting for the characteristics of shoreline morphology documented at this site.

Shoreline Rhythmicity On A Natural Beach

by

Holly C. Garrow

A THESIS

submitted to

Oregon State University

in partial fulfillment of  
the requirements for the  
degree of

Master of Science

Completed June 28, 1984

Commencement June 1985

APPROVAL:

Redacted for privacy

---

Associate Professor of Oceanography in charge of major

Redacted for privacy

---

Dean of Collège of Oceanography

Redacted for privacy

---

Dean of Graduate

Date thesis is presented June 28, 1984

Typed by Holly C. Garrow for Holly C. Garrow

## ACKNOWLEDGEMENTS

Most important to this study was the field help offered by a handful of individuals; Margaret Sparrow, Erik Grann, Sara Culley, Peter Howd, Carlos Lopez, and Drs. David Rea and Paul D. Komar. Dr. Robert A. Holman accompanied many of the field excursions and is owed many thanks for his help with the field work - we saw an awful lot of rain but there were lots of rainbows too.

Also important were a number of people, some of whom may be unaware of the occasional, yet very important, boost(s) to my spirits they each provided; David Murray, Anne Matherne, Kim Murphy, Cathy Fisher, Sarah Hoffman, Donna Moore, Miriam Ludwig (thanks a 'bunch') and Drs. Dallas Abbott, Louis Gordon, Kenneth Scheiddeger, and Verne Kulm.

Special thanks for their support, encouragement and discussion of various aspects of this research are due to Sarah Culley, Aage Gribskov and Drs. Robert A. Holman and Paul D. Komar.

And finally, very special thanks are owed to a few others. First to my family for their support and understanding, and for always reminding me that my happiness is one of the most important things in the world to them. Also, to Dr. Henry Hanson for helping me to learn what great happiness I can find in trying to understand better the world around me. Thanks are also due to Henry for his continued interest in my development as a scientist and as an individual within that profession. Finally, thanks are given to Carlos Lopez for helping me to learn the joy I can find in the

comfort of a warm puppy, the closeness of another human being and the mountains, lakes and deserts in the world around me.

This project was funded in part by the Sea Grant College Program under award number NA81AA-D-00086.

## TABLE OF CONTENTS

INTRODUCTION	1
EDGE WAVES	10
Brief Review of Theory	10
Edge Wave Forcing	14
Edge Waves and Topography	16
Edge Wave Observations On Natural Beaches	19
AERIAL PHOTOGRAPHS	21
Introduction	21
Digitization	27
Qualitative Data Analyses	28
Quantitative Data Analyses	29
Conclusions	36
FIELD EXPERIMENT	39
Methods	39
Wave, Tide and Weather Conditions	44
Beach Profiles	53
Beach Topography: Qualitative Analyses	56
Beach Topography: Statistical Analyses	61
Beach Topography: R-mode Analyses	75
Beach Topography: Conclusions	95
Time Lapse Films Of Run-up	98
Run-up and Incident Waves	104
Spectral Characteristics Of Run-up	113
DISCUSSION	118
Models	118
Waves, Tides, Weather and Topography	133
CONCLUSIONS	139
REFERENCES	140
APPENDIX 1 High water lines for each set of air photo mosaics	144
APPENDIX 2 Spectra of the high water lines	151
APPENDIX 3 Spectra of the 'mean-subtracted' high water lines	158
APPENDIX 4 Topographic maps of the beach for excursions 04 through 26	165

## LIST OF FIGURES

<u>Figure</u>	<u>Page</u>
1. A map of the north-central Oregon coast	2
2. Plan and profile views of Wright and Short's six morphologic beach states	6
3. The offshore profiles of mode 1, 2 and 3 edge waves and a reflected incident wave	13
4. Government Point to the Siletz River Inlet	22
5. Plots of the mean high water line (top) and high water line variance (bottom)	30
6. Typical spectrum of an air photo highwater line	34
7. Typical spectrum of a 'mean subtracted' high water line	37
8. Map of the field site on Siletz Spit	40
9. Weekly mean and maxima of significant wave heights, August 1982 - July 1983	46
10. Ten year monthly means and 1982-83 monthly means of significant wave height.	47
11. Three year monthly means and 1982-83 monthly means of incident wave period	47
12. Weekly mean sea levels, August 1982 - June 1983	49
13. Ten year monthly means and the 1982-83 monthly means of sea level	50
14. Weekly means and minima of barometric pressure, August 1982 - June 1983	51
15. Ten year monthly means and 1982-83 monthly means of barometric pressure	52
16. Representative of the fall and early-winter beach profiles from ranges N3, N1 and S3	54
17. Beach profiles taken November 30, 1982	57
18. Mean beach topography calculated from all 18 complete profile sets	62

19.	Mean beach topographies for the fall/early-winter (a), winter (b), and spring (c)	64
20.	Standard deviation in beach elevations calculated from all 18 complete profile sets	67
21.	Standard deviation in beach elevation for the fall/early-winter (a), winter (b), and spring (c)	68
22.	Mean station elevations versus their standard deviations in elevation	73
23.	Mean station elevations versus their standard deviations for each profile range	74
24.	The seawardmost available topographic contours (top) and the first R-mode factors (bottom) for each of the 18 surveys	79
25.	a) Mean contour and first R-mode factor of data depicting a stable longshore rhythmic pattern with amplitude variations; b) Mean contour and first and second R-mode factors of data depicting a stable longshore pattern with amplitude variations and overall on/offshore movement	81
26.	Mean contours and first and second R-mode factors for data depicting a longshore rhythmic pattern with amplitude variations and, a) 90 degree phase shifting; b) 180 degree phase shifting and c) 360 degree phase shifting	83
27.	The mean contours and first R-mode factors for each of the seven Siletz Spit contour data sets	86
28.	The mean contour, and the first and second R-mode factors for the seawardmost contour of the Siletz Spit data set	87
29.	The sum of the mean contour and (top) the most positively weighted and (bottom) most negatively weighted first R-mode factors	89
30.	The sum of the mean contour and (top) the most positively weighted and (bottom) most negatively weighted second R-mode factors	90
31.	The mean contour, and the first, second and third factors from R-mode analysis of the normalized -5.75 m contour data matrix	94
32.	Spectra from multiple digitizations of film run 11 by three operators	102

33.	Spectra from multiple digitizations of film run 13 by three operators	103
34.	Plots of normalized run-up, set-up and swash versus the Irribaren number for the Siletz Spit data	107
35.	Plots of normalized run-up, set-up and swash versus the Irribaren number with data from Holman and Sallenger (in press) and this study	110
36.	Summary plot of all film spectra	114
37.	The predicted shoreline pattern from the proposed model of two topographically constrained edge waves extending northward together from Government Point.	127
38.	The mean shoreline position versus longshore position (normalized) of the rhythmic pattern	129
39.	A schematic illustration of the time averaged drift velocities on the foreshore as predicted by the proposed model	131
40.	Mean significant wave height versus mean shoreline position	134
41.	Mean significant wave height versus rhythmicity amplitude	137
42.	Mean shoreline position versus rhythmicity amplitude	138

## LIST OF TABLES

<u>Table</u>		<u>Page</u>
1	Air photo mosaics used in this study, their scale, coverage and comments on their quality	23
2	Air photo mosaic dates, characteristics important in spectral analyses and peaks of greater than 80% confidence in power spectra	33
3	Air photo mosaic dates, characteristics important in spectral analyses and peaks of greater than 80% confidence in power spectra for the mean-subtracted water line data set	35
4	Field excursion dates and numbers and a summary of the data obtained on each outing	42
5	Offshore extent of each beach profile from its reference marker	43
6	Field observations of beach topography for each field excursion	58
7	Tabulation of numbers expressing on/offshore position of the shoreline, rhythmicity amplitude and longshore location of rhythmic features for each of the field excursions.	92
8	The statistics of replicate digitizations of the same run-up films	101
9	Percentage of low frequency (<0.05 hz) energy on the foreshore for all film digitizations	116

## LIST OF SYMBOLS

a	amplitude
$a_b$	breaker amplitude
$a_n$	amplitude of mode n edge wave
B	bandwidth
C	covariance matrix
D	original data matrix
$e_i$	eigenvectors
f	frequency, hz
g	gravitational acceleration
$H_{1/3}$	significant wave height
J	identity matrix
$k'$	an integer
L	wave length
$L_t$	wavelength of local rhythmic topography
$L_R$	data record length
m	alongshore mode number (also used to indicate variables within a data matrix)
n	offshore mode number (also used to indicate samples within a data matrix)
$n'$	an integer
$N_f$	half-filter width
$R_T^v$	total run-up
$R_v(t)$	run-up time series
$\bar{R}_v$	mean run-up
$R_{1/3}$	significant swash height

$t$	time
$T$	wave period (also used as a super-script to denote the transpose of a matrix)
$u$	on/offshore velocity
$u_*$	offshore behavior of on/offshore velocity
$v$	alongshore velocity
$v_*$	offshore behavior of alongshore velocity
$x$	on/offshore position
$y$	alongshore position
$y_{ij}$	R-mode factor scores
$\xi_0$	Iribaren number
$\phi$	velocity potential
$\sigma$	radian frequency, $2\pi/T$
$\lambda$	wave number, $2\pi/L$
$\lambda_y$	alongshore wave number
$\kappa$	wave number, $1/L$
$\phi(x)$	offshore behavior of waveform
$\eta$	sea surface elevation
$\bar{\eta}$	set-up
$\bar{\eta}_t$	offshore tidal elevation
$\beta$	beach slope
$\beta_0$	initial beach slope
$\beta'$	rate of change of beach slope, $\partial\beta/\partial y$
$\nu$	degrees of freedom
$\epsilon$	surf-scaling parameter
$\omega$	incident wave radian frequency
$\Lambda_i$	eigenvalues

## SHORELINE RHYTHMICITY ON A NATURAL BEACH

### INTRODUCTION

Rhythmic, cusped topography has been observed on many beaches of the world at a variety of length scales. In some areas it can be an important contributing factor to dune erosion. On the east coast of the United States it has been related to the overwashing of barrier islands (Dolan and Hayden, 1981). On the northern coast of Oregon cusped topography has been associated with major episodes of dune erosion.

A number of previous studies have concentrated on documenting erosion of unconsolidated beach and dune sands on the northern Oregon coast (Terich and Komar, 1974; Rea, 1975; McKinney, 1977; Komar, 1978). In northern Oregon such coastal environments are located primarily on sand spits, the four largest of which are Siletz, Nestucca, Netarts and Tillamook (Bayocean) Spits (Figure 1). Of particular interest are the studies of Rea, documenting erosion on Siletz Spit during the winter of 1972-73, of McKinney, detailing the spring of 1976 erosion on Siletz Spit, and of Komar, describing erosion on Nestucca Spit during the winter of 1977-78. All three of these major erosional episodes can be characterized by a similar

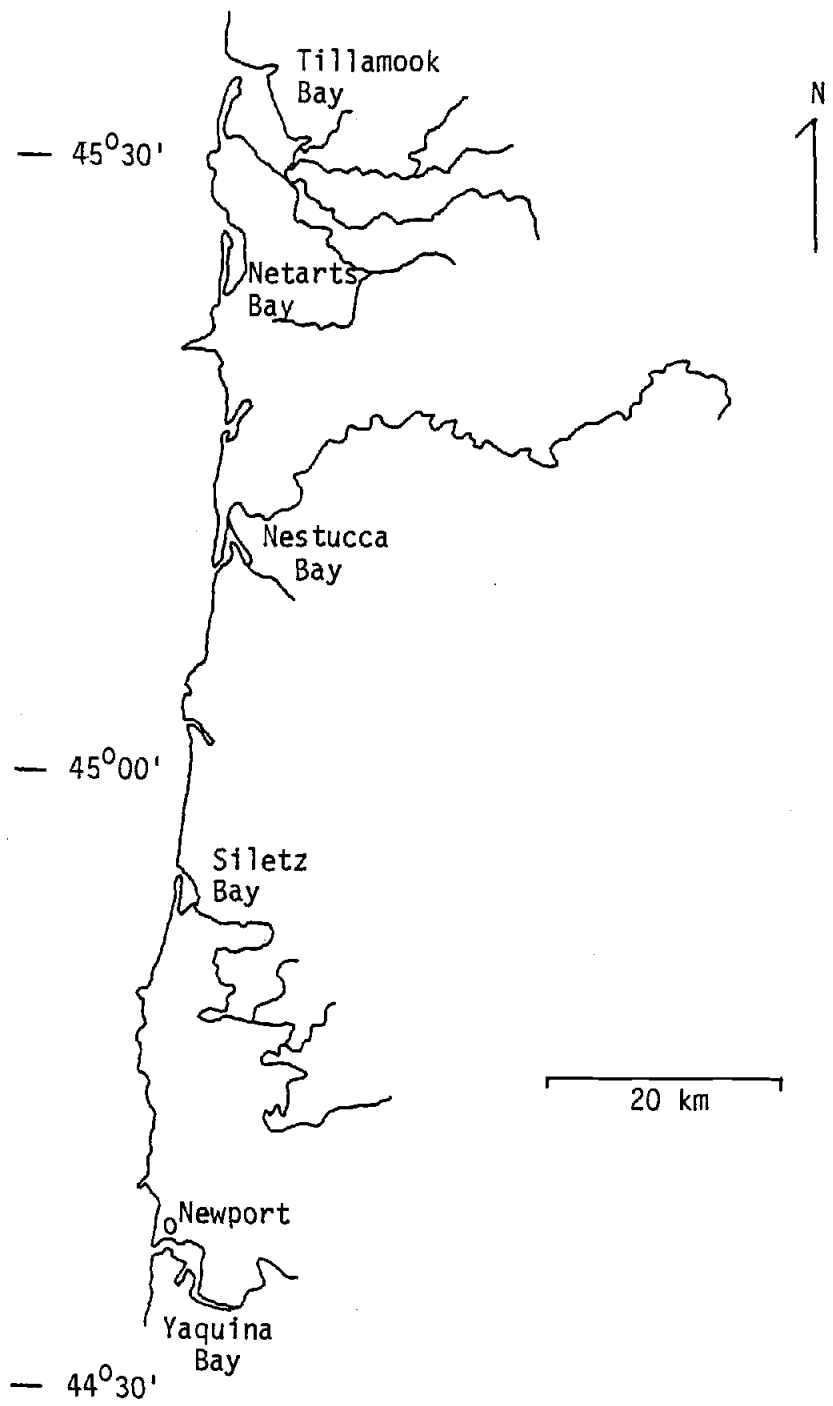


Figure 1. A map of the north-central Oregon coast. The four largest sand spits, shown above, have been the sites of major episodes of dune erosion related to the presence of cusped topography.

scenario. Storms during the fall and early winter move sand from the summer berm to the offshore, and thus reduce the buffer zone between the ocean and the dunes. The amount of shoreline recession often varies alongshore and areas of minimum recession, cusps, and maximum recession, embayments, are usually regularly spaced. This rhythmic shoreline and the longshore position of cusps and embayments stabilize, allowing rip currents occupying the embayments to scour channels and increase water depths very close to shore. If a large storm then occurs incident wave energy is not effectively buffered at embayed areas because the waves travel very near to shore before breaking and the backshore is either very narrow or non-existent. Such conditions can result in direct wave attack on the dunes and hence produce extensive localized coastal erosion and associated property damage. In a review of erosion on Siletz Spit, Rea states that in 1970-71 a 200 meter long section of the foredune retreated six to nine meters. At the same time, approximately 1600 meters to the south, foredune erosion occurred along 670 meters of the beach with a maximum dune recession of 15 meters. In 1971-72 a 200 meter section of this same area retreated up to an additional 20 meters. During a severe erosional episode in 1972-73 a house under construction was destroyed, others nearby had to be protected by the emplacement of riprap. A 650 meter section of foredune was effected and the maximum dune bluff recession was 30 meters during a three week period. By 1976 much of the foredune on Siletz Spit was protected by riprap, reducing property damage. However, some erosion of the riprap took place and a small overwash occurred at one location. The 1977-78 erosion episode on Nestucca Spit resulted in a

breach of the spit which subsequently closed and revegetated naturally.

Komar and Rea (1976) made a detailed qualitative study of air photos of Siletz Spit which revealed cycles of erosion and reformation of the dunes. They also noted that erosion of the dunes in the early 1970's exposed numerous sawed drift logs. This evidence combined with the available photographs indicated that periodic erosion and reformation of the dunes has occurred at least throughout the last century. There has been no measurable net change in the size or position of the spit during this time.

Rhythmic shoreline features have been noted and described on many shorelines of the world. The wavelengths of this topography range from 10 cm (Komar, 1973) to 40 km (Dolan et al., 1979). Until recently, the nomenclature for rhythmic shoreline forms has been based upon the observed morphology, particularly the spacing between features. Beach cusps are generally considered the smaller forms with spacings less than 25 m. Larger cusp forms typically have spacings of tens to hundreds of meters and terms such as 'sand waves', 'storm cusps', 'giant cusps' and 'rhythmic topography' are commonly employed. Komar (1983) presented an initial attempt at a genetic classification of rhythmic shoreline forms. He described four classes, the first of which, reflective beach cusps, corresponds to most of the observations of 'beach cusps' and three others, rip current embayment-cusp system; crescentic bar-cusp system; and transverse and oblique bars, which correspond to the observations of 'rhythmic topography'.

Wright et al. (1983) considered the morphodynamics of both reflective and dissipative beach systems in southeastern Australia, suggesting a classification into six distinct morphologic states, each with a characteristic nearshore rhythmicity, figure 2. Many beaches can be described as varying between these six states as the incident wave climate changes. The two extremes, the dissipative and reflective configurations can be distinguished by a dimensionless surf-scaling parameter. These morphologic states will be compared with the observations of this study in the section, Beach Topography; Qualitative Analyses.

A number of hypotheses have been suggested to explain the formation of rhythmic topography. Sonu (1972) proposed a model dependent on undulations in surf-zone topography and resultant periodic variations in mean water level which then affect foreshore topography. Perturbation theories make no predictions of initial spacings. A regular rhythmic pattern would presumably develop with time as large cusps grow and encroach on smaller ones. Sonu's theory does not explain the origin of the regularly spaced inshore topographic perturbations needed to produce rhythmic shoreline topography.

Other hypotheses rely on regularly spaced variations in the incident wave field or in the surf zone. Hino (1975) develops a hydrodynamic instability theory for the formation of rip currents and a cusped shoreline in which the surf zone width is the critical parameter. Dalrymple (1975) has suggested that intersecting wave trains produce alongshore variations in set-up and thus govern

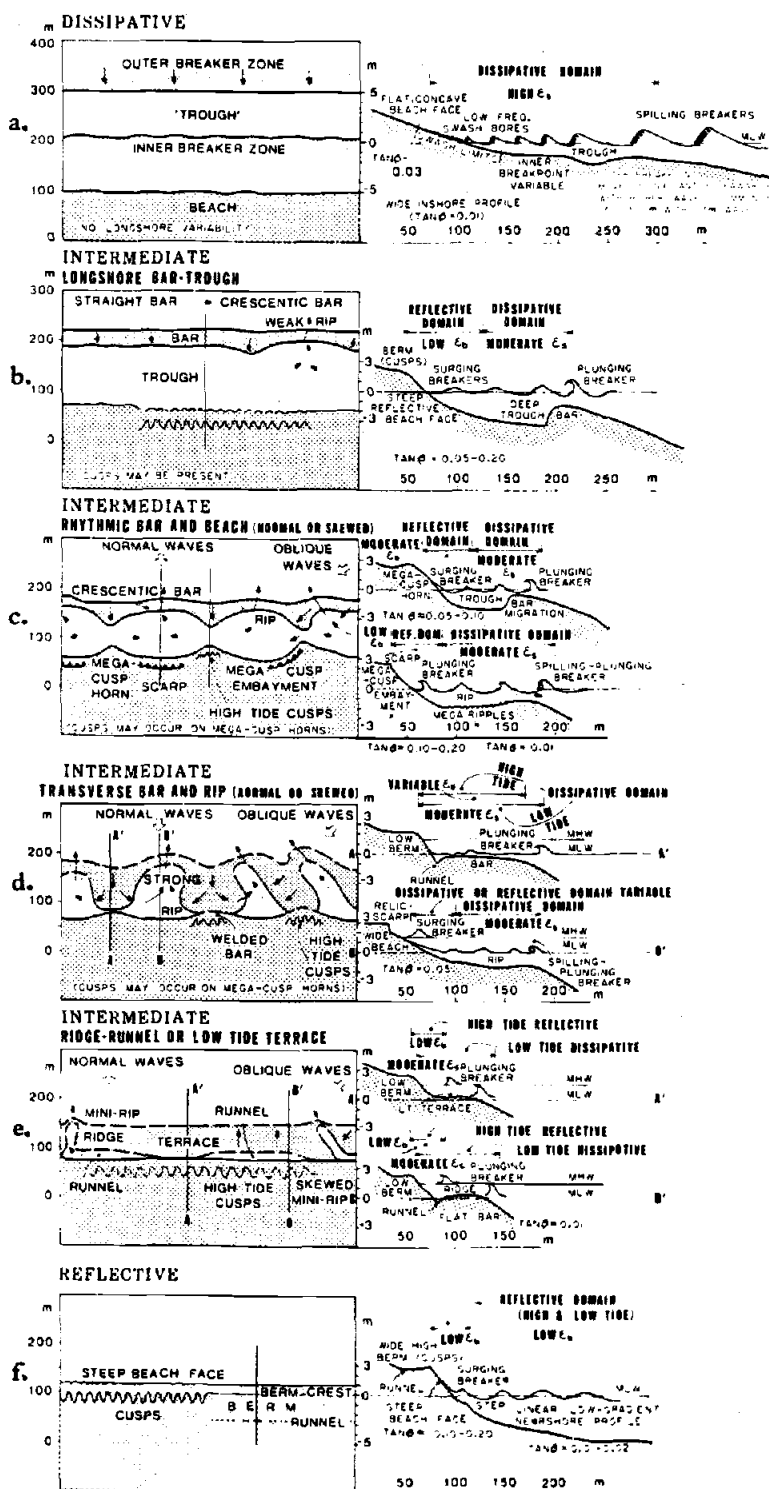


Figure 2. Plan and profile views of Wright and Short's six morphologic beach states. Siletz beach generally ranges from dissipative in the winter to reflective in the summer. Figure from Wright and Short (1983).

formation of the features. The pertinence of these theories to the Siletz beach system will be considered in the discussion.

Recently, theories based on standing or synchronous edge waves have received considerable attention. Theoretical, laboratory and field studies during the last fifteen years suggest that edge waves may be the most likely, and physically sound, mechanism for the formation of some beach cusps and most rhythmic topography. Edge waves are waves trapped in the nearshore which travel in an alongshore direction. Part of their appeal is that they have a natural longshore scale which can be quantitatively linked to the topographic lengthscale of rhythmic topography. Much of the work done relating edge waves to nearshore topography has been based on evaluations of the drift velocities associated with edge waves. Bowen and Inman (1971) explain the formation of crescentic bars in the nearshore. Guza and Inman (1975) account for the formation of large scale beach cusps. Holman and Bowen (1982) evaluate the effects of two and three edge waves acting together on a beach and are able to explain a variety of longshore rhythmic topographies by considering edge waves with different characteristics. Edge wave theory and the details of work relating edge waves to nearshore and foreshore topography will be reviewed briefly in the next section.

Shoreline rhythmicity seems clearly related to the most recent periods of erosion of unconsolidated beach and dune sands along the northern Oregon coast. Thus, more information was needed on the nature of shoreline rhythmicity in this area. The actual investigation is of Siletz Spit only, though some of the conclusions may be applicable to the other similar coastal areas mentioned

earlier. The focus of the work is to determine, in as quantitative a fashion as the data allows, the following:

- 1) The presence and consistency of longshore periodic shoreline features. (Can a characteristic longshore wavelength be determined for the features each time they occur? If so, does this wavelength vary? When present, do the cusps and embayments always occur in the same place?)
- 2) A process or processes responsible for the formation of the longshore periodic shoreline features. (Can we predict where and when longshore rhythmic topography will develop and whether major beach erosion will result?)

Two different means are employed to describe and assess the nature of the shoreline rhythmicity of Siletz Spit. First, and of great importance to this study, is a collection of 24 air photo mosaics of Siletz Spit dating from 1939 to the present. These mosaics provide a valuable historical record on erosion and rhythmic topography on the spit. From them qualitative assessment is made of shoreline rhythmicity. Twenty of the 24 mosaics are of sufficient quality to permit identification and digitization of high water lines, which were assumed to be lines of constant elevation. The ability to describe each water line by a series of x-y coordinate points makes possible both statistical and spectral analyses of the topography.

The second approach was a program of field work carried out from September 24, 1982 to June 27, 1983 on Siletz Spit. During this time surveys of an 830 m long section of beach were made at two week intervals. All measurements were referenced to an absolute x,y,z

coordinate system. The survey data gathered during the nine months of field work at Siletz Spit permit qualitative assessment of topographic change, simple statistical analyses and more complicated R-mode factor analysis of beach topography. On each of these field excursions and on two other occasions, during large storms, time lapse movies were taken of the up-wash and back-wash of the swash. These films provide information necessary to assess the hypothesis that edge waves were responsible for the generation of the rhythmic shorelines on Siletz Spit. The time lapse films make possible an estimation of swash energy and its frequency distribution on the foreshore. Also, comparisons are made to some recently proposed relationships between a surf similarity parameter and run-up, set-up and swash (Holman and Sallenger, in press). In addition, wave, tide and barometric pressure data were available from the Marine Science Center in Newport, Oregon, approximately 35 km south of Siletz Spit.

The information acquired on the rhythmic topography of this beach is used to evaluate hypotheses for the formation of cusped shorelines. A model of two topographically constrained edge waves beating together is proposed and accounts for the characteristics of shoreline morphology documented at this site.

## EDGE WAVES

Brief Review of Theory

Edge waves are waves trapped against the shoreline by refraction (their energy decays asymptotically in the offshore direction). They were first identified as a solution for the equations of motion by Sir George Stokes in 1846. The motions described by the solutions had not yet been identified in the natural world and study in this area was not pursued for more than a century. The development of increasingly sophisticated instrumentation permitted Munk (1949) and Tucker (1950) to conclude from water elevation data that low frequency (60-100 sec period) motions were low-frequency motions as free waves released by the breaking of grouped incident waves, this discovery of low-frequency motions in the littoral zone created renewed interest in all the solutions for the equations of motion relevant to this environment.

Eckart (1951) solved the linear shallow water equations of motion for a plane beach. The full solution for the wave form in terms of velocity potential,  $\phi$ , is

$$\phi(x,y,t) = (ag/\sigma)\phi(x)\cos(\lambda y - \sigma t) \quad (\text{eqn.1})$$

where  $a$  is the wave amplitude at the shoreline,  $\sigma$  is the radial frequency ( $2\pi/T$ , where  $T$  is the edge wave period),  $\lambda$  is the wave number ( $2\pi/L$ , where  $L$  is the longshore wavelength of the edge wave),

$x$  is distance offshore,  $y$  is distance alongshore and  $t$  is time.  $\phi(x)$  is the offshore behavior of the wave form. If it is assumed that the wave is trapped to the shore, that is  $\phi \rightarrow 0$  as  $x \rightarrow \infty$  then the offshore behavior is

$$\phi(x) = \exp(-\lambda x) \text{Ln}(2\lambda x) \quad (\text{eqn.2}).$$

$\text{Ln}$ , a Laguerre polynomial, can be found using the recursion relation

$$L_n(x) = \frac{\exp(x)}{n!} \frac{d^n(x^n \exp(-x))}{dx^n} \quad (\text{eqn.3})$$

where  $n$  is the offshore modal number (the number of offshore zero crossings in the waveform). The offshore form of the edge wave can also be expressed in terms of the sea surface elevation,  $\eta$ , by

$$\eta = \frac{-1}{g} \frac{d\phi}{dt} \quad (\text{eqn.4}).$$

Eckart's solution obtains the dispersion relation

$$\sigma^2 = g\lambda(2n+1)\tan\beta \quad (\text{eqn.5})$$

where  $\beta$  is the beach slope. The shallow water assumption requires that  $(2n+1)\tan\beta \ll 1$  for utilization of this equation.

Ursell(1952) solved the linear equations of motion for an inviscid fluid on a plane beach. He determined the dispersion relation,

$$\sigma^2 = g\lambda \sin((2n+1)\beta) \quad (\text{eqn.6})$$

describing a similar relationship between the same variables as (5). Equation 6 has the constraint that  $(2n+1)\beta \leq \pi/2$ . The mode for which  $(2n+1)\beta = \pi/2$  is called the cutoff mode. Ball (1967) found that on an exponential beach there are a suite of cutoff modes occurring at progressively higher frequencies. It should be noted that both of these equations produce very similar results for small values of  $\beta$ , that is for beaches of low slope. Eckart's solution is restricted by the shallow water assumption and thus deviates from Ursell's solution for steeper beach slopes or higher edge wave modes.

Eckart's solution appears more restricted, and hence less satisfactory than Ursell's at this stage. However, his solution for the offshore behavior of the wave is much easier to deal with. It is, therefore, typical to use Eckart's solution for edge waves but to restrict one's examination to edge waves of low modal number and thereby satisfy the shallow water assumption.

Edge wave energy is a maximum at the shoreline and decays in a roughly exponential manner with distance offshore. In contrast, incident waves have their minimum energy at the shoreline. Since most sediment transport occurs in the nearshore zone it is not surprising that edge waves are gaining increasing recognition as important factors in determining coastal morphology. Figure 3 shows plots of  $\phi$  versus a non-dimensional offshore distance for the four lowest edge wave modes. A reflected normally incident wave is shown for comparison. The similarity in the offshore structure of

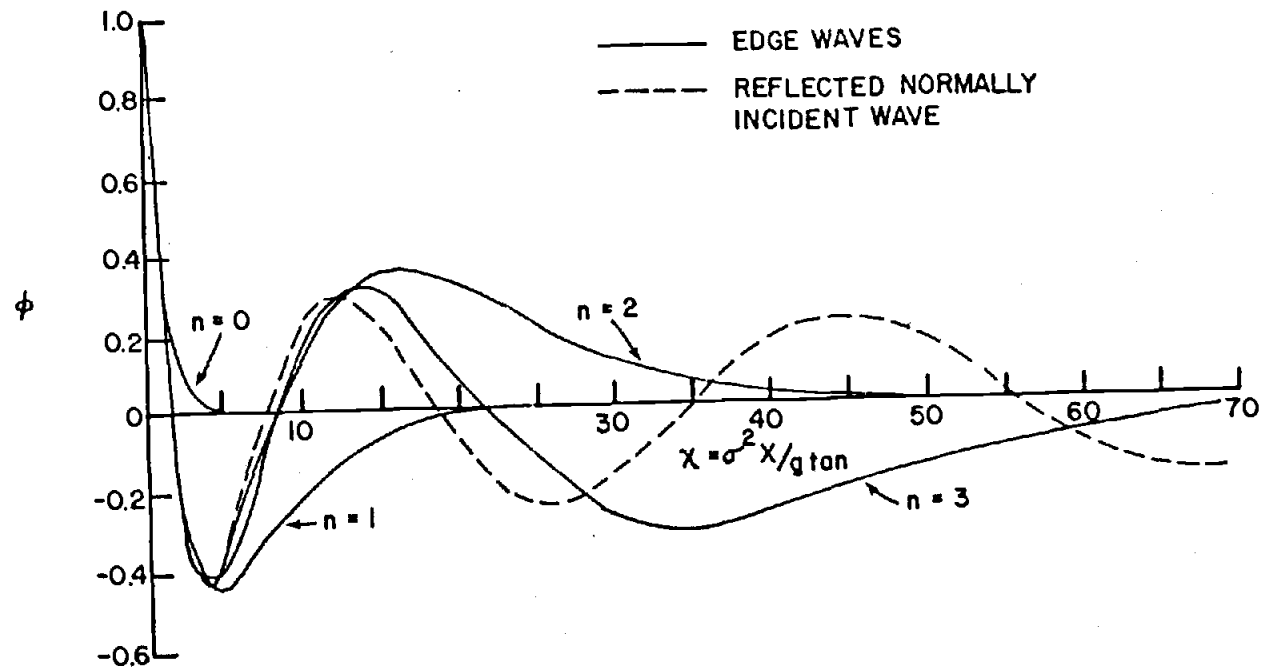


Figure 3. The offshore profiles of mode 0, 1, 2 and 3 edge waves and a reflected incident wave. Note the similarity in structure between higher mode edge waves and the reflected incident wave.

reflected incident waves and edge waves should be noted. This similarity requires that field studies seeking to identify edge waves in the nearshore environment have the capabilities to detail either the offshore structure or the longshore structure of low frequency motions. The two waves are distinguished by the fact that  $\sigma^2 \leq g\lambda_y$  for edge waves and that  $\sigma^2 \geq g\lambda_y$  for reflected incident waves, often called leaky modes ( $\lambda_y$  is the alongshore wave number).

It is important to remember that these equations were solved under the assumption of a planar beach profile. Holman and Bowen (1979) examined the validity of the planar beach assumption for a typical concave beach by numerical solution of the edge wave equations, concluding that prediction of the edge wave length "can be wrong by  $\pm 100\%$  at a fixed mean sea level with a further error of  $\pm 50\%$  introduced by tides." One can reduce this error and still use the simple solutions based on the planar beach assumption if the beach slope is chosen carefully. They suggested using the mean slope out to an offshore distance of  $1/11$  of  $(2n+1)$  times the edge wave wavelength, a relationship which must be solved iteratively since the wavelength in turn depends on the beach slope.

#### Edge Wave Forcing

Gallagher (1971) showed that low frequency waves in the nearshore can theoretically derive energy from non-linear interactions between two incident waves. Using perturbation analysis of the shallow water equations of motion, he derived a transfer function which, under proper incident wave angle and frequency

conditions, describes the forcing of edge waves on a straight, planar beach.

Bowen and Guza (1978) pursued and simplified the hypothesis developed by Gallagher. Whereas Gallagher considered stochastic waves (the complete incident wave spectrum) Bowen and Guza looked at deterministic waves. They considered specific combinations of incident waves first in a theoretical context and then in laboratory experiments. They concluded that low frequency response at the shoreline can be in the form of edge waves (as predicted) and that this response is strongest when resonance conditions for their growth are satisfied.

Guza and Davis (1974) showed that a surging incident wave (large standing component) is unstable to edge wave perturbation and will resonantly force a pair of oppositely-progressing edge waves. Only edge waves with frequencies lower than those of the incident waves are forced by this mechanism. When viscous effects are considered, indications are that edge waves with one half the frequency of the incident waves are preferentially excited (hence the name subharmonic resonance mechanism).

This should not be looked upon as an exclusive list of forcing mechanisms. It should, however, indicate the importance of incident wave characteristics such as angle of incidence, breaker type (wave steepness) and the incident wave spectrum on the forcing of edge waves.

### Edge Waves and Topography

Certain edge wave/edge wave or edge wave/incident wave interactions result in regularly-spaced longshore variation in the nearshore environment. Such variations in conditions can produce regularly spaced longshore topographic features. Bowen (1972) provides a straightforward review of the two most accepted models for the generation of rhythmic topography by edge waves.

One of these, referred to as the synchronous mechanism, is developed theoretically by Bowen (1969). The essence of this idea is that if edge waves are present which have the same period as the incident wave there will be regularly-spaced, longshore locations where the two waves are always additive (in phase) and produce large amplitude surface waves as well as other longshore locations where they are completely out of phase and produce small amplitude surface waves. This longshore variability in wave height gives rise to variable set-up. The associated longshore pressure gradients drive longshore currents towards the areas of small waves and low set-up. Rip currents occur at the convergences of flow. Circulation patterns of this form are usually referred to as nearshore circulation cells. It is common for rip currents to erode the foreshore where they form and produce an embayed area on the beach. Such a pattern is rhythmic in the longshore and has a wavelength equal to the wavelength of the edge waves. Bowen and Inman (1969) showed evidence from laboratory experiments which confirm the validity of this mechanism. The laboratory observations are compared

to a set of field observations made in the Gulf of California indicating the probable importance of this mechanism in generating rip currents with spacings of up to 600 m on natural beaches.

The second commonly accepted model concerns only standing edge waves. Standing waves can be produced by reflection of a progressive edge wave at a longshore barrier. The motion of the water surface alongshore is then the result of the combined effects of the two waves travelling in opposite directions. The model for the development of rhythmic topography by standing edge waves results from the second order (drift velocity) terms in the edge wave solution. Using a simple sediment transport model Bowen and Inman (1971) showed that standing edge waves can produce crescentic bars with offshore bar locations at offshore nodes of the edge waves and "points" at longshore nodes. A corollary of their model is that bars will only form for edge wave modes 1 or greater. In a discussion of the implications of their model on the formation of shoreline cusps, Bowen and Inman noted that drift velocities near the foreshore are strongest, and are directed offshore, at edge wave antinodes. One therefore, would expect to find embayed areas associated with antinodes. Bowen and Inman cite examples in the literature of cusped shorelines with offshore crescentic bars on real beaches. This model for the development of rhythmic topography produces a longshore topographic wavelength one half that of the edge wave length.

Guza and Inman (1975) extended the study of subharmonic edge waves to examine their role in the formation of beach cusps. They found that the resulting topographic wavelength would be one half

that of the edge wave length and the system would be constrained by the need for the edge wave to have twice the period of the incident waves.

Guza and Bowen (1981) studied the amplitude of beach cusps for the case of subharmonic edge waves described above. The theoretical analysis they performed suggests that cusp growth produces a negative feedback to edge wave growth, leading to the conclusion that there exists an equilibrium cusp amplitude for a given set of wave conditions. Their main conclusion is that equilibrium cusp amplitude increases with increasing beach slope and increasing incident wave period. Field observations support these conclusions.

Two studies, Bowen (1980) and Holman and Bowen (1982), combined the orbital and drift velocity analyses with Bagnold's sediment transport equations, modelling topographic changes under various edge wave conditions. Bowen (1980) concentrated on the position of offshore bars and the determination of equilibrium profiles. He concluded that this model accounts for field observations more fully than does the null-point theory. Holman and Bowen (1982) broadened this approach by generating a variety of longshore rhythmic topography from the combination of two edge wave modes of the same frequency. In addition, they demonstrated that what appears to be very complex, non-rhythmic longshore topography can be produced by three edge waves of the same frequency acting concurrently.

### Edge Wave Observations On Natural Beaches

Huntley and Bowen (1975) published the first observations of nearshore flow velocities which directly identified subharmonic edge waves. The measurements are consistent with mode zero edge waves with a wavelength of approximately 34 m. Extrapolation of flow velocities to the foreshore permitted estimation of the antinode elevation amplitude of 0.27 m. Huntley (1976) identified low frequency spectral peaks between 0.014 hz and 0.05 hz in nearshore electromagnetic current meter data. The offshore structure of the current amplitudes compares well to calculated offshore edge wave amplitude variations. The assignment of the four lowest frequency peaks to edge wave modes  $n=1$  through 4 is suggested because they match the predicted frequencies for edge wave cutoff modes 1 through 4. Holman, et al. (1978) published results from an offshore array of electromagnetic current meters showing a 0.01 hz spectral peak. Conclusive identification of infragravity edge waves was not possible due to the similarities between reflected waves and edge waves and the proximity of the current meters to an offshore zero crossing. Other investigations (Wright et al., 1978; Sasaki et al., 1976) have encountered similar difficulties in conclusively identifying infragravity edge waves. Examinations of longshore variations of waveforms have proved to be important as definitive evidence for the presence of infragravity edge waves. Using an array of 19 current meters, Huntley, Guza and Thornton (1981) identified edge waves of modes 0 and 1. They found a separation of modes by frequency with

mode zero waves dominating the 0.006-0.011 hz frequency band and mode one waves dominating the 0.015-0.025 hz frequency band. Very good agreement was found between calculated and predicted dispersion relations. Katoh (1981) examined longshore differences in wave run-up suggestive of an edge wave standing against a breakwater. However, his technique did not permit spectral analyses to determine the frequencies of the predicted edge wave modes. Holman and Bowen (in press) found a standing edge wave with a wavelength of 5-10 km. It had a significant edge wave height at the antinode of 1.3 meters, a period of 140 seconds and a mode number in the range 3 to 7.

It is clear from these studies that edge waves are not uncommon features in the nearshore zone. In addition, a foreshore edge wave amplitude of 0.27 m results in swash excursions of 5.4 m at their antinodes on a beach with a slope of 0.1 (Huntley and Bowen, 1975). A foreshore edge wave height of 1.3 meters on a beach of slope 0.04, as found by Holman and Bowen (in press), results in maximum swash excursions of 33 meters. These motions might easily effect the deposition and erosion of beach sand.

## AERIAL PHOTOGRAPHS

### Introduction

Analysis of historical air photographs is the most reliable means of determining an area's characteristic shoreline morphologies. The availability of such a collection of photographs was an important factor in the choice of Siletz Spit as the location of this study. A total of twenty-four sets of air photographs were obtained covering all or part of the Oregon coast between Government Point and the Siletz River (Figure 4). The dates of these photos and certain of their characteristics (to be discussed later in this section) are listed in table 1. Critical to this study was the identification of some particular feature, continuous along the shoreline, that was representative of the beach topography at the time each photograph was taken. Study of the mosaics demonstrated that high water lines were easily and objectively identifiable on all photo series. It is assumed that high water lines represent longshore points of equal elevation. Dolan et al. (1979,1981,1983) used this approach to study shoreline periodicities on the southeastern coast of the United States and presented a quantitative analysis of its errors (1983). On three mosaics two high water lines can be identified, one a result of the previous high tide and the other a result of a storm tide or a higher high tide. The shape and location of the high water line(s) on each photo mosaic were examined, recorded and analyzed.

There are certain characteristics of air photographs which must be considered before and during their use in topographic

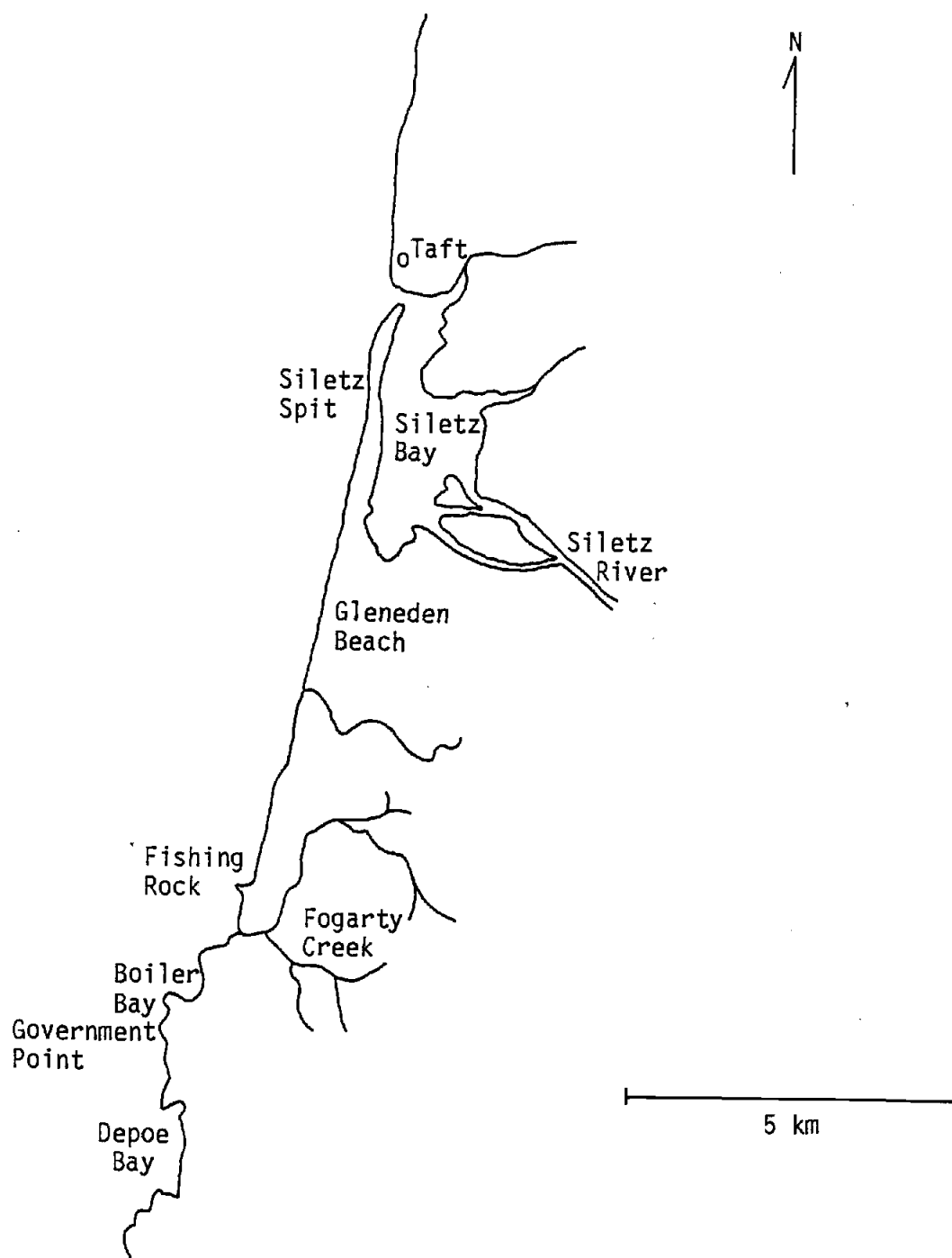


Figure 4. Government Point to the Siletz River Inlet: twenty-four sets of air photographs, which covered all or part of the shoreline in this area were studied.

DATE	SCALE m/cm	STEREO COVERAGE	COMMENTS
00/00/39	103	partial(w)	
09/19/45	109	yes	reference photo
07/02/62	194	yes	
05/28/63	127	no	
10/04/64	85	yes(w)	
09/23/65	62	yes(w)	
09/03/67	62	yes(w)	
08/06/71	122	yes	
05/24/72	241	yes(w)	
07/17/72	126	single image	nsqa
02/06/73	121	yes	reference photo
02/08/73	99	yes	
04/08/73	57	no	
05/11/73	121	yes	reference photo
02/02/74	27	.....	nsqa
03/02/74	83	.....	nsqa
03/15/74	112	.....	nsqa
02/05/76	61	no	
10/07/76	150	no	
04/25/79	137	no	
05/23/82	338	yes	
01/11/83	57	yes(w)	
05/19/83	65	yes(w)	
07/28/83	66	yes(w)	

nsqa: not suitable for quantitative analysis.

reference photo: used to align photographs which could not be used to create a semi-controlled mosaic.

(w): some or all image centers located over water.

TABLE 1. Air photo mosaics used in this study, their scale, coverage and comments on their quality.

analyses. Image quality is important in making observations on the photographs. Lighting conditions at the time of film exposure, the film used to record the image, the developing technique, amount of enlargement and paper used all effect the grain and image contrast in the photographs. In none of the photographs used for this study was image quality a limiting factor in the amount of information obtained. The other major considerations in working with air photographs are the flight characteristics of the aircraft and camera mount system. Variations in altitude of the airplane will produce variable scales from image to image. When a number of images must be aligned as a mosaic of the study area, scale variability will interfere with some qualitative observations and all quantitative observations. Tilt of the camera unit during an exposure will result in scale variations across a single image. The consequences on observations from a mosaic of such images will be similar to those from altitude variations. Unless a level and altimeter are visible in the field of view of the camera or ground truthing is available for the geographic area, such variations are difficult to compensate for. The photographs used in this study have no level or altimeter in the field of view and ground truthing the area at the appropriate scale was not feasible. It did prove possible, however to estimate amounts of relative error and identify images with large tilt effects or discrepant image scales.

The amount of overlap between images is also important when working with photo mosaics. Different methods exist for aligning photos depending on the amount of accuracy desired. All methods require at least a small amount of overlap between images. The

easiest approach is to visually match features along the image margins. This was done for all sets of images resulting in twenty-four 'uncontrolled' mosaics. Using an electronic, computer operated digitizing system, which will be described in more detail later in this section, the high water line on each image was recorded. All digitized records were then plotted to the same scale. Comparisons between plots immediately revealed high sensitivity to alignment. It was concluded that a more sophisticated means of aligning the images was necessary.

Increased accuracy can be achieved by constructing semi-controlled photo mosaics. This approach entails estimating the flight path of the aircraft from the geometry of adjacent stereo pairs (>50% overlap) and thus estimating the orientation of each photograph individually. This method is described in most introductory texts on the interpretation of aerial photographs (ex. Lillesand and Kiefer, 1979). A further constraint in aligning photographs for this study is that the center of each image must be located over an identifiable landmark. Applying this method to all the available sets of images is not possible. Some of the sets consist of every second image in a stereo sequence, with less than 30% overlap and many of those that do have stereo coverage have their centers located over moving surface water. Table 1 indicates which image sets have suitable stereo coverage for the successful application of this method.

It was decided that the three semi-controlled mosaics of greatest geographic coverage should be used as references to align the photo sequences to which this method was not directly applicable.

Two means were used to arrive at consistent photo alignment. First, slides were taken of the three reference mosaics. These were projected at the same scale as the photo series being aligned and by a combination of aligning the photo image with the projected image and matching points on adjacent photo images a satisfactory mosaic was produced with no identifiable false trends. Little difficulty was encountered in aligning the projected images with the mosaics. The reliability of this approach was evaluated by projecting a mosaic's image on the mosaic itself and by projecting each mosaic image on the other two reference mosaics. All of these evaluations were impressively successful. Image tilt or scale variations were identified by areas where the projected image and photograph could not be matched. Such areas are not extensive and should have little or no effect on the analyses performed.

A second means of producing photo mosaics was required for the three 1983 photo sets since their scale was too large to allow alignment by comparison with the projected images. The alternative devised was to digitize easily identified houses, roads and concentrations of riprap on one of the reference mosaics and then plot them at the scales of the 1983 photographs. This plot was traced on clear acetate, overlain on the uncontrolled mosaics and the necessary corrections were made. This method was evaluated by plotting the digitized record at the scale of one of the other reference mosaics, tracing and overlaying it to verify the fit. Agreement was quite good and this approach was determined to be satisfactory.

Throughout the process of aligning photographs to produce reasonably accurate mosaics, four of the photo sequences proved difficult or impossible to work with. They are identified in table 1 as not suitable for quantitative analysis. Three of these consist of many 4.5 x 4.5 inch format images with fairly large scales and much more scale variation than noted in other series. The fourth is only a single image and noticeable scale variation exists across it. Since this photograph covers only a portion of the area (less than 3 km of a total of approximately 10 km) attempts were not made to correct the variation.

#### Digitization

Digitization is the process of assigning orthogonal x-y coordinates to designated points. In this study the process was assisted by a computer controlled Hitachi electronic digitizer with 0.001 inch resolution. Thus, digitization involves fixing the mosaic to the digitizer table, setting a viewer with cross-hairs over a desired point and pushing a button. For tracing a line the button can be held down while the viewer is moved. Coordinates are recorded every time either the x or y coordinate changes by 0.254 mm. Digitizer output is in absolute coordinates, either inches or centimeters, from the lower left corner of the digitizing table.

Three reference points were chosen just east of the dunes on the spit such that at least two would be identifiable on all mosaics. Careful measurements were made on all mosaics containing all three points and each of the three points was assigned x-y coordinates in a

ground referenced coordinate system. These reference points then allowed transformation of all mosaics to this common coordinate system. Data sets were then plotted at the scale of their respective photo mosaic, traced and overlain on the mosaic to check for discrepancies. When all data sets were verified they were plotted at a scale of 118 m/cm in the alongshore direction and 30 m/cm in the onshore/offshore direction. Reduced versions of these plots are reproduced in appendix 1.

#### Qualitative Data Analyses

A casual scan through the plots in appendix 1 or the available photo mosaics of the Siletz Spit area suggests that topographic rhythmicity along this shoreline is not unusual. The record dated 02/05/76 was photographed soon after significant dune erosion occurred during a large storm. A few rough measurements on this and other records suggests that rhythmicity resulting in large amounts of beach and dune erosion has a longshore wavelength in the neighborhood of 1000 m. Only two of the mosaics have no visible rhythmicity, 09/19/45 and 05/23/82. At other times there is evidence of rhythmicity but the onshore/offshore amplitude appears very small. The mosaics from 08/06/71 and all three 1983 mosaics have such an appearance. On most of the records, however, rhythmicity is evident, whether it be only 1 to 3 cycles of modest amplitude (04/25/79, 09/23/65, 09/03/67, 07/02/62 and 05/28/63) or a number of cycles of intermediate or large amplitude (1939, 10/04/64, 05/24/72, 02/06/73, 02/08/73, 04/08/73, 05/11/73, 02/05/76, 10/07/76). First,

longshore embayment locations varied widely through time. Second, the rhythmicity tends to concentrate along the spit, with the beach tending to straighten to the south. Similarly, the onshore/offshore amplitudes of the cusped patterns seem to be greatest to the north and decrease to the south. A final observation concerns the southernmost 1-2 km of this beach. It is only recorded on four of the mosaics and observations concerning it are therefore tenuous at best. However, on these four there is a suggestion of increased rhythmicity near Government Point, particularly in 1939 and on 10/7/76, and less so on 5/24/72.

#### Quantitative Data Analyses

All water line records were combined and a mean water line was calculated. At the same time the variance at 10 m alongshore increments was calculated. The mean high water line and the high water line variance are shown in figure 5. The beginning and ending of both the mean and variance plots look peculiar. This is due to the variation in record lengths. For calculations containing a small number of records the presence or absence of a single record makes a noticeable difference in the result. In all analyses using these data, only that portion of the record based on 12 or more data points is considered. The mean water line is seen to be concave and has no appearance of topographic rhythmicity. This supports the previous observation that the alongshore location of embayments is not stable over long periods of time. Examination of the water line variance plot supports this observation. If embayments always formed in the

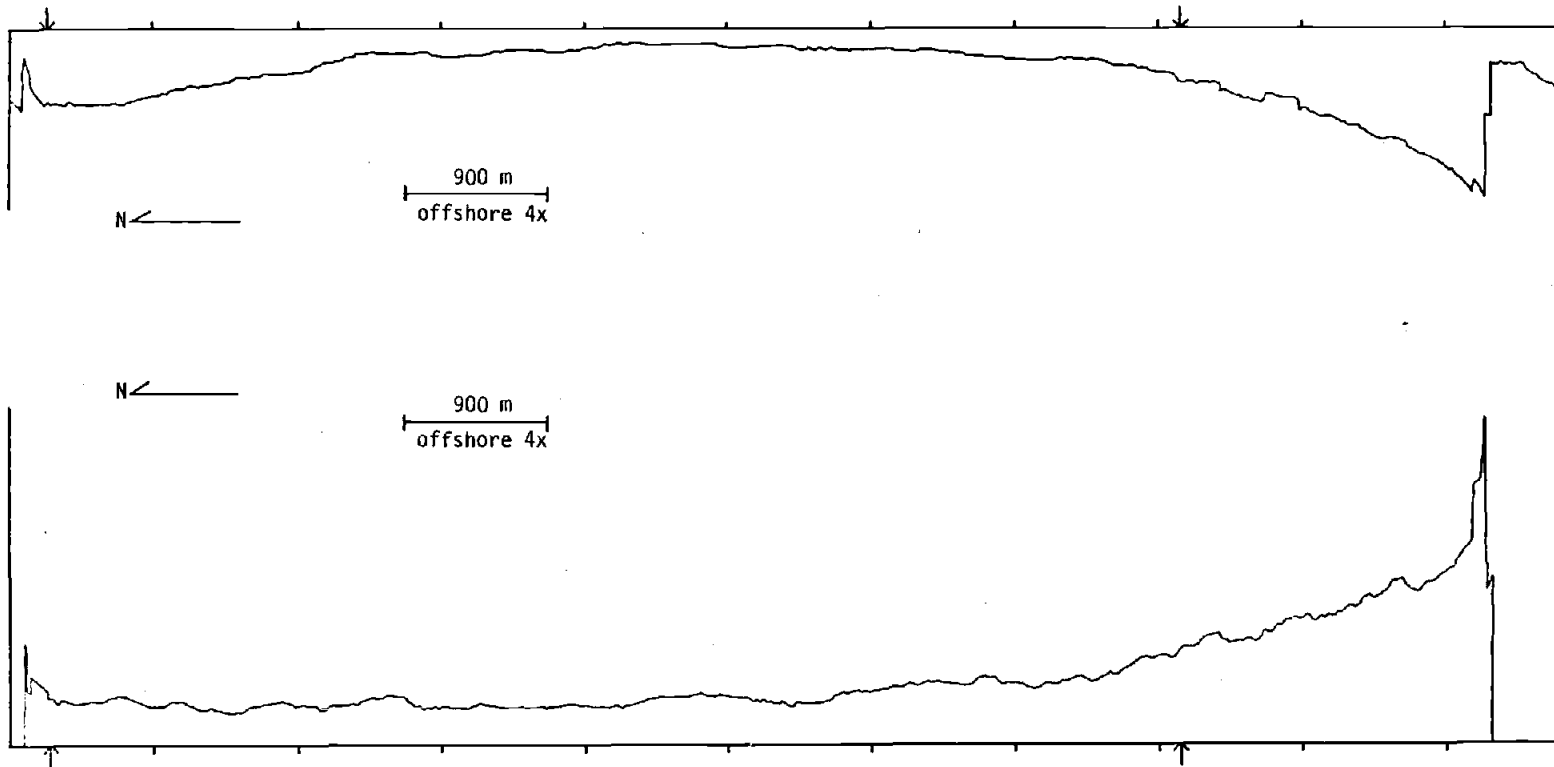


Figure 5. Plots of the mean high water line (top) and the high water line variance (bottom). The arrows indicate the points between which more than 12 records were included in calculations. Note the absence of any longshore rhythmicity.

same locations then areas at the topographic waveform's antinodes (embayments and cusps) would have a high variance relative to its nodes. The variance plot shows little alongshore variation, and spectral analysis of this data set confirms this conclusion.

Three hypotheses are possible given this observation. First, there is no regular longshore rhythmic pattern. Second, there is a single regular longshore rhythmic pattern but that its exact location varies randomly alongshore. Third, there are a number of regular longshore rhythmic patterns each occurring at a different time. For example, there may be a dominant wavelength of 600 m at times, 1000 m at other times and 1500 m at yet other times. Each of these could then have its own stable longshore position but when averaged together produce uniform variance alongshore.

Spectral analysis was performed on each water line record to identify any statistically significant wavelengths of topographic rhythmicity. The two important parameters for determining statistical significance in spectral analysis are the confidence interval and the bandwidth. The confidence interval specifies the necessary peak height for a peak to be statistically significant at some level of confidence. It is a function of the number of degrees of freedom,  $\nu$ . For the Tukey filter used,

$$\nu = \frac{8}{3} (N_f - 1) \quad (\text{eqn.7})$$

where  $N_f$  is the half-filter width. Similarly, the bandwidth, the frequency range over which there is only one independent estimate, is given by,

$$B = \frac{4 (N_f - 1)}{3 L_R} \quad (\text{eqn.8})$$

where  $L_R$  is the length of the record. The longest wavelength which can be distinguished from a record is the one that is a half bandwidth away from zero wavenumber. For the high water line data set the minimum record length is 4147 meters (see table 2 for a listing of all record lengths). Even in this worst case we can distinguish wavelengths less than 2083 meters using a half-filter width of 4. This is longer than the visually-observed wavelengths.

Plots of spectra for all high water line records are reproduced in appendix 2. All spectral peaks statistically significant at a level greater than 80% were identified and are recorded in table 2. No peaks are found at or very near the 1000 m wavelength. Examination of the spectra however, reveals that many of them are very red, that is energy decreases monotonically with the wavenumber  $\kappa=1/L$ , where  $L$  is wavelength, (ex. Figure 6). This is a result of the general curvature in the mean shoreline. With the thought that the redness may obscure significant peaks, the mean water line was subtracted from each of the data series and the spectra were recalculated. Record lengths are restricted in some cases by the shortened mean water line data series. Table 3 lists the bandwidths for the 'mean subtracted' data sets. The shortest record is now 02/08/73 and the longest wavelength that can be determined as significantly different from zero is 1538 m. This is rather close to 1000 m, but all other records have their maximum

DATE	LENGTH m	MAX L DISTINGUISHABLE FROM 0 FREQUENCY	SPECTRAL PEAKS
00/00/39	9216	4651	
09/19/45	7782	3922	
07/02/62-1	7065	3509	
07/02/62-2	7065	3509	80% @ 560-824m
05/28/63	5120	2564	80% @ 855-2564m
10/04/64	4147	2083	
09/23/65	4608	2299	
09/03/67	4352	2174	
08/06/71-1	5120	2564	
08/06/71-2	5120	2564	
05/24/72-1	8806	4444	80% @ 506-655m
05/24/72-2	8806	4444	
02/06/73	9113	4545	
02/08/73	3123	1563	
04/08/73	4454	2222	
05/11/73	5120	2564	
02/05/76	5120	2564	
10/07/76	9011	4545	
04/25/79	9011	4545	
05/23/82	6860	3448	
01/11/83	7270	3636	
05/19/83	7475	3704	
07/28/83	7373	3704	

TABLE 2. Air photo mosaic dates, characteristics important in spectral analyses and peaks of greater than 80% confidence in power spectra.

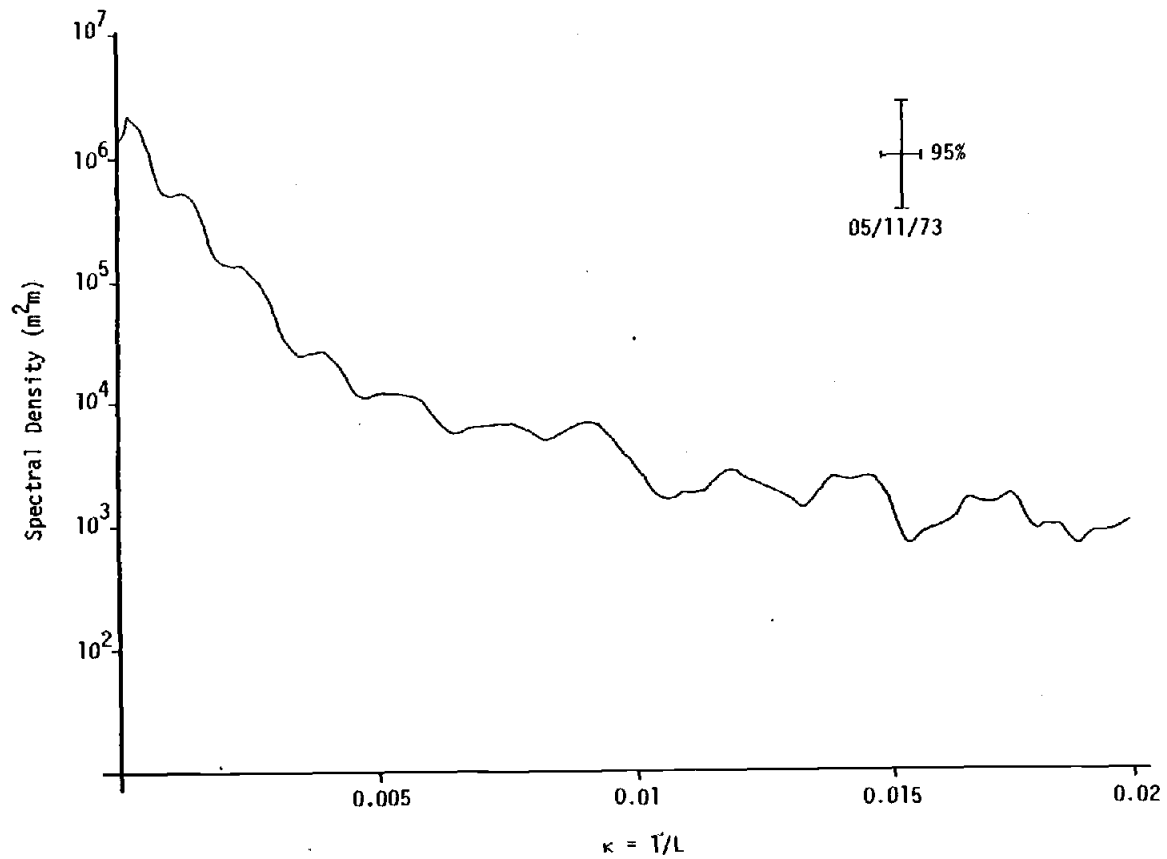


Figure 6. Typical spectrum of an air photo high water line. Note that energy (spectral density) decreases monotonically with increasing wavenumber ( $k=1/L$ ).

DATE	LENGTH m	MAX L DISTINGUISHABLE FROM 0 FREQUENCY	SPECTRAL PEAKS
00/00/39	6942	3448	
09/19/45	7036	3509	
07/02/62-1	7045	3509	
07/02/62-2	7045	3509	
05/28/63	5121	2564	
10/04/64	4148	2083	95% @ 676-1923m
09/23/65	4708	2353	99% @ 656-1481m
09/03/67	4395	2198	80% @ 570-1183m
08/06/71-1	5527	2778	
08/06/71-2	5527	2778	
05/24/72-1	6899	3448	
05/24/72-2	6907	3448	99% @ 840-1639m
02/06/73	7034	3509	
02/08/73	3130	1538	
04/08/73	4296	2151	
05/11/73	5323	2667	95% @ 635-1212m
02/05/76	5689	2857	80% @ 645-1176m
10/07/76	7030	3509	
04/25/79	7035	3509	
05/23/82	6674	3333	
01/11/83	6994	3509	
05/19/83	7014	3509	
07/28/83	6924	3448	

Table 3. Air photo mosaic dates, characteristics important in spectral analyses and peaks of greater than 80% confidence in power spectra for the mean-subtracted water line data set.

detectable wavelength at 2000 m or more so the analyses can still provide useful information. The spectra of these data sets are reproduced in appendix 3 and are summarized in table 3. Six of the twenty-three spectra now show peaks in the 800-1000 m range with greater than 80% confidence (ex. Figure 7). Of these six peaks two are significant at the >80% level, two at the >95% level, and two at the >99% level. Consideration of the bandwidths for these records and the repetition of two spectral analyses with a half-filter width of 2 indicates that there is only a single regular rhythmic pattern on this section of coast and that its wavelength is 800-1000 m. A more exact identification of the wavelength is not possible given the record lengths and apparent localization of the signal.

### Conclusions

Two conclusions concerning the nature of shoreline rhythmicity between Government Point and the Siletz River can be drawn from this study of air photo mosaics. First, spectral analysis revealed that when rhythmicity was present it had a lengthscale of 800-1000 m. This was identified by subtracting the mean water line from each data set and then performing spectral analyses on the resulting record. Qualitative observation suggests that there is a localization of this rhythmicity on the northern part of Siletz Spit and that the amplitude of the rhythmicity is greatest at its northern extent. The southernmost part of the study area, within about 2km of Government Point, may also be subject to a very similar rhythmic topography but data in this region are limited.

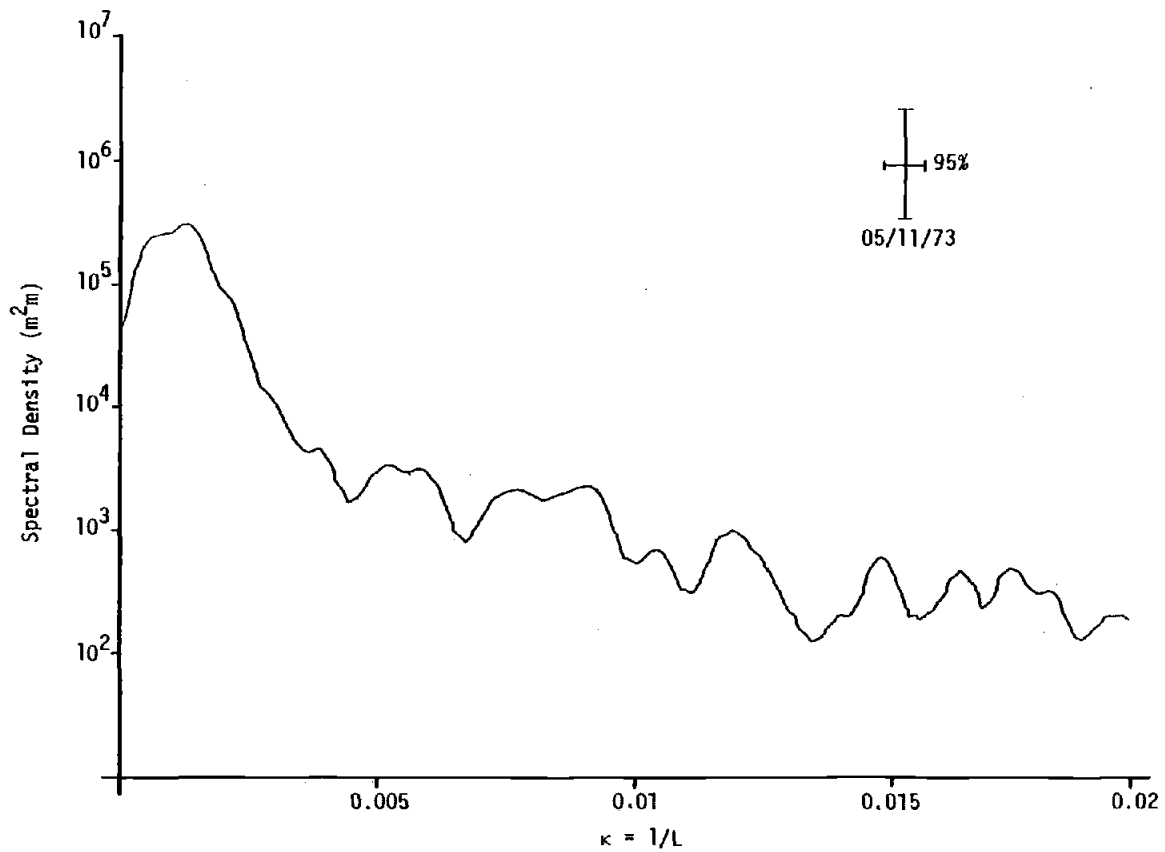


Figure 7. Typical spectrum of a 'mean-subtracted' high water line. Note the energy (spectral density) peak in the 800-1000 m ( $k=0.001$ ) range.

Second, though always of the same wavelength when present the exact longshore position of the cusate pattern varies widely. In the area affected by the rhythmicity there are no positions where an embayment is more likely to form than at others.

## FIELD EXPERIMENT

### Methods

A field study of an 830 m section of Siletz Spit was undertaken from September 24, 1982 to June 27, 1983. The purpose was to document the topographic changes in beach configuration through an annual cycle. It was also desirable to try to relate the observed changes in topography to various environmental parameters such as significant wave height, water level, and barometric pressure.

The field site is identified on figure 8. Four reasons can be given for the choice of this location. First, as previously stated, the general area of Siletz Spit was chosen because of the large number of aerial photographs available to document past beach morphologies. Second, it is the most conveniently located sand spit on the coast with respect to Corvallis and enabled a field excursion to be completed in a single day. Third, there are headlands to both the north, Cascade Head, and south, Government Point, which might lead to the generation of rhythmicity by standing edge waves. Fourth, this 830 m of beach between Government Point and Siletz Spit showed the greatest rhythmicity on the historical photographs. It was hoped that development of a large embayment might be documented.

Field excursions were made once every two weeks, at the time of spring tides, and also during and/or soon after large storms. On each excursion beach profiles were recorded during low tide at marked locations in the 830 m study area. Also on each excursion, a 35

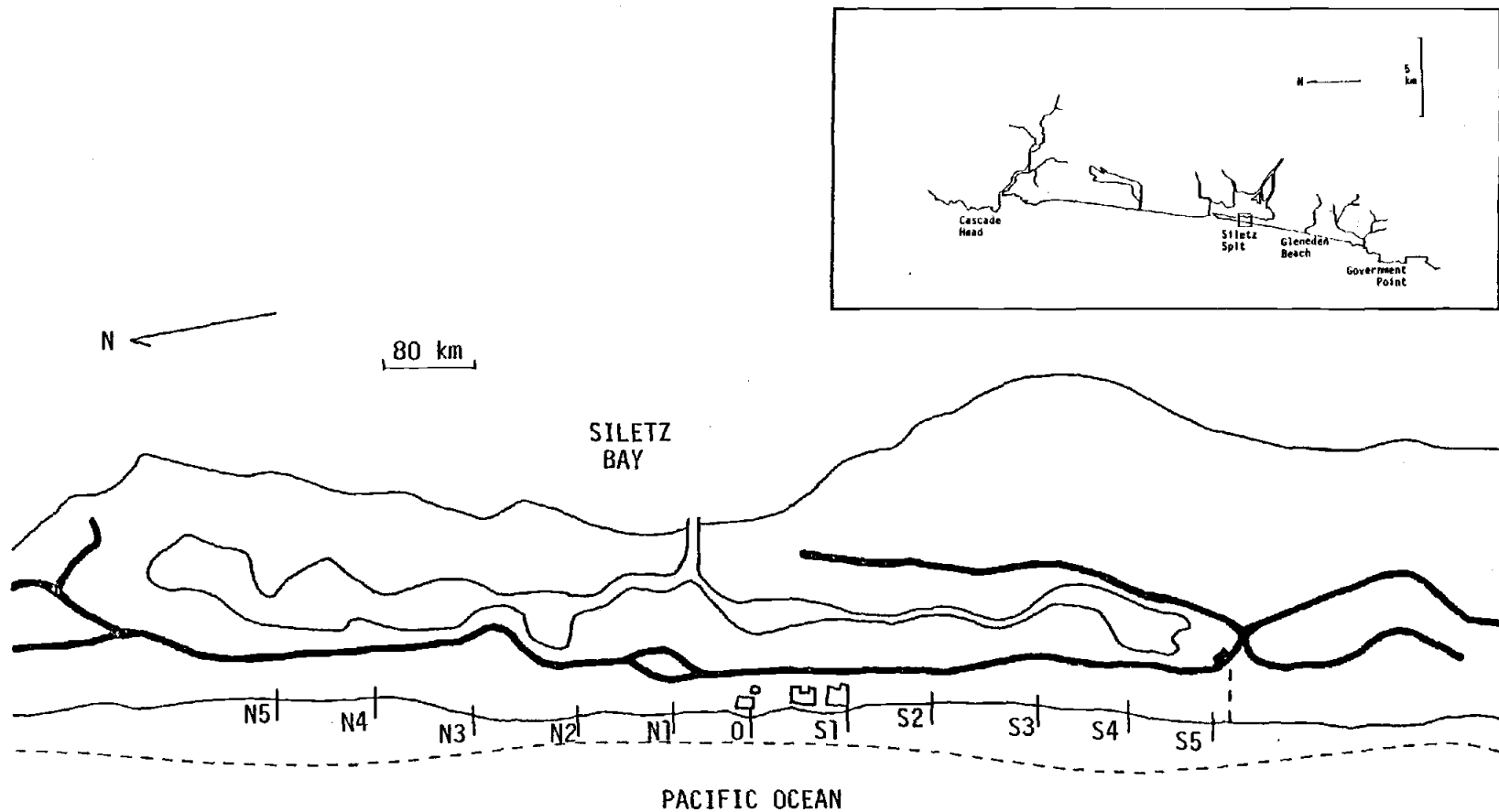


Figure 8. Map of the field site on Siletz Spit. The labelled profile ranges are approximately 80 m apart. Profiles were usually measured at bi-weekly intervals from September 24, 1982 to June 27, 1983.

minute time lapse movie was taken during high tide. Due to adverse weather conditions and two equipment failures, not all the desired data were actually collected on all excursions. Table 4 lists the excursion dates and the data obtained on each.

A total of 11 profile lines, distributed through the study area at approximately 80 m intervals, comprised the profile grid used to document beach topography (Figure 8). The landward extreme of 10 of the profiles was located 5-10 m east of the dune crest and was marked by a wooden dowel driven into the dune or by the corner of a house porch. At one profile line a house extended over the dune crest and here the landward extent of the profile was at the dune to beach slope change. The site was marked by a drift log which remained stationary all winter. The distance between the sand surface and the top of the reference marker was recorded each time a profile was measured. Emery Boards (Emery, 1961) were used to measure the profiles; changes in elevation were recorded at 5 m intervals across shore. The accuracy of this surveying method is discussed in Emery (1961) and Davis (1976). The most critical concerns with this method are the stability of the sediment surface, the visibility to and clarity of the horizon, and the possibility of cumulative error along a profile. The seaward extent of each line was usually determined by the existing wave conditions, though on several occasions, at exceptionally low tides, time was a limiting factor. Surveys rarely extended more than 5 m into the water and hence sediment movement at the survey stakes was not a problem. Visibility was a serious problem on only one excursion (11/16/82) preventing the complete topographic documentation. However, the

EXCURSION DATE	EXCURSION NO	DATA OBTAINED
24 SEPT 1982	04	film and all profiles
16 OCT 1982	05	film and all profiles
30 OCT 1982	06	film and all profiles
16 NOV 1982	07	film only
18 NOV 1982	08	film and all profiles
30 NOV 1982	09	film and all profiles
8 DEC 1982	10	profiles only
15 DEC 1982	11	film and every other profile
21 DEC 1982	12	film and all profiles
30 DEC 1982	13	film and all profiles
13 JAN 1983	14	film and all profiles
26 JAN 1983	15	film only
27 JAN 1983	16	film and all profiles
12 FEB 1983	17	film and all profiles
26 FEB 1983	18	film and all profiles
13 MAR 1983	19	film and all profiles
27 MAR 1983	20	film and all profiles
12 APR 1983	21	film and all profiles
28 APR 1983	22	qualitative evaluation only
12 MAY 1983	23	film and all profiles
28 MAY 1983	24	film and all profiles
12 JUNE 1983	25	qualitative evaluation only
27 JUNE 1983	26	film and all profiles
12 JULY 1983	27	qualitative evaluation only

Table 4. Field excursion dates and numbers and a summary of the data obtained on each outing.

EXCURSION	PROFILE RANGE										
	N5	N4	N3	N2	N1	00	S1	S2	S3	S4	S5
04	125m	125m	120m	115m	130m	105m	110m	95m	105m	100m	90m
05	80	90	70	95	115	115	105	85	100	110	105
06	70	80	80	85	150	120	100	85	90	85	80
07	...	...	...	...	...	...	...	...	...	...	...
08	65	75	65	80	90	75	60	55	60	105	55
09	65	90	95	100	135	100	100	90	115	120	130
10	125	135	140	140	130	130	100	95	120	115	115
11	...	...	...	...	...	...	...	...	...	...	...
12	80	95	80	75	70	65	70	85	100	90	85
13	95	135	125	105	95	195	150	155	135	130	240
14	85	85	65	75	100	105	125	115	120	115	160
15	...	...	...	...	...	...	...	...	...	...	...
16	55	80	80	75	85	85	90	80	85	100	95
17	45	70	60	60	115	80	95	90	105	95	70
18	80	105	105	100	180	105	115	105	105	105	100
19	105	110	105	105	115	95	115	85	90	75	70
20	105	105	105	105	160	125	115	120	125	80	80
21	125	120	155	125	155	115	120	115	140	125	130
22	...	...	...	...	...	...	...	...	...	...	...
23	125	130	120	105	135	95	115	105	120	120	120
24	150	155	135	130	165	240	135	125	140	135	130
25	...	...	...	...	...	...	...	...	...	...	...
26	135	130	120	110	115	100	100	95	115	110	115

TABLE 5. Offshore extent of each profile from its reference marker.

eleven profiles were measured on a return trip 11/18/82. In the worst possible case a cumulative error of 1 to 2 cm at each survey station might occur. Over profiles of 45-60 m in length maximum errors of 18 to 48 cm could be incurred. The total vertical relief over this cross-shore distance was 6 to 9 m and thus errors of less than 8% can be expected. The possible magnitudes of these errors and the continuity of profiles through time suggests that these errors do not effect significantly the analyses and conclusions of this study.

An absolute coordinate system was established for the site with an Omni Total Station laser surveying unit during the spring of 1983. The coordinate system is oriented with its origin located at the top of the S1 reference marker (corner of porch floor) and the y-axis trending along the dune crest. Figure 8 shows the profile grid with each profile labelled. The offshore extent of each profile for each excursion is noted in table 5. It should be noted that the area documented by all 18 surveys extends only 45-60 m from the dune base and hence is rather narrow. Quantitative analysis of the beach topography will be restricted to this backshore area.

#### Wave, Tide and Weather Conditions

Wave, tide and barometric pressure data recorded at the Marine Science Center, Newport, Oregon are available for the period of field work on Siletz Spit. Wave height and period are measured by recording microseisms produced by the waves on an analog seismic recording system (Quinn, Creech and Zopf, 1974; Komar et al., 1976). Wave data are recorded for ten minutes every six hours. Wave height

(in 13 m water depth) estimates are determined from calibrated templates overlain on the seismic records. Wave periods are twice the period of the microseisms. A tide gauge is located in the Newport Harbor; hourly water elevations and times of high and low tides are tabulated from its output. Hourly barometric pressure is tabulated from the barometer output.

It is of interest to compare the general wave and weather characteristics during the nine months of field study with the monthly means calculated from the preceding ten years. Figure 9 shows the weekly mean and weekly maximum significant wave heights from Aug. 8, 1982 to June 27, 1983. The maximum significant wave height was 6.0 m for one week, but exceeded 5.0 m during 4 separate weeks and 4.8 m during 2 additional weeks. Weekly mean significant wave heights reached almost 4.0 m on one occasion and over 3.5 m on another. Figure 10 shows the ten year (1971-1981) means of monthly mean significant wave height and the monthly mean significant wave height for 1982-1983. There is no noticeable difference in wave climate, as expressed by monthly means, between 1982-1983 and the preceding ten years. For a comparison of maximum wave conditions, Komar et al. (1976) state that the largest significant wave height measured by the seismometer from 1971 until early 1976 was 7.0 m. This occurred in late December 1972 and corresponded with a period of severe erosion on Siletz Spit. Incident wave periods also showed no noticeable difference between 1982-1983 and the preceding three years (Creech, 1981). As shown in figure 11 wave periods of 12 to 15 seconds are typical.

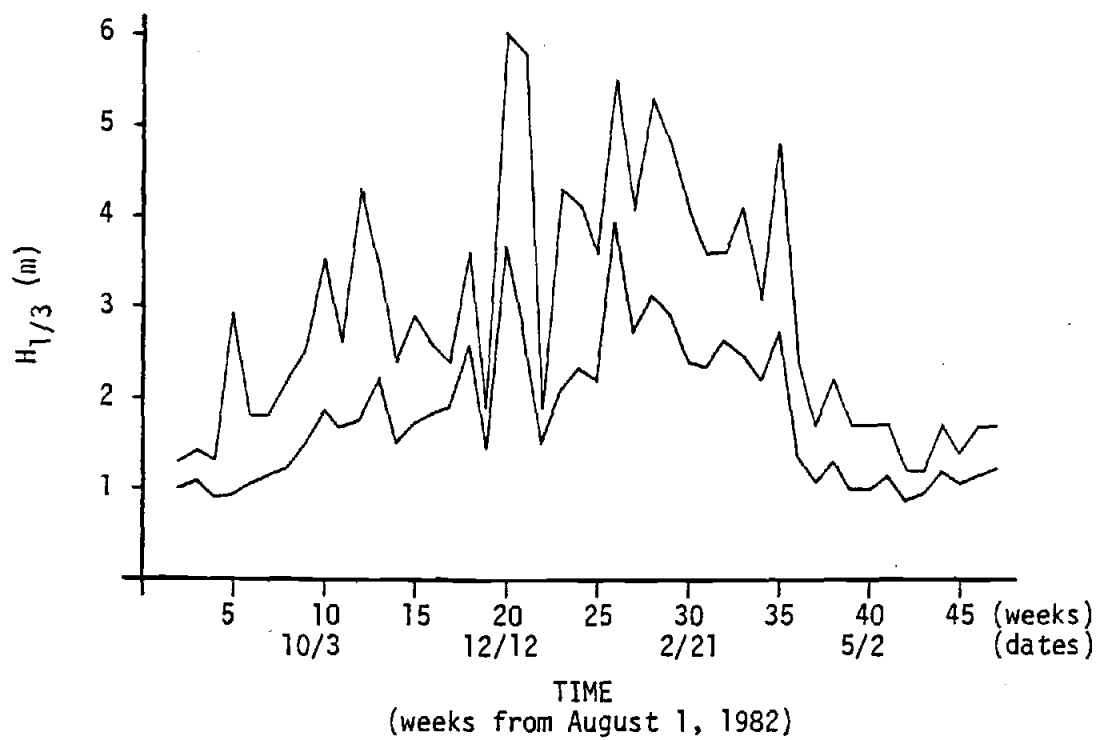


Figure 9. Weekly means and maxima of significant wave heights, August 1982-June 1983. Weekly maxima exceeded 5.0 m on four occasions.

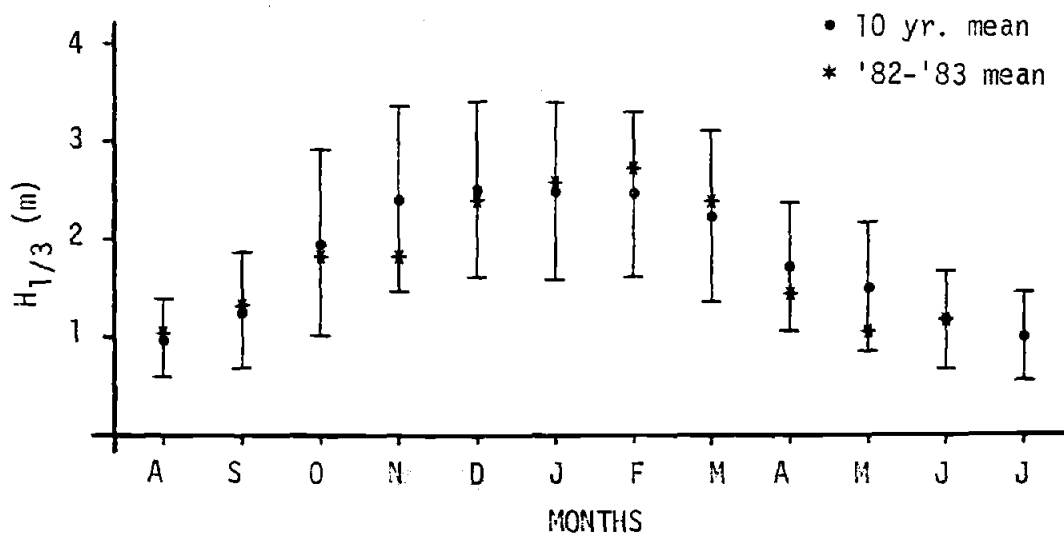


Figure 10. Ten year monthly means and 1982-83 monthly means of significant wave height. The bars extend one standard deviation about the ten year mean.

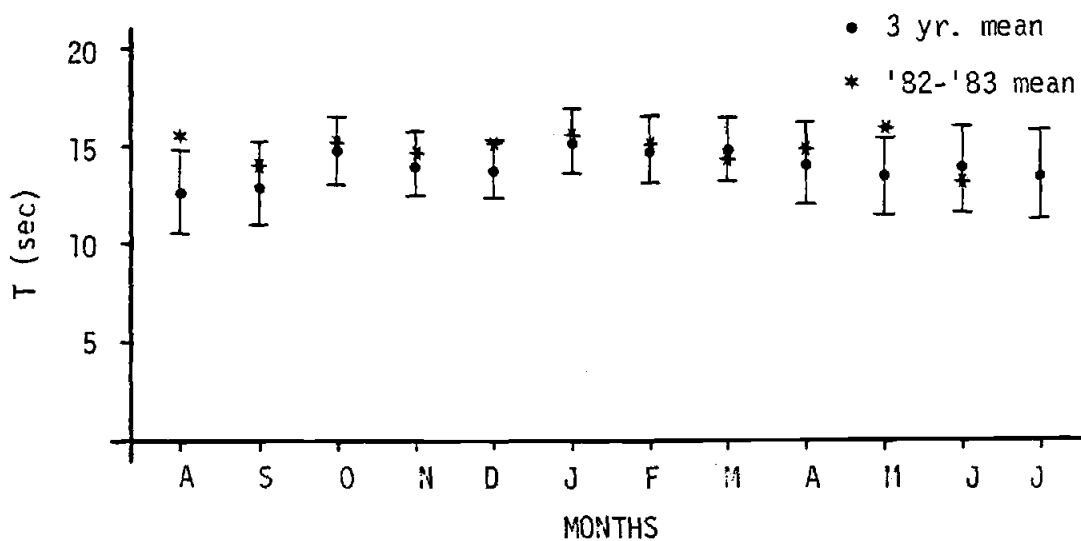


Figure 11. Three year monthly means and 1982-83 monthly means of incident wave period. The bars extend one standard deviation about the three year mean.

The weekly means of hourly water level data during the field study, figure 12, show a maximum from mid-October through March. Comparison of 1982-83 records to those of the preceding ten years shows that 1982-83 mean water levels exceeded levels since sometime before 1970. Figure 13 shows the ten year mean of monthly mean sea level for 1971-81, and the monthly mean sea level for September 1982 through September 1983. Sea level during the time of this study was clearly anomalously high (Huyer et al., 1983).

Plots of weekly mean and minimum barometric pressure are shown in figure 14. Weekly minimum barometric pressures reached well below 995 mbars during 8 weeks and the weekly mean pressure was less than 1000 mbars once during the Siletz Spit field study (1013.25 mbars is standard atmospheric pressure at sea level). Changes in atmospheric pressure will give rise to corresponding changes in sea level, the "inverse barometer" effect. As a rough rule of thumb, sea level will rise 1 cm per mbar drop in atmospheric pressure. A comparison of the 1982-83 barometric pressure data with the ten year means (Figure 15) shows anomalous lows through the winter months of the study period (Huyer et al., 1983). The inverse barometer effect was a maximum in early 1983, contributing 28 cm to a total sea level anomaly of +111 cm. It typically accounted for up to 25% of the total sea level anomaly.

The large variations in sea level and barometric pressure from the fall of 1982 through the summer of 1983 can be attributed to the El Niño event experienced throughout the central and eastern Pacific during this time (Huyer et al., 1983). The high water conditions and low atmospheric pressures on the central Oregon coast

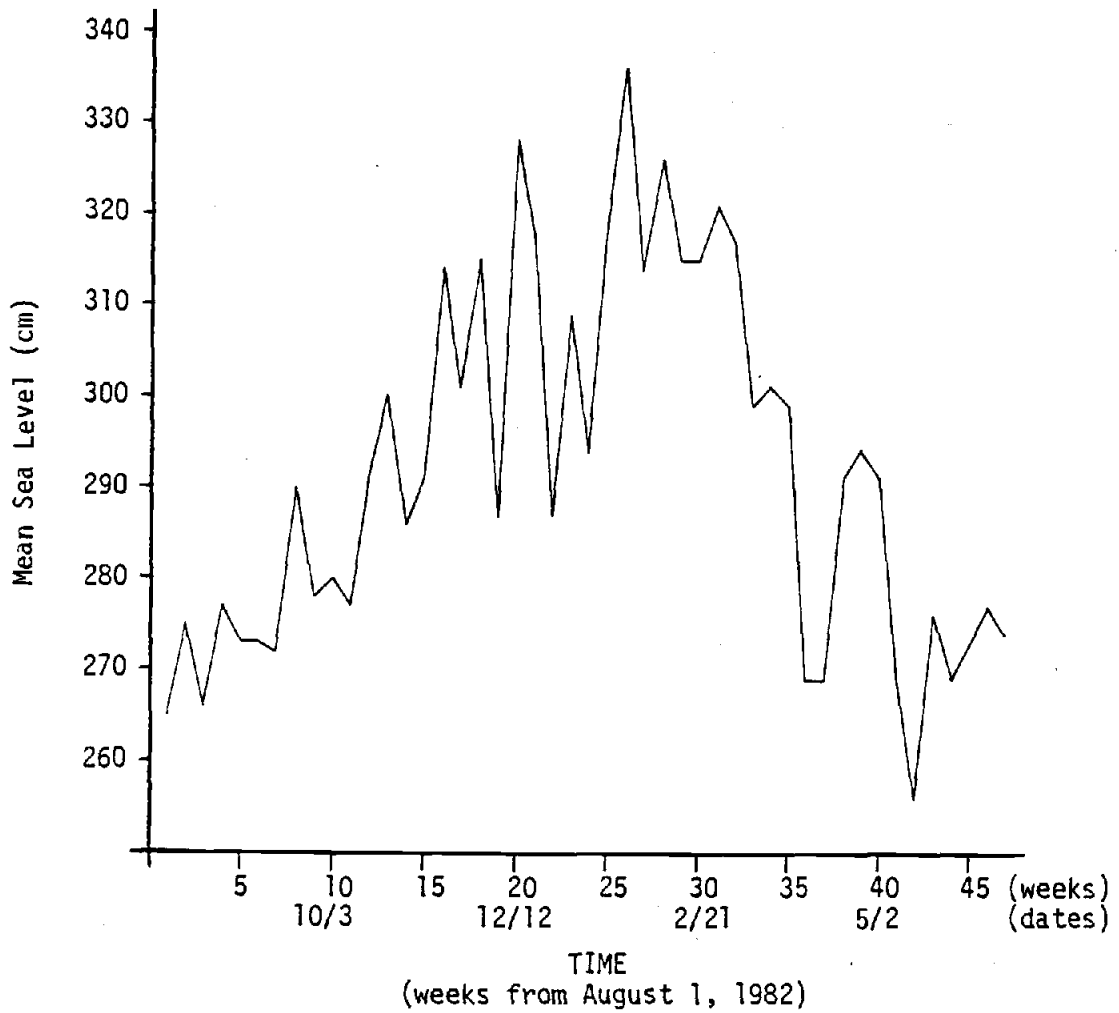


Figure 12. Weekly mean sea levels, August 1982-June 1983. Note the increased levels from mid-October through March. Values are relative to MLLW.

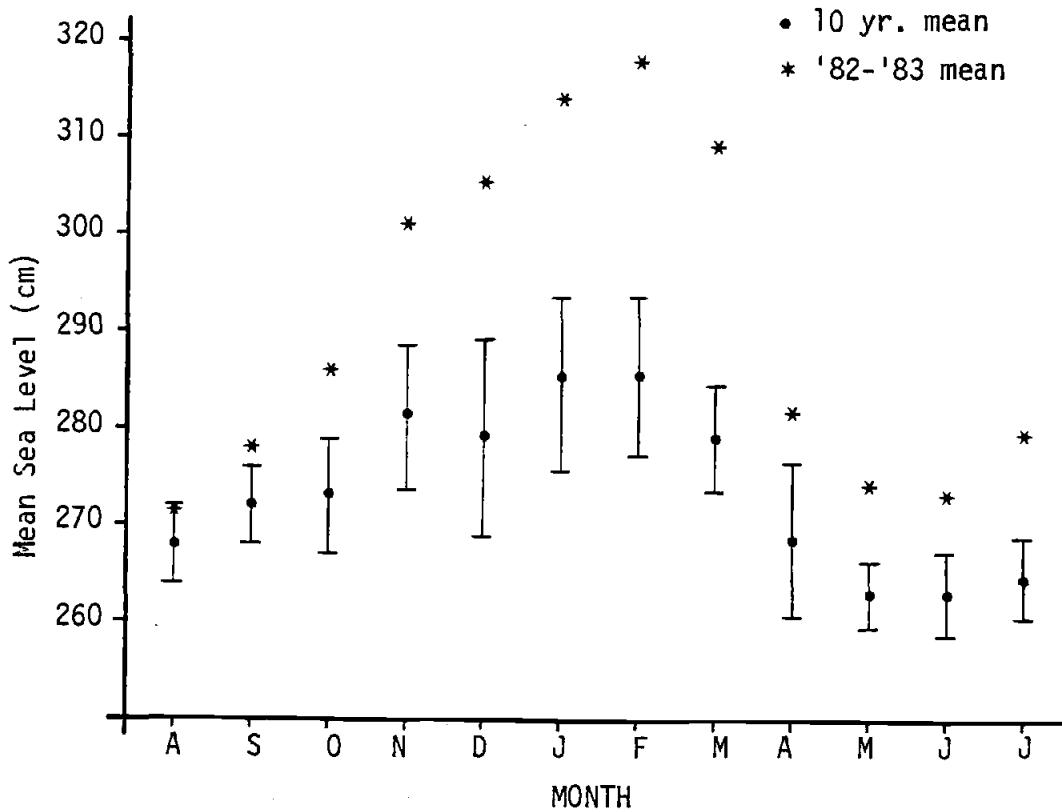


Figure 13. Ten year monthly means and the 1982-83 monthly means of sea level. Note the anomalously high sea levels from November through March of 1982-83. The bars extend one standard deviation about the ten year mean. Values are relative to MLLW.

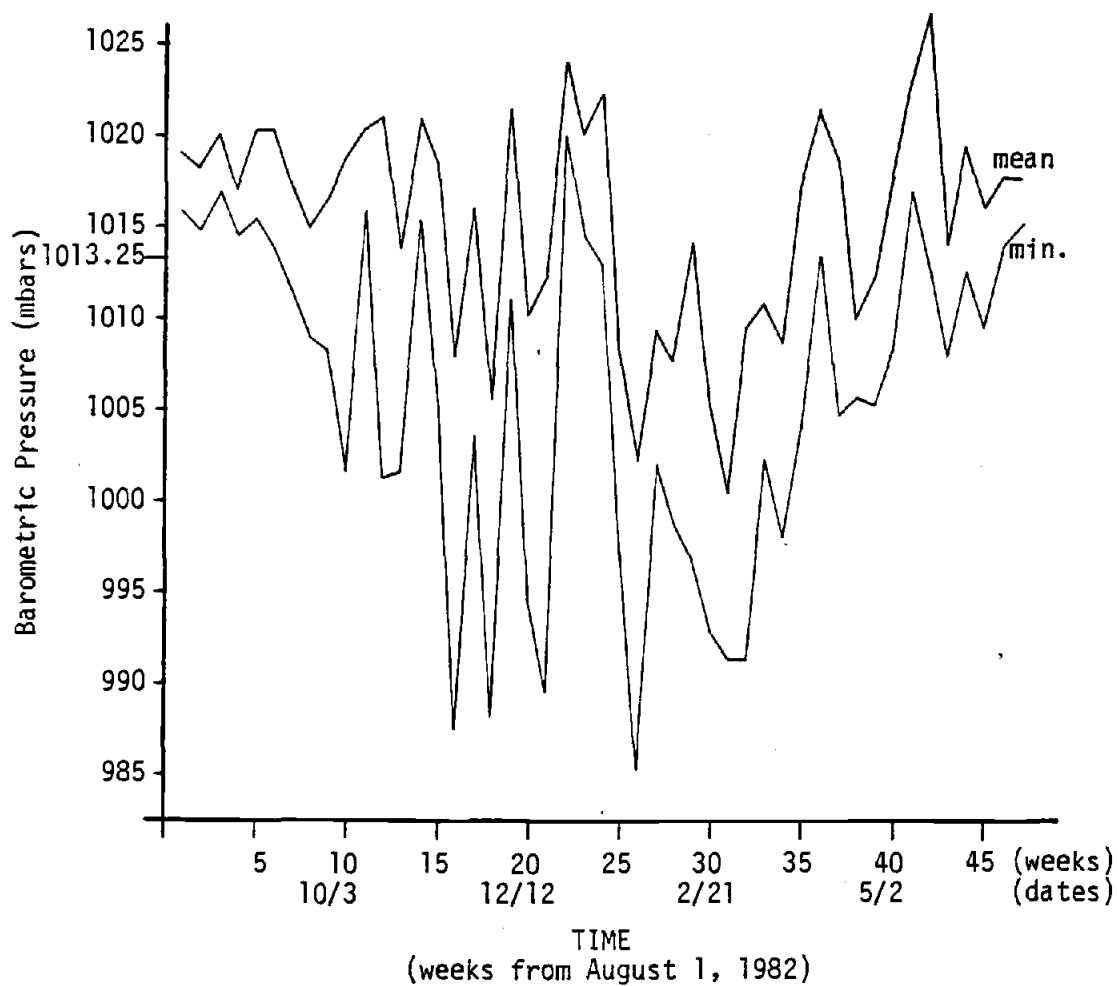


Figure 14. Weekly means and minima of barometric pressure August 1982-June 1983. Note the extreme lows in pressure from November through March. Standard atmospheric pressure (1013.25 mbar) is labelled for reference.

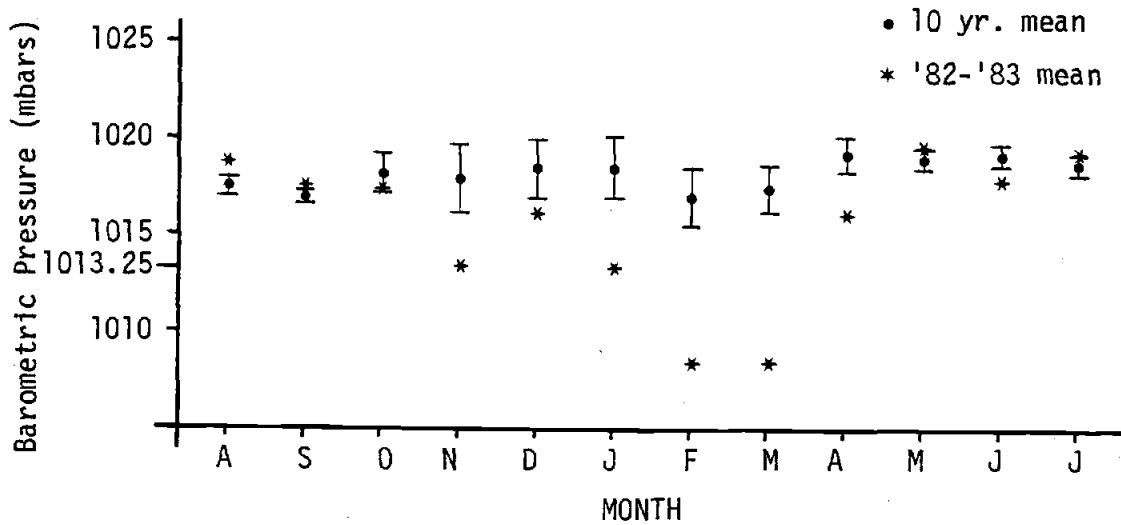


Figure 15. Ten year monthly means and the 1982-83 monthly means of barometric pressure. Note the anomalously low values through the winter months of 1982-83. Standard atmospheric pressure (1013.25 mbar) is labelled for reference. The bars extend one standard deviation about the ten year mean.

are believed to be the direct result of 1) thermal expansion associated with an increase in nearshore water temperature, 2) a shift in the atmospheric pressure system to the south, bringing low pressure storm centers closer to the central Oregon coast than usual and 3) either a large coastal-trapped wave propagating north from the equatorial region or a large scale atmospheric disturbance (Huyer et al., 1983; Enfield and Allen, 1980).

### Beach Profiles

Qualitative evaluation of the beach profile data confirms previous work on profile changes on the Oregon coast (Aguilar-Tufoñ and Komar, 1978). Representative profiles from ranges N3, N1 and S3 are shown in figure 16. Each range shows the classic transition from a swell or summer beach profile to the storm or winter beach profile as sediment moves offshore in the fall storms. The three ranges demonstrate the alongshore variability of the seasonal changes. On the whole the swell profiles look very similar with a wide berm sloping to the backshore landward of the berm crest. The storm profiles also look quite similar. All are concave, though variations in steepness can be seen through time at any one location and concurrently at different longshore locations. The greatest longshore variations in profiles seems to occur in the fall as the summer berm is eroding. At ranges S3 and N3 the berm disappears quite suddenly while at range N1 it moves onshore and is slowly reduced in size before finally disappearing in late November. Longshore variation in profiles was very small by the time winter

Figure 16. Representative fall and early-winter beach profiles from ranges N3, N1 and S3. Note the alongshore variations in the transition from swell to storm profiles. Also, note the similar shapes of all three late summer, swell, profiles.

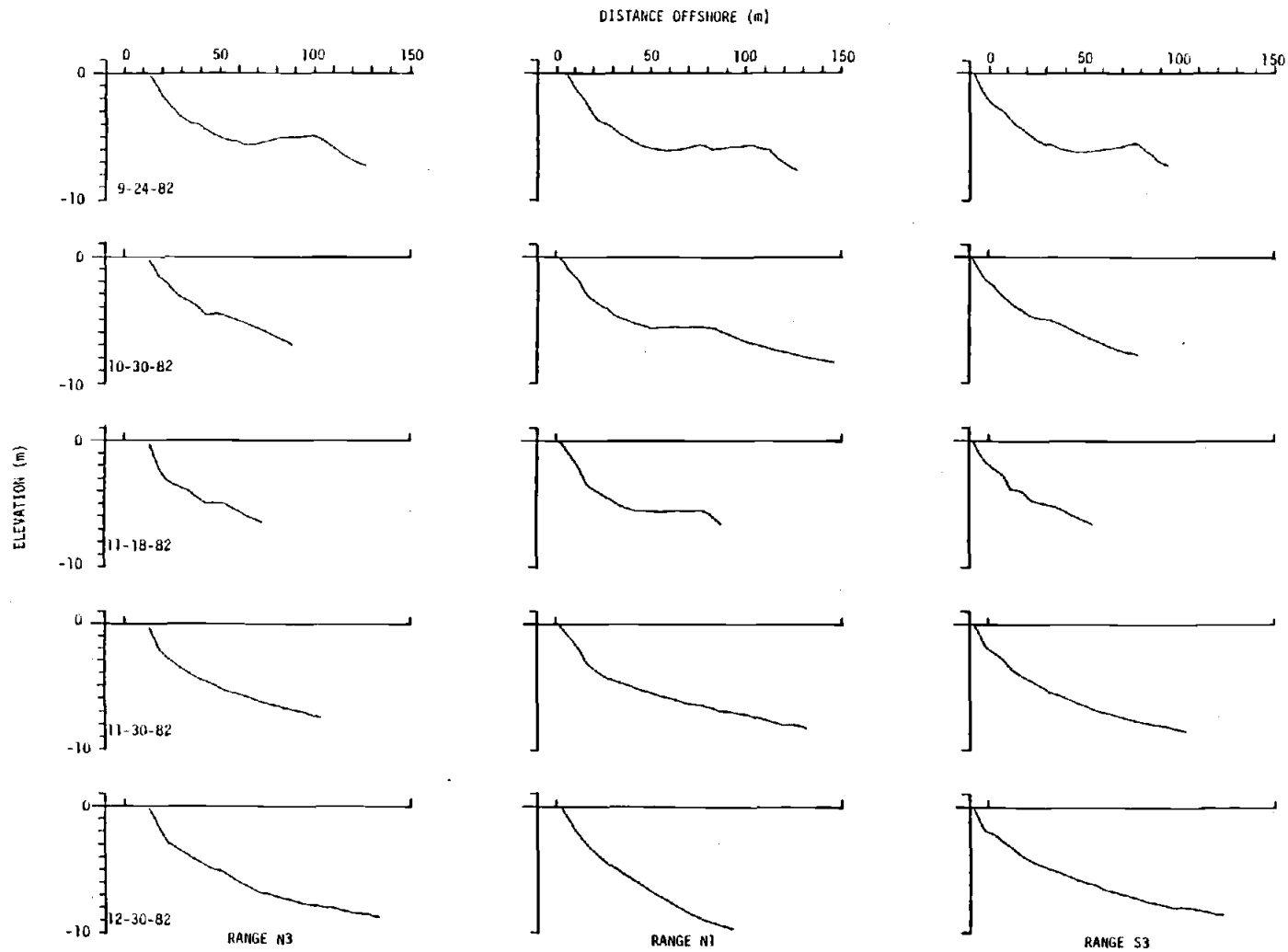


Figure 16.

storms and the associated high wave energies occurred for the first time in mid-December (Figure 17).

### Beach Topography: Qualitative Analyses

A brief summary of field observations is appropriate before entering into the discussion of the quantitative analyses. Table 6 lists brief descriptions of the observed topography for each excursion. The overall topography appears to change from rhythmic and cusped in the fall and early winter to generally straight through the middle of the winter. The transition was accompanied by temporary development of a smaller scale, approximately 200 m, rhythmicity. In late February welded bars and their associated rhythmic topography developed leading to a return to the generally rhythmic and cusped shoreline, similar to that observed the previous fall. Even the locations of embayments and cusps correspond from fall to spring.

Overall, Siletz would be considered to have a high-energy dissipative beach/inshore system. Wright and Short (1983) distinguish their reflective and dissipative beach configurations by a dimensionless surf-scaling parameter,  $\epsilon$ ,

$$\epsilon = \frac{a_b \omega^2}{g \tan^2 \beta} \quad (\text{eqn.9})$$

where  $a_b$  is breaker amplitude,  $\omega$  is incident wave radian frequency ( $2\pi/T$ , where  $T$  is period),  $g$  is acceleration of gravity and  $\beta$  is

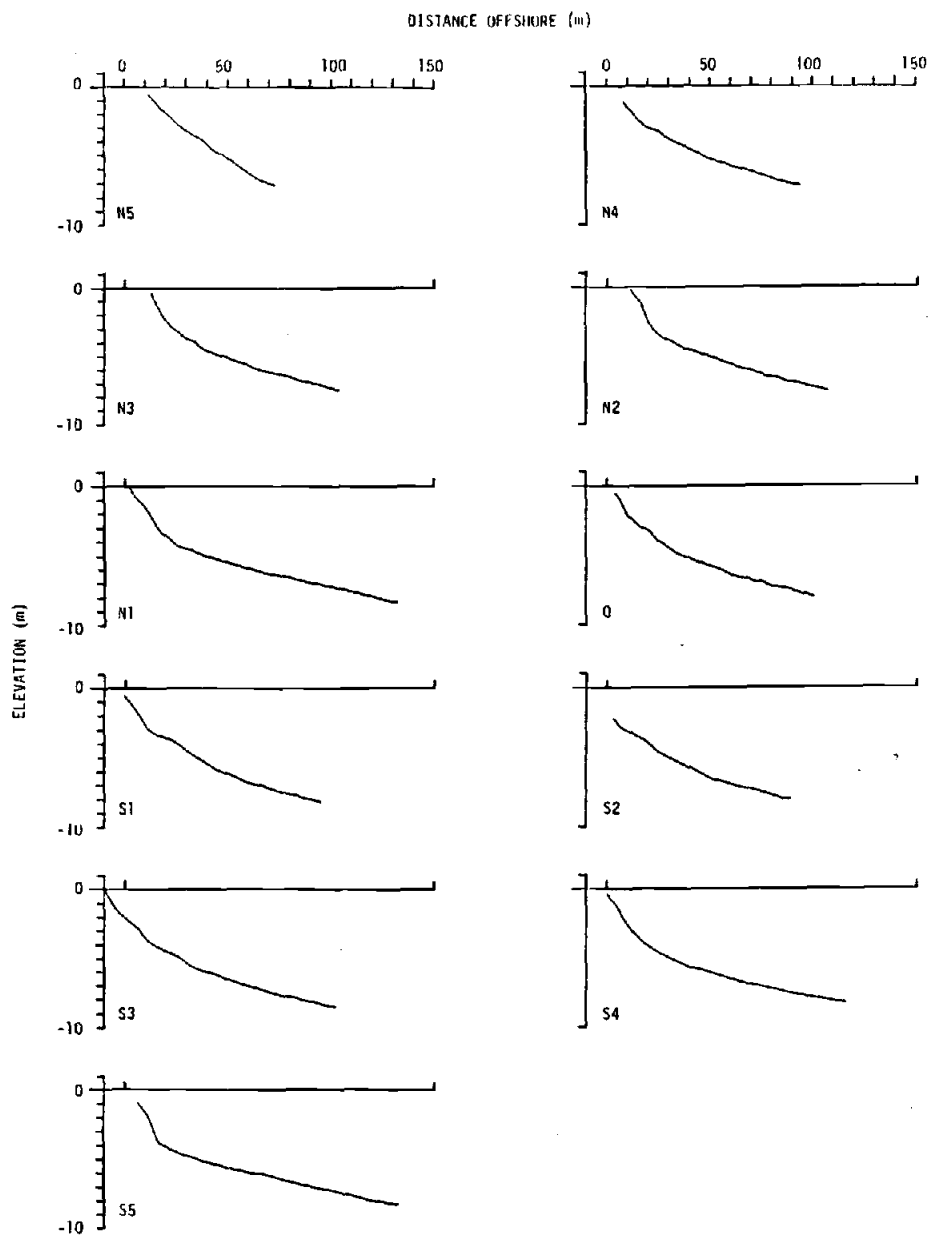


Figure 17. Beach profiles taken November 30, 1982. Note that there was little alongshore variation in profiles by the time the first large winter storms occurred in mid-December.

DATE	NUMBER	OBSERVED TOPOGRAPHY
24 SEPT 82	04	embayments at s2 and n1 cusp at 00
16 OCT 82	05	embayment between s2 and s3 cusp 80m south of s5 and at n2 straight north of n5
30 OCT 82	06	embayment between s2 and s3 and north of n5 cusp 40m south of s5 and at n2
16 NOV 82	07	embayments at s2 and n1 cusps at s5 and a small one at s1 cusp/welded bar attachment at n3, bar points south
18 NOV 82	08	embayments at s1 and just north of n5 cusps 20m south of s5 and between n1 and n2
30 NOV 82	09	embayment at n3 cusps 20m south of s5 and between n2 and n3 straight north of n5
8 DEC 82	10	embayment at s2 small embayments at n1 and north of n5 cusps 20m south of s5 and at 00 small cusp at n2
15 DEC 82	11	appeared straight but very high water
21 DEC 81	12	embayments south of s5, at 00 and north of n5 cusps at s4 and n2(low amplitude)
30 DEC 82	13	embayments at s4, s1 and between n1 and n2 cusps at s5, s2 and n4 actually very complex welded bar topography
13 JAN 83	14	small embayments s5 and between s3 and s4 straight in the northern part of the site
26 JAN 83	15	pretty straight
27 JAN 83	16	small embayment north of n5 small cusp at n3 pretty straight overall
12 FEB 83	17	rip occupied embayment north of n5, scarp on dune small embayment at s4
26 FEB 83	18	large embayments at s5 and between n4 and n5 welded bar attachments south of s5 and at 00 bars point north gravel lag deposits in embayments

TABLE 6. Field observation of beach topography for each excursion.  
These observations tend to be dominated by the topography of the seawardmost exposed beach.

13 MAR 83	19	embayments south of s5 at n1 and 150m north of n5 cusps at s2 and n4
27 MAR 83	20	embayments at s4, 00 and n3 welded bar attachments s2, n1 and n5 bars point north
12 APR 83	21	small embayment at n1 small amplitude cusps at s4 and n4 pretty straight overall
28 APR 83	22	
12 MAY 83	23	embayments between s1 and 00 cusps at s5 and n4
28 MAY 83	24	embayments at s4 and between n2 and n3 welded bar attachments at s3 and n5 small lag deposits in embayments
12 JUNE 83	25	embayments between s2 and s1 and between 00 and n1 cusps at s3 and n2 coarse sediment in embayments
27 JUNE 83	26	embayment at s2 cusp at s5

Table 6 (cont.).

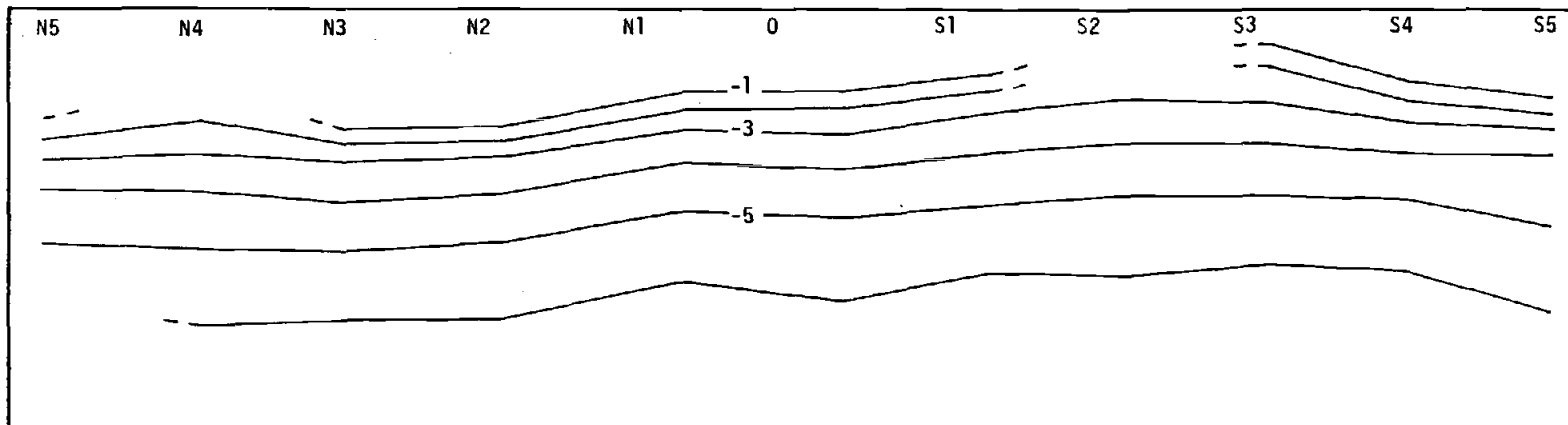
beach or surf zone slope.  $\epsilon$  ranges from 1 to 3 in the reflective configuration and from 30 to well over 100 in the dissipative configuration.  $\epsilon$  values at Siletz ranged from approximately 0.5 to 2 in the late summer, 5 to 75 during the winter, and 75 to 150 during large winter storms. Under the more erosive storm conditions of previous years  $\epsilon$  values of approximately 200 to 250 would be expected.

When field work began the beach at Siletz was similar to Wright and Short's state f or e morphology with a well developed, wide berm and generally reflective beach profile in late summer. During the fall and spring states e and d were most common, though the scale of foreshore and nearshore features was much larger (800-1000 m) than that described by Wright and Short (200-300 m). These morphologies are cusped on the foreshore with shoals opposite the cusps in the nearshore. In state d the shoals resemble welded bars. It is likely that states c, b and a were existent during the winter but there were few opportunities to observe any nearshore topography. The low amplitude rhythmicity observed during the winter and the rip current occupied embayment observed at site N5 in mid-February do not preclude state c, b or a beach configuration. Wright and Short point out that "on strongly embayed and headland-bounded beaches such as those near Sydney, very strong large scale rips frequently accompany the dissipative conditions that occur during storms." It will be shown that unlike the beaches studied by Wright and Short there is no evidence that rip or embayment spacing decreases with decreasing wave energy in the Siletz system.

In trying to relate the field observations to the statistical analyses about to be discussed, it should be kept in mind that the data sets used are limited by the minimum profile length in the set. Therefore, the quantitative analyses often fail to correspond to the observed field conditions. That these analyses are in fact correct can be confirmed by examining the topographic maps produced for each complete survey (appendix 4) . The difference is that whereas the quantitative analyses evaluate the backshore region, where change occurs relatively slowly, the field notes pertain more to the foreshore area where topographic change occurs relatively more rapidly. As a result the foreshore and backshore beach morphologies do not always correspond.

#### Beach Topography: Statistical Analyses

The mean beach topography, as represented by the average of the eighteen complete surveys from September 24, 1982 to June 27, 1983, is shown in figure 18. All elevations are relative to the corner of a house porch located at the landward extent of range S1. A cusate feature is present in the northern part of the area with its horn extending from range N2 to N4. An embayment is located to the south with its maximum landward extent between ranges S1 and S4. The northern extreme of the study site, range N5, is located on the north side of a cusp while the southern extreme, range S5, is located on the south side of an embayment. In an alongshore rhythmic pattern these two sites are topographically equivalent and suggest a lengthscale of 800-850 m. Mean beach topographies for the fall/



N ←

75 m  
 contour interval 1 m  
 offshore exaggeration 2x

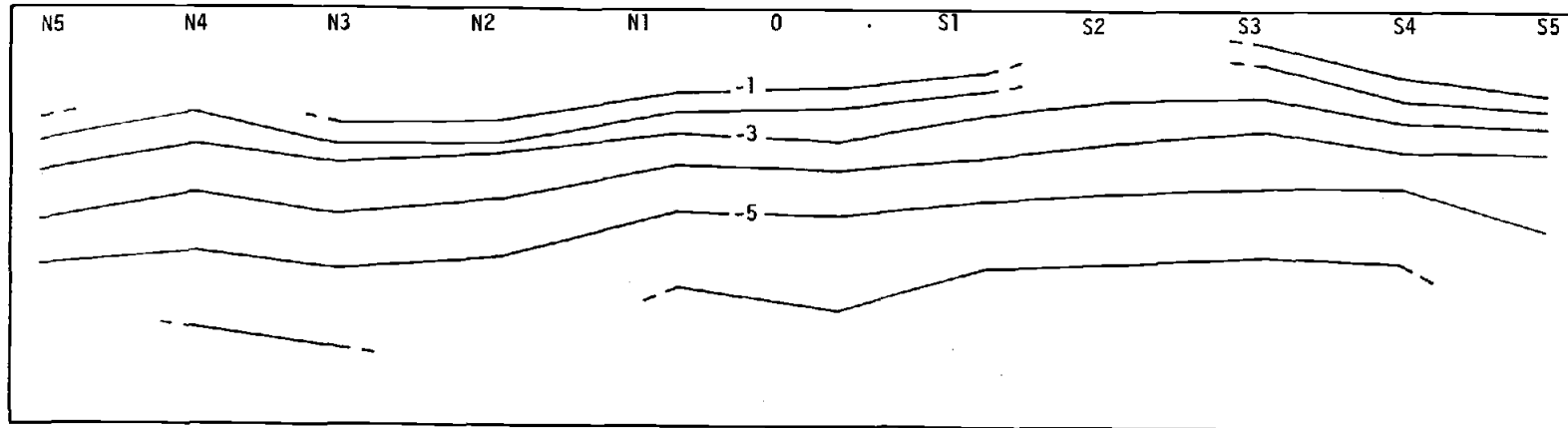
Figure 18. Mean beach topography calculated from all 18 complete profile sets. Note the cusplate feature in the northern part of the site and the embayed area to the south. Values are in meters, relative to a local datum.

early-winter (September to early January), winter (early January to mid-March) and spring (mid-March to June) are shown in figure 19. Each map shows the presence of a rhythmic shoreline in which the northern and southernmost ranges are topographically equivalent, suggesting a longshore wavelength of 800-850 m. The amplitude of this pattern varies considerably, being quite large in the fall/early-winter, very small in the winter and intermediate the following spring. All three shorelines are roughly sinusoidal, though more rectangular, or less peaked, than a true sinusoid. Furthermore, the embayment appears broader on the fall/early-winter map than on the spring map. Examination of the topographic maps produced for each excursion (appendix 4) suggests this is due to the migration of topographic features during the fall. Steady northward migration of the embayment can be observed from range S4 on October 30 to range N1 on December 21, documenting a migration rate of 400 m in 50 days during this time.

For each survey station the standard deviation in elevation was calculated and the results are plotted and contoured in figures 20 and 21. Figure 20 shows the values calculated for all eighteen surveys. Standard deviations generally increase in the offshore direction but also show variations alongshore. The values are largest in ranges N5, 0 and S5, midway between horns and embayments. In this topographic location a small shift in longshore position of the rhythmic features would produce a large change in sediment volume and hence elevations. This longshore variation of standard deviations supports the lengthscale estimate of 800-850 m and some alongshore migration of rhythmicity during the time of observation.

Figure 19. Mean beach topographies for the fall/early-winter (a), winter (b), and spring (c). Note the decrease in rhythmicity amplitude from fall to winter and the increase from winter to spring.

a) FALL / EARLY-WINTER

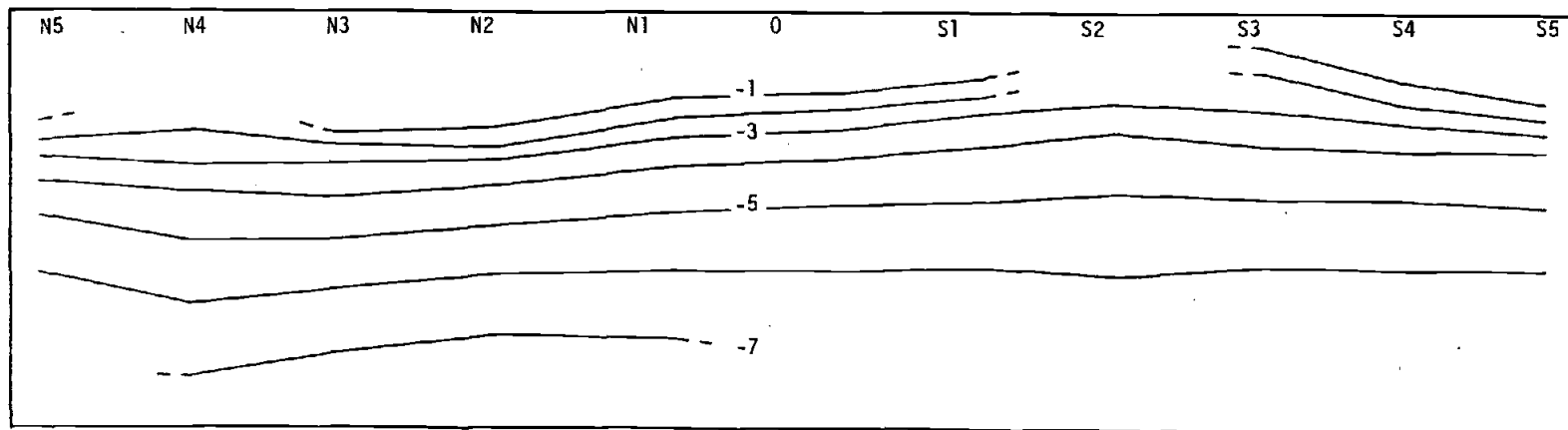


N ←

75 m

contour interval 1 m  
offshore exaggeration 2x

b) WINTER



N ←

75 m

contour interval 1 m  
offshore exaggeration 2x

Figure 19.

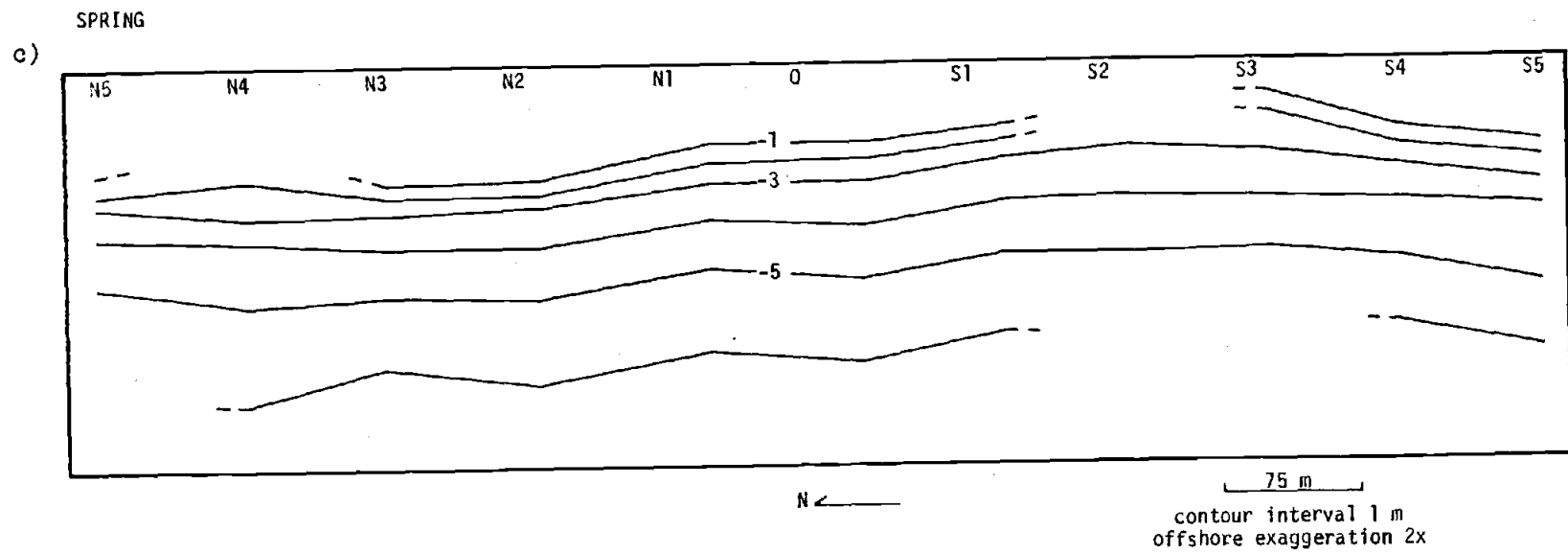


Figure 19 (cont.).

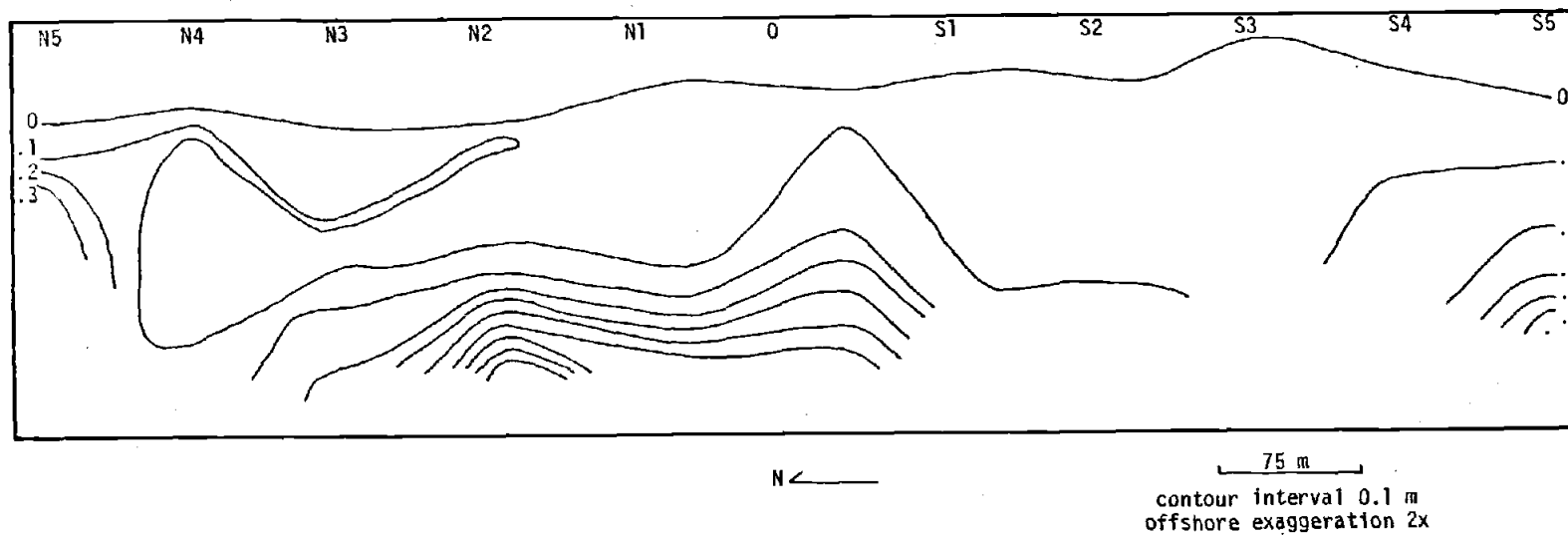
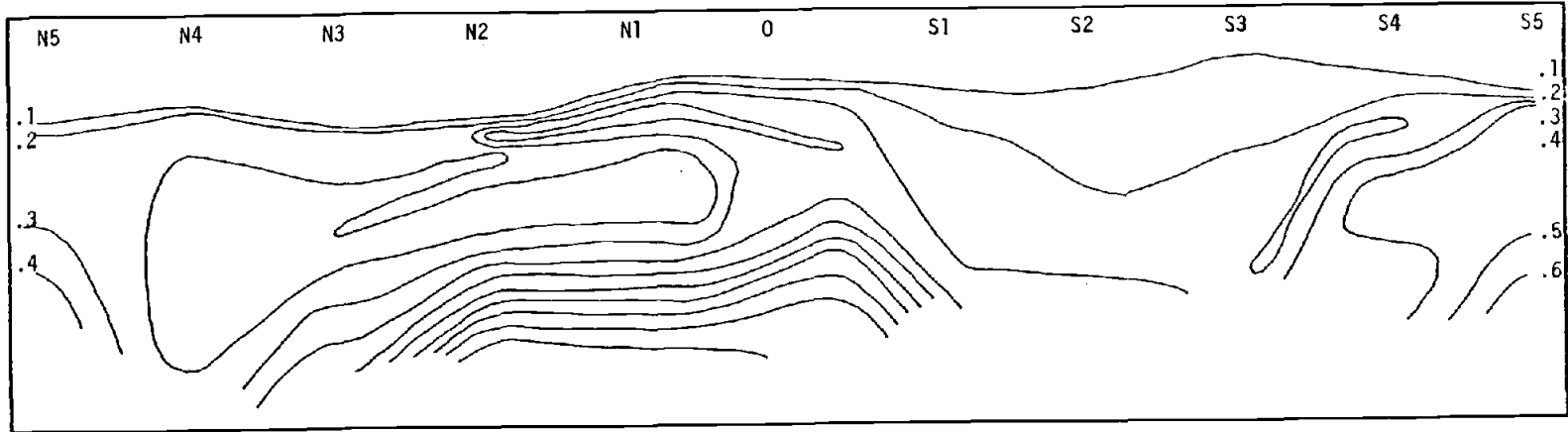


Figure 20. Standard deviation in beach elevations calculated from all 18 complete profile sets. Note the alongshore variation in values, particularly the large values associated with ranges N5, 0 and S5.

Figure 21. Standard deviation in beach elevations for the fall/early-winter (a), winter (b), and spring (c). Large values at ranges N2, N1 and 0 in the fall reflect migration of the embayment.

FALL / EARLY-WINTER

a)



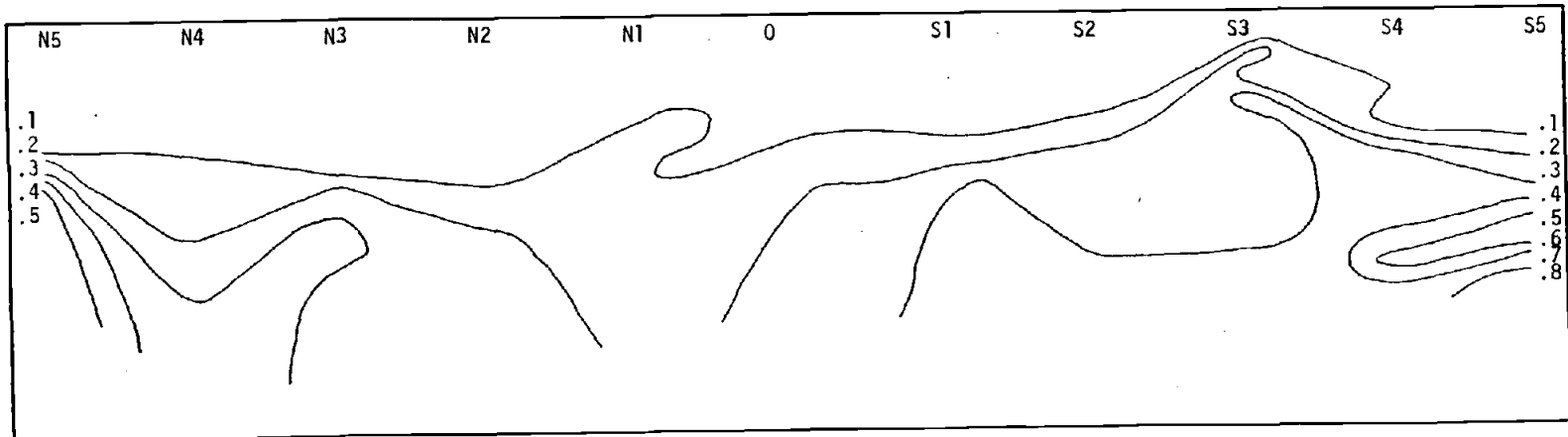
N ←

75 m

contour interval 0.1 m  
offshore exaggeration 2x

WINTER

b)



N ←

75 m

contour interval 0.1 m  
offshore exaggeration 2x

Figure 21.

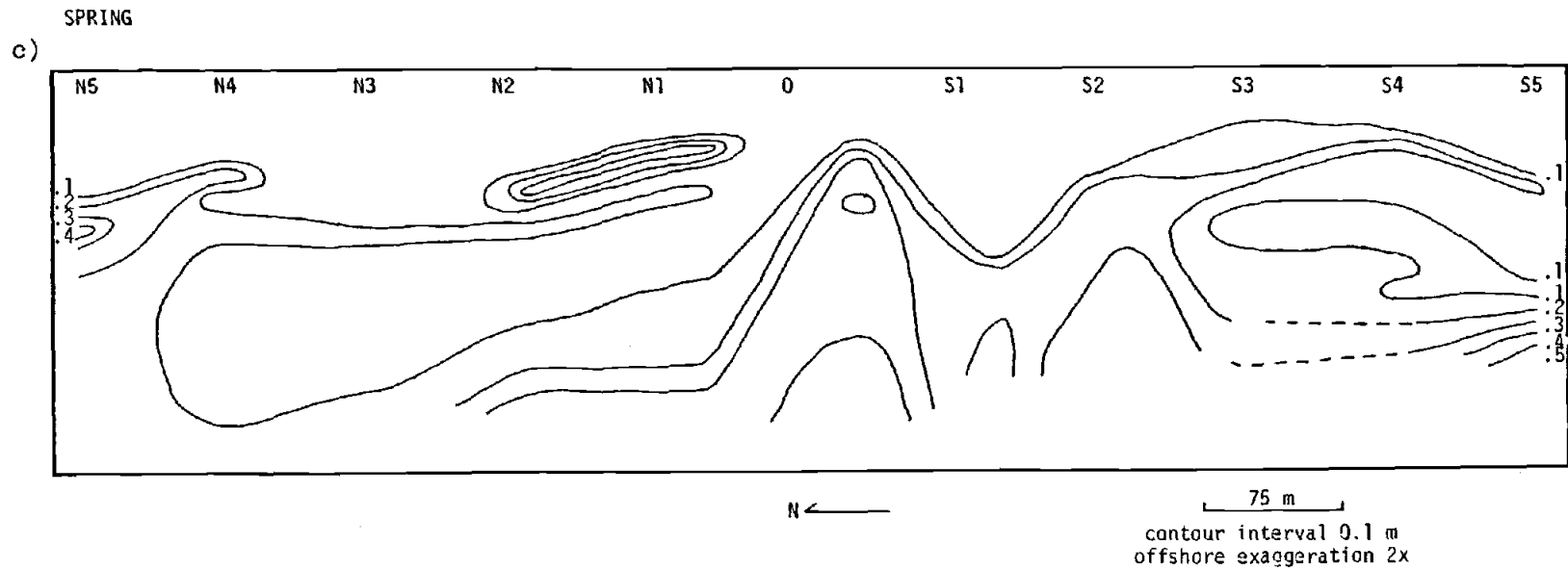


Figure 21 (cont.).

Figure 21 shows the standard deviations in elevation for each of the three seasons. The same pattern is observed in the fall/early-winter and spring as that previously discussed. Large standard deviation values on the seawardmost portions of ranges N2, N1 and 0 during the fall reflect the northward migration of the embayment. Large values are more restricted, found only on range 0, in the spring when no longshore migration was observed. The winter map shows no interpretable pattern, but given the small amplitude of the winter shoreline rhythmicity this should not be surprising. The large values on range N5 are a result of the rip-occupied embayment at that site in early February which eroded through the beach and began eroding the dunes.

It can be concluded that the fall 1982 and spring 1983 beaches were quite similar. During both of these times the shoreline was rhythmic and was roughly sinusoidal in shape with a wavelength of 800-850 m. Longshore migration of this pattern was documented. As Rea (1975) also documented northward migration of beach topography from February 1 through March 1974, longshore migration of rhythmic topography would not seem to be uncommon.

Linear regression was used to further delineate the relationship between mean elevation and variations about that elevation. The hypothesis that the standard deviation in elevation at a station should be a function of the mean elevation of that station seems reasonable for the beach environment. Such a functional relationship would mean that frequency and duration of direct contact with the ocean is the primary variable in determining deposition and erosion of sediment. The result of linear regression

on a data set of all mean station elevations and their standard deviations is shown in figure 22. It reveals that only 28% of the variation in elevation is explained by mean elevation. No relationship other than a linear one is suggested for these variables by the distribution of data points on the plot. This low correlation suggests more complex nearshore sediment transport processes than initially hypothesized. Evaluations of this relationship for individual profile ranges is summarized in figure 23. On ranges N3 (the average cusp position), and S1 and S2 (the average embayment position), more than 75% of the variation in elevation can be accounted for by a station's mean elevation. At longshore locations N2, N1 and S5 less than 65% of the variation is explained by a linear relationship between the two variables. These longshore variations in the hypothesized relationship would suggest that at certain longshore locations some variable(s) other than mean elevation (or frequency and duration of direct contact with the ocean) is important. The additional parameter(s) must have a longshore, rhythmic variation in importance, with approximately a 400 meter wavelength.

If the shoreline approximates a sinusoid, nodes of the topographic waveform are much more sensitive than the antinodes (cusps and embayments) to small ( $< 1/2$  wavelength) longshore migration of rhythmic topography. At nodes a small longshore migration of features would result in a large change in sediment volume and hence, a lesser percentage of variance would be explained by elevation. This explanation is consistent with the results of analyses of the topographic data. The important parameter not

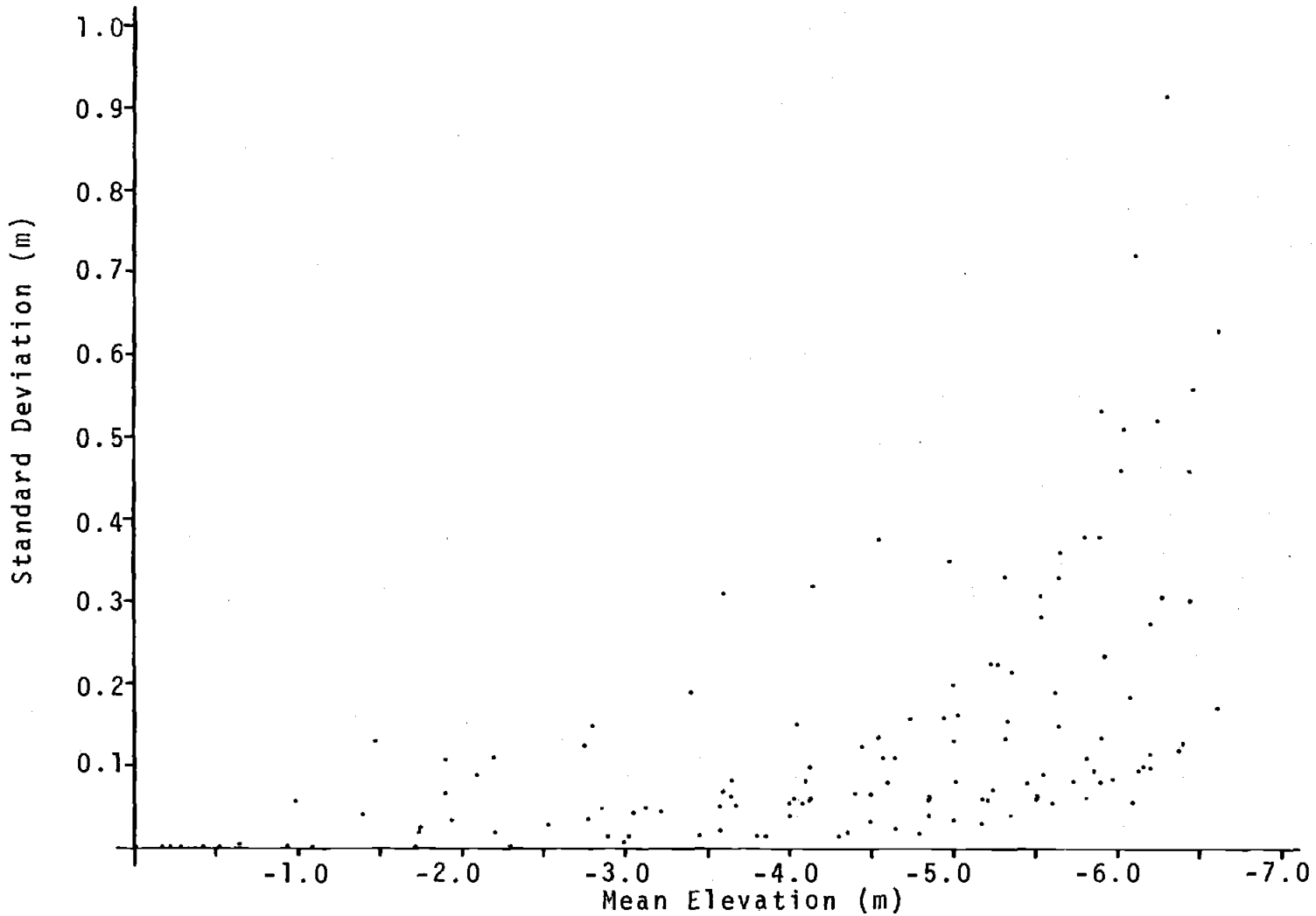


Figure 22. Mean station elevations versus their standard deviations in elevation. Only 28% of the variation in elevation is explained by a linear relationship to mean elevation.

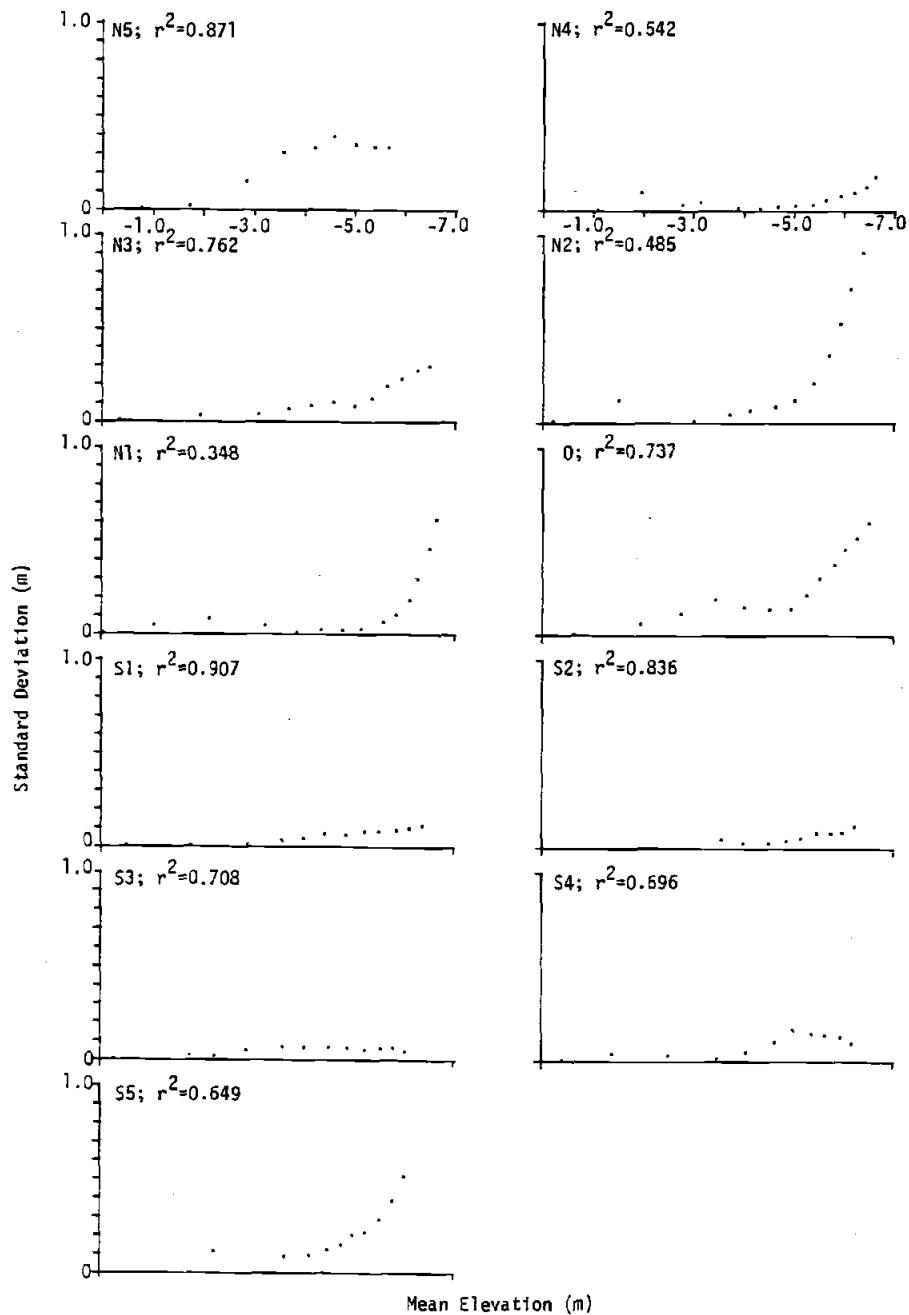


Figure 23. Mean station elevations versus their standard deviations in elevation for each profile range.

considered in the linear regression seems to be the longshore position relative to the longshore rhythmic pattern.

#### Beach Topography: R-mode Analyses

It is particularly useful to develop a parameter or parameters which represent important characteristics of shoreline morphology. Such parameters would enable one to quantitatively evaluate the role of waves, winds, currents or other such forces on the development or modification of beach topography. R-mode factor analysis is a mathematical evaluation of the associations among variables in a data matrix for the purpose of simplifying the original data. The simplification consists of reducing the number of variables which need to be considered. New variables, or factors, are created by the combination of interdependent and hence redundant variables in such a way that the total variance exhibited by the original variables is still accounted for. In this study variables are expected to be interdependent because they represent topographic locations and hence respond to the same dominant forces or processes, though apparently to different extents. R-mode analysis of the profile data was pursued extensively because the factors may describe characteristic shoreline morphologies. Explanations of the details of R-mode analysis can be found in most texts considering mathematical analyses of multivariate data (ex. Davis, 1973). The approach will be briefly outlined here.

Consider an original data matrix,  $D$ , with dimensions  $n \times m$ , that is, it contains  $n$  rows ( $n=1, j$ ), or samples, and  $m$  columns

( $m=1,i$ ), or variables. First, the covariance or correlation matrix for the data is calculated,

$$C=(1/(n-1))[D-JD/n]^T[D-JD/n] \quad (\text{eqn.10})$$

where  $J$  is an  $n \times n$  matrix containing all 1's and  $T$  indicates the transpose.  $C$  is the covariance matrix. It is a square and symmetrical,  $m \times m$ , matrix and as such it has  $m$  eigenvalues,  $\Lambda_i$ , and  $m$  orthogonal eigenvectors,  $e_i$ . The sum of the eigenvalues,  $\sum_{(m=1,i)} \Lambda_i$ , equals the total variance in the original data, and the quotient of an eigenvalue and the total variance expresses how much of the total variance is explained by that eigenvector. The eigenvectors are called factors and have  $m$  elements,  $e_{ij}$ , that are frequently referred to as loadings. For each vector  $n$  linear equations can be written in which the loadings represent coefficients of their corresponding elements of the original data matrix. Each set of  $n$  equations can be solved for  $n$  values, referred to as scores,  $y_{ij}$ , which indicate the similarity between the eigenvector from which it was calculated and the original data sample (row). The weighting of each factor's importance for a specific sample is given by,

$$y_{ij} (\Lambda_i)^{-1/2} \quad (\text{eqn.11}).$$

The output of most R-mode analyses consists of a list of the factors, or eigenvectors, ranked by the amount of variance they account for in the original data set, their associated eigenvalues, and a list of scores for each of the factors. Usually only a few factors are

needed to explain most (90-100%) of the variance in the data set, vastly simplifying matters.

This technique can be applied to the analysis of beach profile data if one envisions a matrix of topographic data from the study site with a column representing each of the eleven profile ranges. R-mode analysis of this matrix will produce eleven or fewer factors (eigenvectors), each with 11 elements, which can account for all of the variance in the data. Each factor will represent an alongshore topographic pattern or morphology. The hope is that most of the variance in the dataset will be accounted for by several dominant morphologies which may be associated with known or hypothesized nearshore processes.

In deciding to do such an analysis the question remained as to what the actual elements of the data matrix should be. A number of possibilities were tried and evaluated for each survey individually with the specific goal of better understanding the nature of shoreline rhythmicity at the field site. The results were evaluated by plotting the two most dominant factors for each matrix and subjectively determining whether one or both of them had patterns clearly related to the longshore rhythmicity documented on the topographic map for that survey. As noted in the previous paragraph the variables in all of the matrices evaluated represented longshore position. Several different types of samples were evaluated and discarded. These included: 1) elevations at different offshore distances; 2) local beach slope at different offshore distances; and 3) local alongshore beach slopes at different offshore distances.

An inverse approach of using the offshore distance to particular topographic contours proved highly successful. R-mode analysis of these matrices consistently produce single factors which explain 90-100% of the variance in the data and which record the longshore rhythmicity shown in the seaward-most portion of that survey's topographic map. Figure 24 shows plots of the first R-mode factor and the seawardmost available topographic contour for each of the eighteen surveys. The greater similarity of the first factor to the seaward-most contour than to other contours is a result of the seawardmost elements of the data matrix having the largest magnitude values.

The above approach shows offshore distance to different contours to provide a good descriptor of apparent rhythmicity for a particular profile data set. The success of these analyses suggests the use of cross-shore position to a particular contour as a function of time to study the variability of rhythmicity through the 18 separate surveys. If the changes in beach morphology through time are relatively simple then the mean contour calculated from such a matrix should describe a reasonable longshore topography and R-mode analysis of such a matrix should produce one or two meaningful factors to account for most of the variance.

One's understanding of the results of this analysis on the Siletz Spit data set is enhanced by first examining results of this analysis on hypothetical data matrices representative of ideal beach topographies. The first and simplest case is that of a straight beach extending different distances offshore at different times (accreting and eroding). The mean contour is straight and R-mode

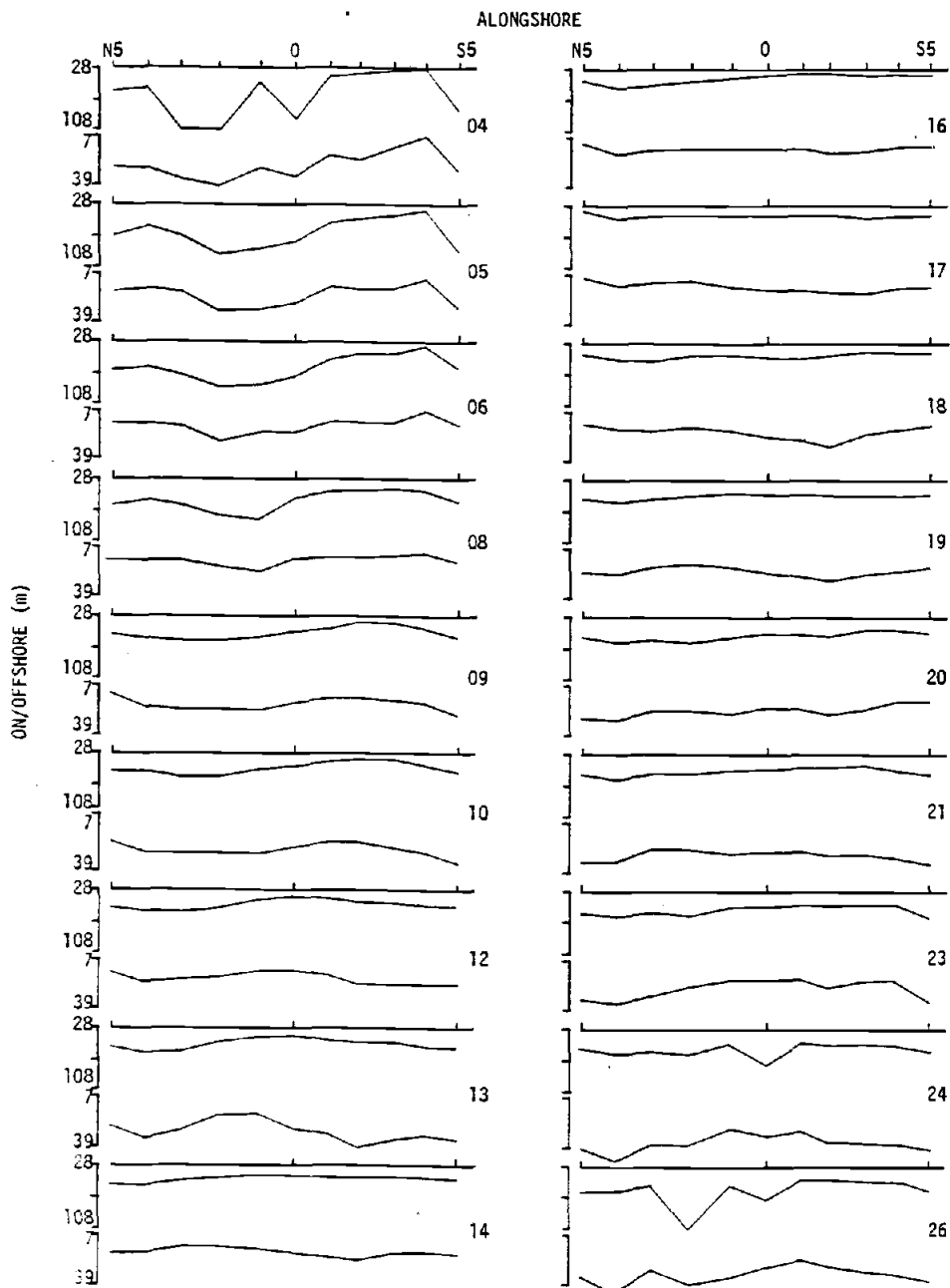


Figure 24. The seawardmost available topographic contours (top) and the first R-mode factors (bottom) for each of the 18 surveys.

analysis determines a single dominant factor. This factor is straight alongshore and the factor scores indicate the amount of accretion (positive scores) or erosion (negative scores) about the mean contour location. An additional factor is present in this and all the following cases, though it accounts for at most only a few percent of the variance. This factor represents noise in the data.

A more interesting case for the study of longshore rhythmicity is that of a cusped shoreline exhibiting sinusoidal topographic contours. One can imagine a number of changes such a shoreline may experience including variations in amplitude and longshore phase, as well as combinations of these with general erosion and accretion. If the sinusoidal pattern remains stable in the longshore but varies in amplitude the analysis produces a sinusoidal mean and a single sinusoidal factor 180 degrees out of phase with the mean, figure 25a. The factor scores describe 'how much' of the factor must be added to (positive scores) or subtracted (negative scores) from the mean to regain the original data. In this simple beach environment the factor scores can be used directly to describe the amplitude of the rhythmicity present at the time of each survey.

Results from a rhythmic shoreline exhibiting changes in both on/offshore position and amplitude through time is just a combination of the above cases. There is a sinusoidal mean and there are two dominant factors, figure 25b, one representing variations in amplitude, the other representing erosion or accretion. The percentage of variance explained by each of these factors depends on

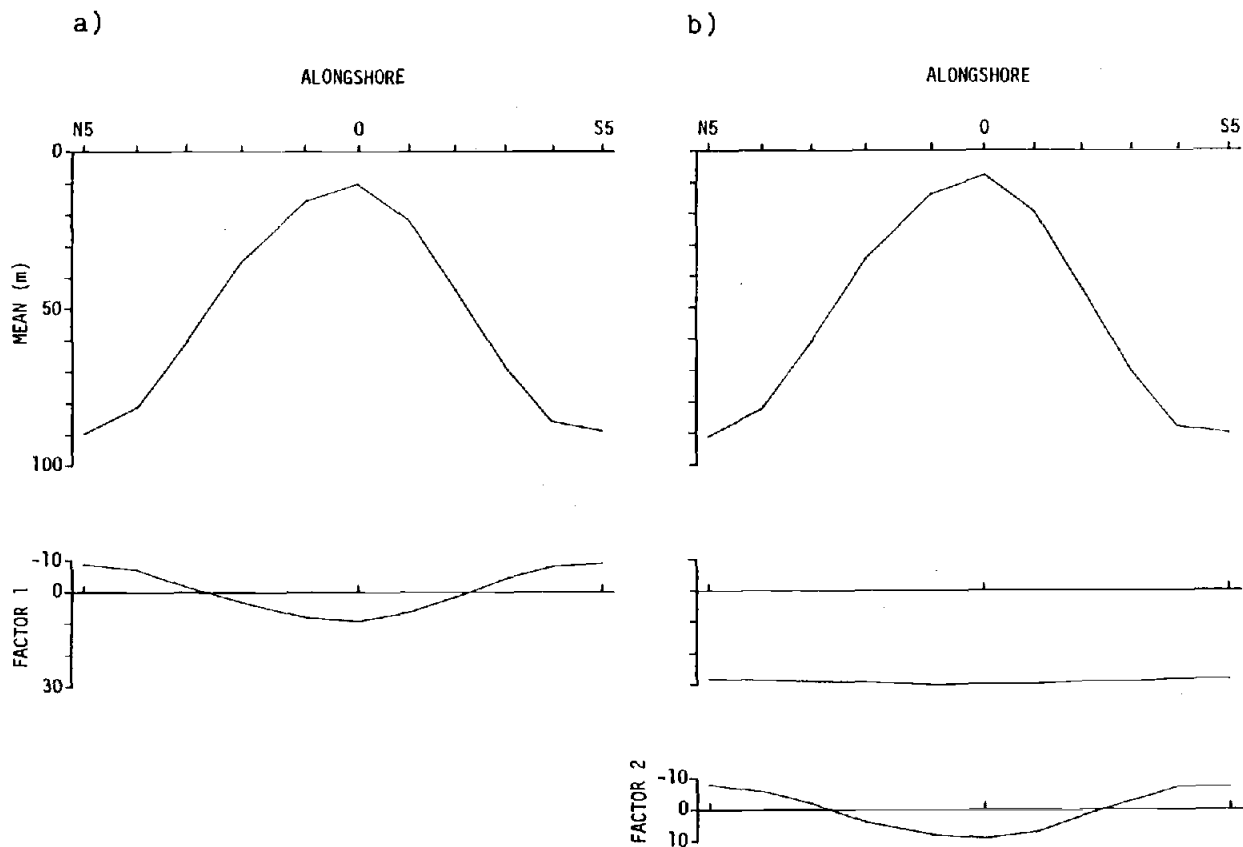


Figure 25. a) Mean contour and first R-mode factor of data depicting a stable longshore rhythmic pattern with amplitude variations; b) Mean contour and first and second R-mode factors of data depicting a stable longshore pattern with amplitude variations and overall on/offshore movement.

the relative magnitudes of amplitude variation and change in on/offshore position.

The previously discussed analyses of the study site suggest that a still more realistic hypothetical set of circumstances would include longshore migration, or phase shifting, of the sinusoidal contours. Three cases will be explored using random phase variations within 90, 180, 360 degrees ( $1/4$ ,  $1/2$  and full wavelength, respectively) envelopes. One hundred synthetic contour lines were generated in each case. No on/offshore migration of the beach is included in the analyses discussed here, though inclusion of this signal would not alter the basic results.

The mean contour and the first and second factors calculated by the R-mode analysis for the 90 degree, 180 degree and 360 degree phase variation cases are shown in figures 26a,b and c respectively. Any apparent distortion of the mean contour from a perfect sinusoid is largely a result of the fact that the wavelength is not an even multiple of the spacing between variables. It can be noted that the amplitude of the mean decreases with increasing phase shift envelope. Factors 1 and 2 are sinusoidal and exactly 90 degrees out of phase in all instances. They are also out of phase with the mean by approximately 25 and 205 degrees. This phase offset from the mean is what accounts for the longshore phase shifting in the data. As phase variations in the data increase the second factor becomes increasingly important. The relative importance of the first and second factors is not sensitive to the amount of amplitude variation in the data for phase shifts of less than about 300 degrees. For example, consider a case with a mean amplitude of 40 m. The cases

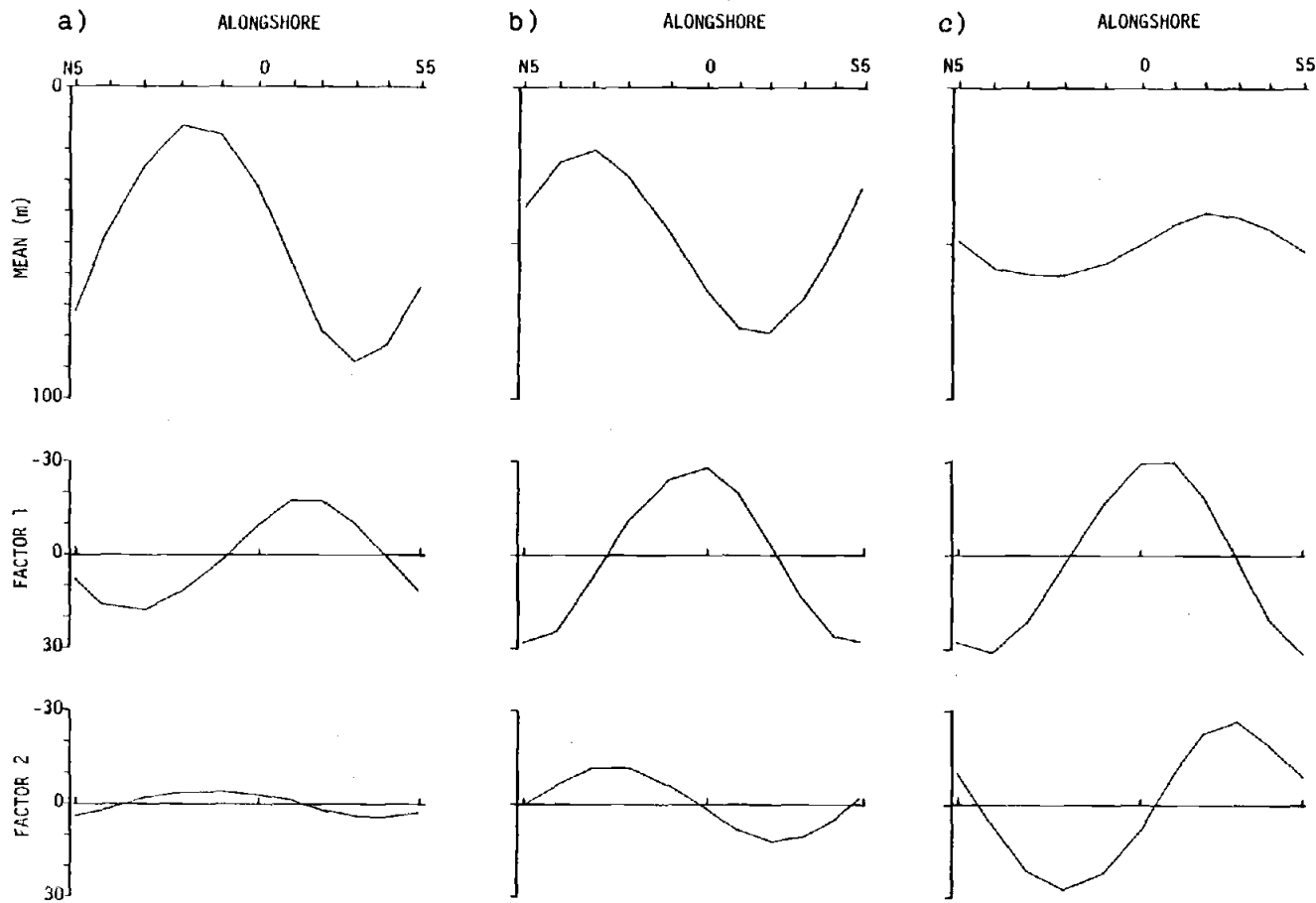


Figure 26. Mean contours and first and second R-mode factors for data depicting a longshore rhythmic pattern with amplitude variations and, a) 90 degree phase shifting; b) 180 degree phase shifting and c) 360 degree phase shifting.

shown in figures 26a,b and c have an amplitude variation of  $\pm 37.5\%$  and the 90, 180 and 360 degree phase shift examples respectively have factor 2 to factor 1 ratios of percents of variance accounted for of 0.067, 0.138 and 0.587. With zero amplitude variation and 180 degree phase shifting the ratio is 0.149 while with 360 degree phase shifting the ratio is 0.754. With longshore migration of a rhythmic shoreline, factor scores still indicate how much of a factor must be added to the mean to regain the original data. However they now include the longshore location of rhythmic features relative to the mean. When analyzing real data, the meaning of the factor scores must be evaluated subjectively based on the shape of the mean, and dominant factors and the phase relations between them.

Finally, the influence of noise in the data was investigated. For the case of a matrix consisting solely of random noise, the mean contour is a straight line. Factor analysis produces the same number of factors as there are variables, all accounting for approximately equal amounts of variance. The factors themselves look irregular when plotted. In an effort to determine how much noise could be present in a matrix based on a longshore rhythmic beach system and still yield interpretable results, many analyses were run on matrices similar to those just discussed but including amplitude variations, on/offshore variations in beach position and varying amounts of noise. It was determined that noise can hinder interpretation of the mean and factors when it is of the same order of magnitude as the amplitude of the rhythmic signal or larger. In general this condition can be identified by the need for more than two or three factors to account for more than 90% of the variance.

For analysis of the Siletz Spit topographic data, factor analysis was run for seven different elevation contours spaced 0.5 m apart. Plots of the means and first factors are shown in figure 27. All mean contours appear rhythmic with approximately the same lengthscale of 800-850 m. For higher elevation contours, those nearest the dunes, the first factors show lower amplitude rhythmicity and account for less of the total variance in their matrices than do the first factors for contours further offshore. The results of R-mode analysis of the seawardmost data are shown more fully in figure 28. The longshore patterns are more irregular than those of the synthetic analyses, as would be expected in a natural system, but they definitely suggest some characteristics of the shoreline rhythmicity. The mean contour is obviously rhythmic with a longshore wavelength of 800-850 m and an amplitude of approximately 20 m. Two factors account for 83% of the variance in the data suggesting that though there is some noise in the system it is probably much less than the amplitude of the rhythmicity signal. The shapes of the first two factors are reassuringly similar to those determined in analyses of the hypothetical rhythmic shoreline with amplitude variations and phase shifting of the pattern. Factor 1 departs from the expected phase relation with the mean for this model in the southern part of the area. The nature of the departure suggests that phase shifting at this site was possibly accompanied by small changes in the wavelength of the rhythmicity. Factor 2 also departs from the expected phase relation with the mean but it is 90 degrees out of phase with factor 1 for most of its length and this is consistent with the model. The amplitudes of the mean, first factor and second



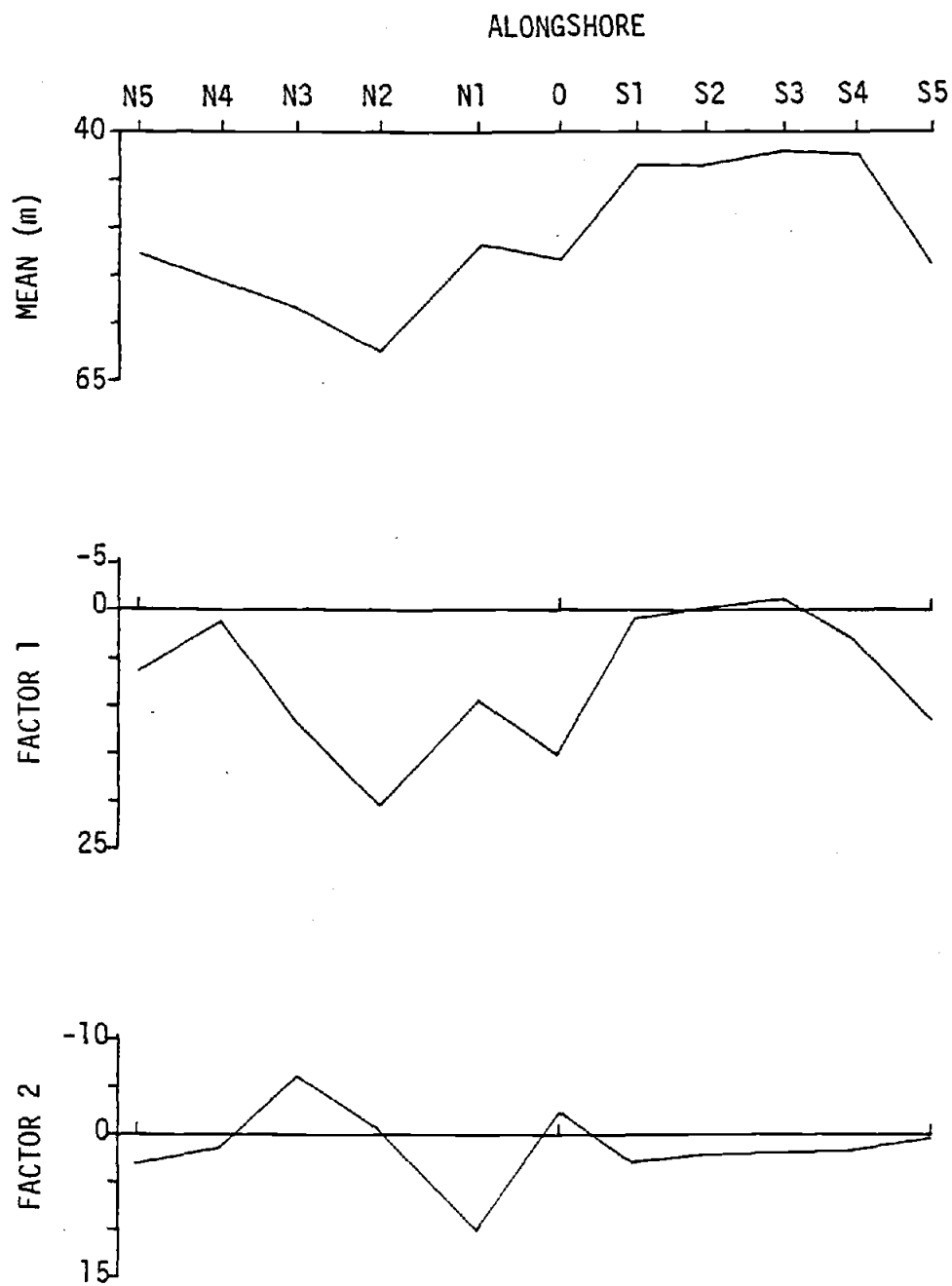


Figure 28. The mean contour and the first and second R-mode factors for the seawardmost contour of the Siletz Spit data set.

factor are 20 m, 25 m, and 15 m respectively. This is very reminiscent of the synthetic data sets with 180 degree phase shifting. The percentages explained by the first two factors from the Siletz data are also similar to this hypothetical case. The ratio of percent explained by factor 2 to that explained by factor 1 de-emphasizes the noise in the natural system. The ratio for the hypothetical example with a 180 degree phase shift is 0.145 and for the Siletz field site is 0.170.

Examination of factor 1 shows it to have a mean of 6.4 m, implying an associated on/offshore movement of the contour. Sites S1, S2, S3 and S4 have values near zero while sites to the north have greater values indicating a greater on/offshore fluctuation in position. Figure 29 shows plots of the sum of the mean contour and the most positively and most negatively weighted first factors in the data set. From these it is concluded that a change from large positive to a large negative first factor scores would describe erosion in the north, a broadening of the embayment in the south and migration of the cusp to the north with a concurrent decrease in amplitude. Though examination of factor 1 alone suggests that it might describe variation in the wavelength of the rhythmicity signal it does not appear to do so within this data set. Factor 2 has a mean near zero and shows most variation in the northern half of the study area. Figure 30 shows plots of the most positively and most negatively weighted second factor in the data set added to the mean contour. A transition from large positive to large negative second factor scores represents a straightening of the beach to the south, a large increase in topographic complexity to the north, and a

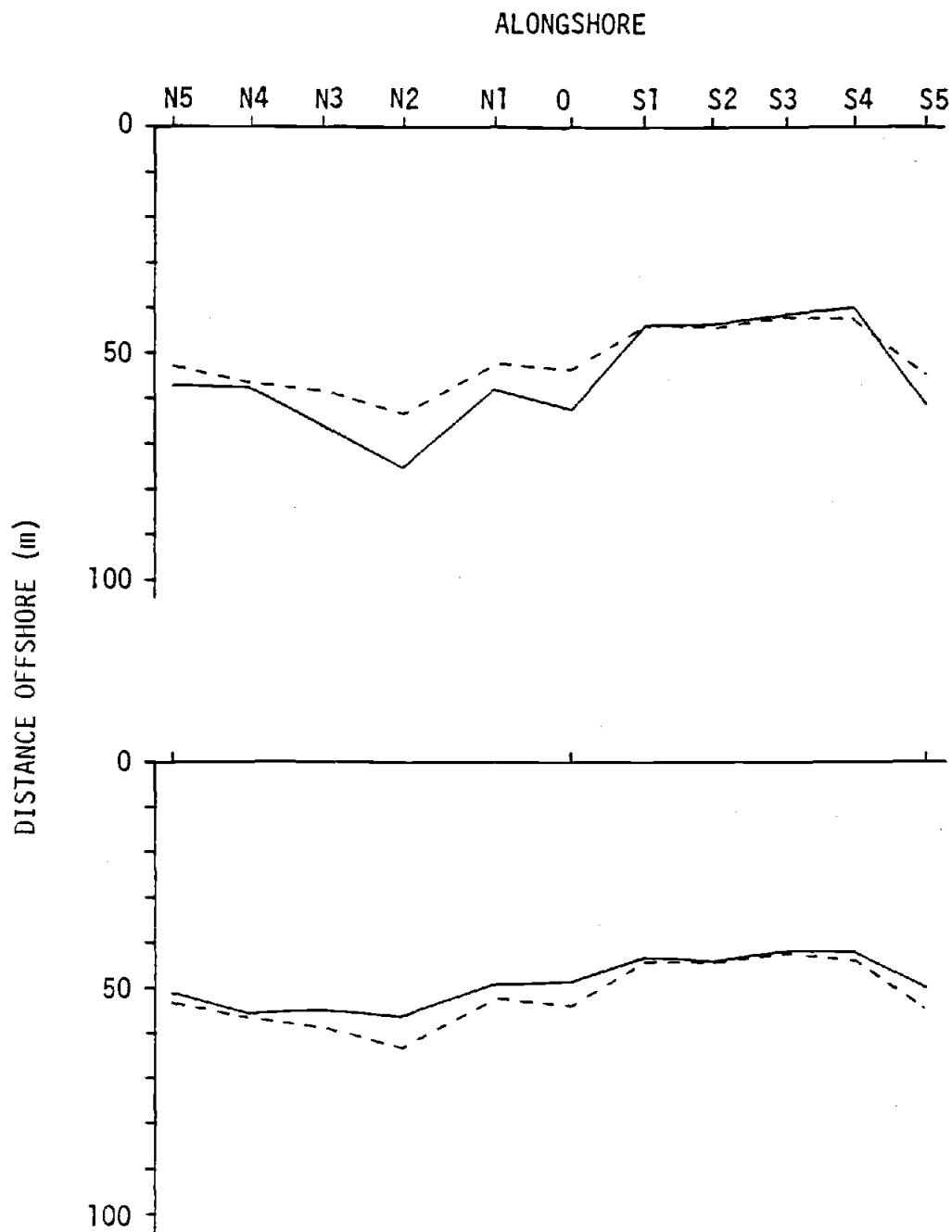


Figure 29. The sum of the mean contour and the most positively weighted (top) and most negatively weighted (bottom) first R-mode factors (solid lines). For reference the mean contour is shown as a dotted line.

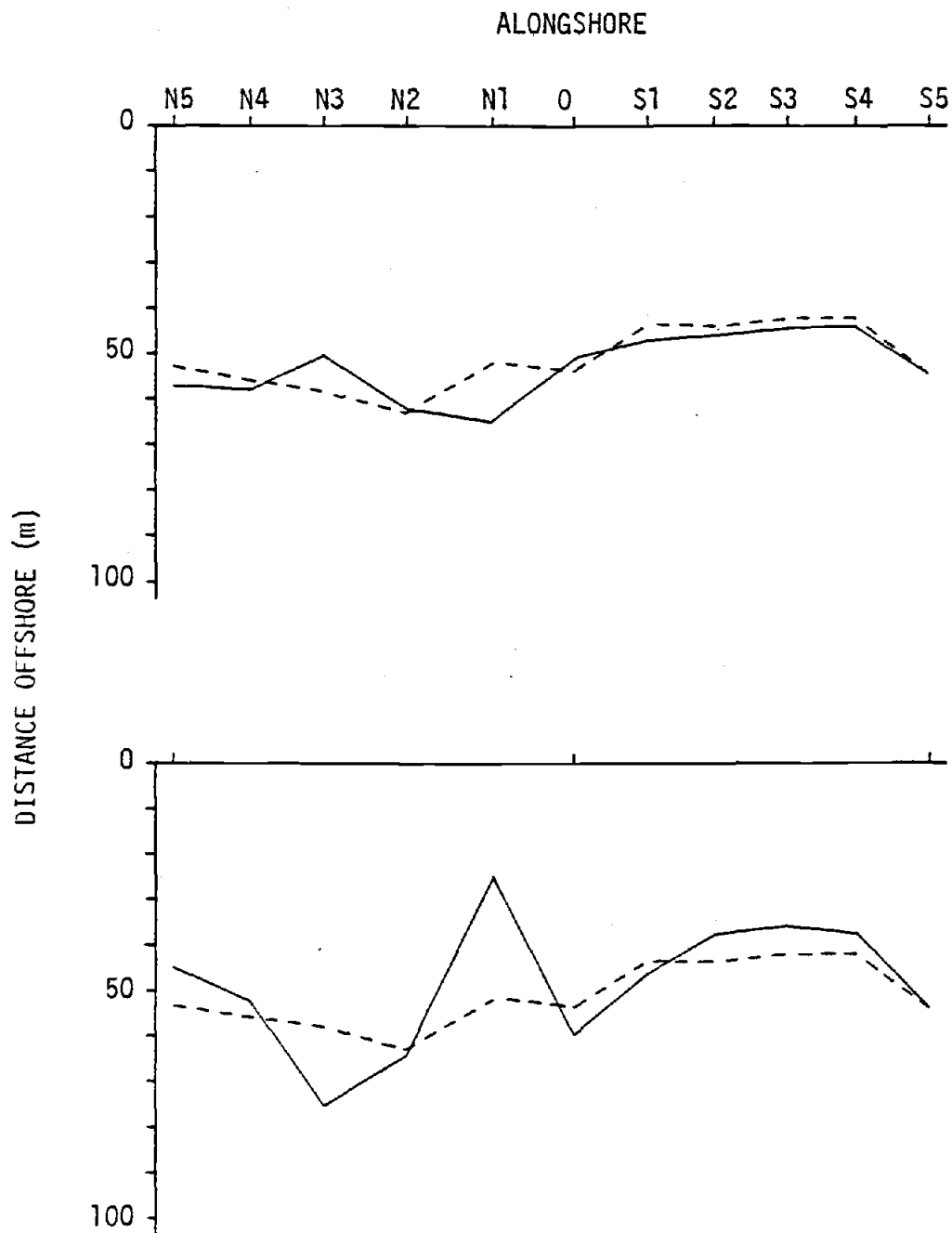


Figure 30. The sum of the mean contour and the most positively weighted (top) and most negatively weighted (bottom) second R-mode factors (solid lines). For reference the mean contour is shown as a dotted line.

concurrent decrease in amplitude and northward migration of the southernmost embayment.

This analysis confirms the visual and survey observations that there are three primary components in the beach variability data. These are general accretion or erosion of the shoreline, amplitude of a dominant 800-850 m wavelength rhythmic pattern and longshore location or phase of the rhythmic pattern through approximately 180 degrees. R-mode factor analysis is useful in verifying the importance of these components as demonstrated here, and in the analyses of the synthetic data. Furthermore, it is capable of separating accretion/erosion and rhythmicity amplitude variations in a simple two component system where these morphologies are independent. Unfortunately, in an interdependent multiple component system or a phase varying sinusoidal system the resulting factors fail to provide a simple separation of the three topographic parameters.

To study relationships between topography and wave and tide conditions it is desirable to try to separate these three signals and express each by a meaningful numerical parameter for each documented topography. On/offshore position and amplitude of rhythmicity can be described by the mean and standard deviation of the distance offshore to a contour at a given time, table 7. One possibility for quantification of longshore position of the signal would be longshore location of extrema. The signal produced by the real data is sufficiently noisy to preclude this approach. For any rhythmic shoreline exhibiting less than about 200 degrees of longshore phase shifting R-mode analysis produces a single factor which describes

EXCURSION	MEAN POSITION OF SHORELINE(m)	RHYTHMICITY AMPLITUDE	LONGSHORE POSITION
04	62.20	30.32	0.5646
05	63.65	19.53	0.9779
06	60.87	17.11	0.9293
08	55.82	13.56	0.7434
09	50.00	8.85	0.3142
10	46.97	7.99	0.1971
12	45.65	6.28	-0.7820
13	47.88	6.59	-1.0810
14	45.49	4.20	-0.8373
16	39.78	6.31	-0.2893
17	40.86	3.06	-0.0866
18	44.33	3.80	0.0899
19	49.83	3.47	-1.2777
20	51.93	5.47	-0.0219
21	49.55	5.46	-0.3168
23	50.89	6.27	-0.0988
24	53.65	8.13	0.3349
26	58.53	17.97	0.6403

TABLE 7. Tabulation of numbers expressing on/offshore position of the shoreline, rhythmicity amplitude and longshore location of rhythmic features for each of the field excursions.

much of the topographic variation. Scores for each excursion then are meaningful numerical descriptors of the overall topography. In this instance if the on/offshore movements of the shoreline and amplitude variation signals can be removed from the data then the first factor calculated by R-mode analysis should describe only the phase shifting, or longshore migration of the rhythmic pattern.

To this end the seawardmost contour data was normalized to the same mean and standard deviation. This normalization results in varying amounts of noise for different excursions, increasing the noise in low amplitude (midwinter) data sets relative to the higher amplitude data sets. Figure 31 shows plots of the mean contour, first, second and third factors from R-mode analysis of the normalized data. The effect of increased noise is that in order to account for 90% of the variance 5 factors are necessary, whereas for the non-normalized data the same amount of variance is explained by only 3 factors. Longshore migration of the rhythmic pattern is described mostly by factor 1. Factors 2 and 3 primarily "fine tune" the shape of the topographic features by narrowing and broadening cusps and embayments.

Comparison of the first factor scores of the normalized data, table 7, to the topographic maps of each excursion, appendix 4, confirms that these scores can be used as quantitative descriptors of longshore position of the rhythmic pattern. Large positive scores describe the fall and spring beaches when an embayment was located in the southernmost part of the field site. Large negative scores describe a number of the winter beaches when the embayment was located in the north central part of the site.

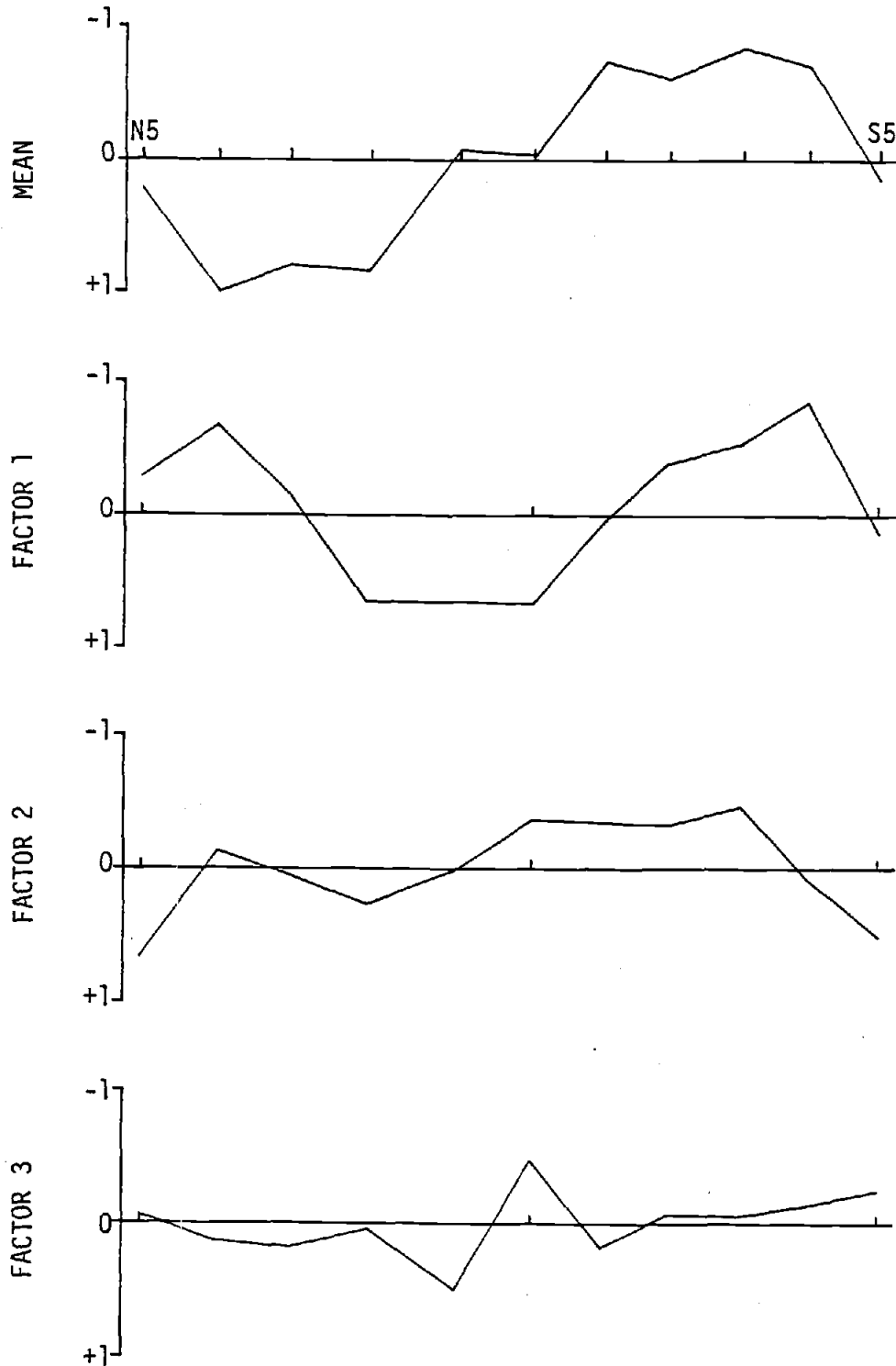


Figure 31. The mean contour and the first, second and third factors from R-mode analysis of the normalized -5.75 m contour matrix

Careful analysis of the topographic data reveals three primary components of topographic change on Siletz Spit and suggests three independent and quantitative parameters to describe them. On/offshore position of the shoreline is best described by the mean distance offshore to a pre-determined contour for each excursion. The amplitude of rhythmic topography is most simply and accurately described by the standard deviation of a contour about its mean offshore distance. The longshore position of rhythmic features is best expressed by the first factor scores calculated by R-mode analysis of the contour data set normalized to the same mean and standard deviation.

#### Beach Topography: Conclusions

In the early fall the beach on Siletz Spit had a wide berm characteristic of swell profiles. With increasing wave energy during the fall, the berm was eroded and before the onset of the first large winter storm all beach profiles resembled the storm profile. However, erosion of the berm occurred at different rates along shore. Calculation of mean beach topography during the first part of the study and during the entire study both show evidence for longshore rhythmicity with a wavelength of 800-850 m. Comparison of these two means suggests longshore migration of the features, an observation confirmed by the individual topographic maps from each survey. This topography apparently migrated 400 m from October 30 to December 21, 1983. The distribution of standard deviations in elevation of each

station supported these conclusions and also showed that the fall and spring beach topographies were very similar.

The relationship between the variation in elevation and the mean elevation at survey stations was evaluated by linear regression. The results demonstrate that only 28% of the variance in elevation was accounted for by the frequency and duration of contact with water. It was further concluded that the amount of variance accounted for fluctuated alongshore; it was high at points about 400 m apart and was low at other points, also about 400 m apart. The nature of the alongshore fluctuations resemble those predicted by longshore migration of a sinusoidal topographic form. Stations on cusps and in embayments experience only a small elevation change when the pattern migrates alongshore. Locations between these positions however, experience greater changes in elevation as a result of large changes in sediment volume.

R-mode analysis of a data matrix of offshore distances to the -5.75 m contour leads to similar conclusions. The variables in this matrix represent longshore position and the samples represent discrete times. The mean contour and first factor both have striking longshore rhythmicity with a wavelength of 800-850 m. Evidence is noted for phase variation within an approximately 180 degree phase envelope, or migration over about 400 m of beach. Careful analysis of the R-mode results demonstrates that there are three primary signals in the topographic data: the on/offshore position of the shoreline, the amplitude of the longshore rhythmicity, and the longshore position of the rhythmic topographic features. However because this is an interdependent three component sinuoidal system,

they do not map onto separate factors. It is concluded that on/offshore position of the shoreline is best described by the mean offshore distance to the seawardmost (-5.75 m) contour and that the rhythmicity amplitude is best described by the standard deviation in offshore distance to the -5.75 m contour. Longshore location of rhythmic features is well described by the first factor scores resulting from R-mode analysis of a matrix in which each row represents the offshore distance to the -5.75 m contour for an excursion and all rows are normalized to the same mean and standard deviation. The variables in this matrix represent longshore position.

Thus it is concluded that during the nine months of field study at this site on Siletz Spit, topographic rhythmicity had a constant wavelength of 800-850 m when it was present. In addition the longshore position of cusped features and embayed areas was not stable but instead migrated over approximately 400 m of beach. The on/offshore position of the shoreline, the amplitude of the rhythmic shoreline topography and the longshore position of the rhythmic pattern can each be described by a single, meaningful number based on simple mathematical analyses of the beach topography.

It is interesting to notice that while analysis of the 1983 photographs does not reveal significant shoreline rhythmicity, analysis of the survey data from that time does show a longshore cusped topography. This is largely a result of the small amplitude of the pattern and the presence of only 1 to 3 cycles during that time. With that small a signal fourier analysis would have little success identifying it.

All analyses of shoreline morphology concur that large scale longshore rhythmicity on Siletz Spit and neighboring beaches has a characteristic length scale of 800-850 m. Thus whenever large scale rhythmic topography can be identified on Siletz Spit it has very nearly the same longshore spacing, though the exact longshore location of topographic features can be expected to vary.

#### Time Lapse Films Of Run-up

Time lapse movies were used to record the run-up for a 35 minute period during high tide on most field excursions. The movie camera was located on the dune crest at the center of the field site and directed at the swash zone on the adjacent 100 m of beach. In this area an additional profile range was added approximately half way between the camera and the nearest range in the survey grid. By installing two flags at known locations on each of these ranges, scale is established and the position of the swash can be located on the beach profile of that range. A time series of the swash position can be determined by playing back the movie and recording the swash position on each frame. This digitization was done with the use of a computerized digitizing system. As the profile of each range is known the conversion from swash location to the vertical foreshore water elevation is easily accomplished. This method of recording swash position is described in detail and compared to the use of run-up sensors in Holman and Guza (1983).

Spectral analysis of each time series was used to describe the frequency distribution of energy on the foreshore, permitting

identification of statistically significant energy peaks and the wave frequency, and hence period, at which they occur. It also allows determination of the relative amounts of low frequency ( $f < 0.05$  Hz or  $T > 20$  sec) energy and incident wave energy ( $f > 0.05$  Hz). These spectral characteristics are useful in evaluating whether long wavelength edge waves may be present at the field site and if so, whether they can account for enough of the nearshore wave energy to be responsible for the observed nearshore and foreshore topographic features.

Two difficulties were encountered in the filming and digitizing process in this project. First is a lack of contrast in the films, a result of the flat lighting conditions typical of the overcast and rainy winter weather on the Oregon coast. This makes identification of the landward extent of the swash difficult on many of the films. The second difficulty results from the low angle of view of the camera at the field site and hence the lack of good longshore visibility. As discussed in the section on edge wave theory, one must have detailed information on either the offshore or alongshore structure of the infragravity energy to establish definitely whether it is the result of edge wave activity. Unfortunately, the relatively low elevation of the dune crest and poor visibility precluded documentation of longshore variability of energy and hence a more definitive analysis for the presence of edge waves. However, these analyses, together with the wave and tide data collected at Newport, Oregon, do allow evaluation of proposed relationships among run-up, set-up and various incident wave parameters.

Twenty films were successfully taken under incident wave conditions varying from 1.0 m to 4.6 m significant wave height. For several of these, replicate digitizations were performed to allow estimation of variance due to operator error. The mean swash elevations and swash variances for replicates are shown in table 8. Variance differences as large as 54% are observed, with an average deviation from the mean variance ( $|\overline{\text{var}} - \overline{\text{var}}| / \overline{\text{var}}$ ) of 23%. This is, in fact, quite large. Holman and Guza (in press) determined an average deviation from the mean variance of 8% for their data, with a maximum variance difference of 20%. Examination of the range of deviation from the mean variance ( $|\overline{\text{var}} - \overline{\text{var}}|$ ) for the Siletz data suggests that the absolute error is nearly the same for replicates of different runs, with a maximum value of 0.06-0.07 m. Thus, for films taken during large wave conditions the error is a small percentage of the swash excursions. Replicates of run 11 ( $H_{1/3} = 4.6$  m) have small deviations from the mean variance, averaging 10%. The relative error is much greater for films taken during small wave conditions. Significant wave height during run 13 was only 1.0 m and replicates show an average deviation from the mean variance of 36%. Figures 32 and 33 show the spectra from multiple digitizations (by three operators) of film run numbers 11 and 13, respectively. The spectral shapes of replicates appears to be very similar.

Though the number of replicates by the same operator is small, two replicates for each of four films, it is worthwhile to examine these values because all films, other than the previously discussed replicates of numbers 11 and 15, were digitized by the same

RUN	OP	MEAN	VAR	$ \overline{\text{MEAN}}-\overline{\text{MEAN}} $	$ \overline{\text{VAR}}-\overline{\text{VAR}} $	$ \overline{\text{VAR}}-\overline{\text{VAR}} /\overline{\text{VAR}}$
Replicates by multiple operators:						
11	S	-5.63	0.42	0.0109	0.0130	0.030
11	A	-5.48	0.39	0.1435	0.0515	0.118
11	H	-5.75	0.50	0.1325	0.0644	0.147
13	S	-5.69	0.10	0.0100	0.0233	0.189
13	A1	-5.54	0.08	0.1600	0.0433	0.351
13	H1	-5.87	0.19	0.1700	0.0667	0.541
						average:0.229

---

Replicates by the same operator:						
13	A1	-5.54	0.08	0.05655	0.00925	0.1380
13	A2	-5.43	0.06	0.05655	0.00925	0.1380
13	H1	-5.87	0.19	0.0163	0.0040	0.0237
13	H2	-5.84	0.18	0.0163	0.0040	0.0237
15	H1	-8.14	0.36	0.0582	0.0103	0.0282
15	H2	-8.26	0.38	0.0582	0.0103	0.0282
24	H1	-7.33	0.05	0.1469	0.0090	0.2360
24	H2	-7.63	0.03	0.1469	0.0090	0.2360

TABLE 8. The statistics of replicate digitizations of the same runup films. Multiple digitizations by the same operator and by different operators are both considered.

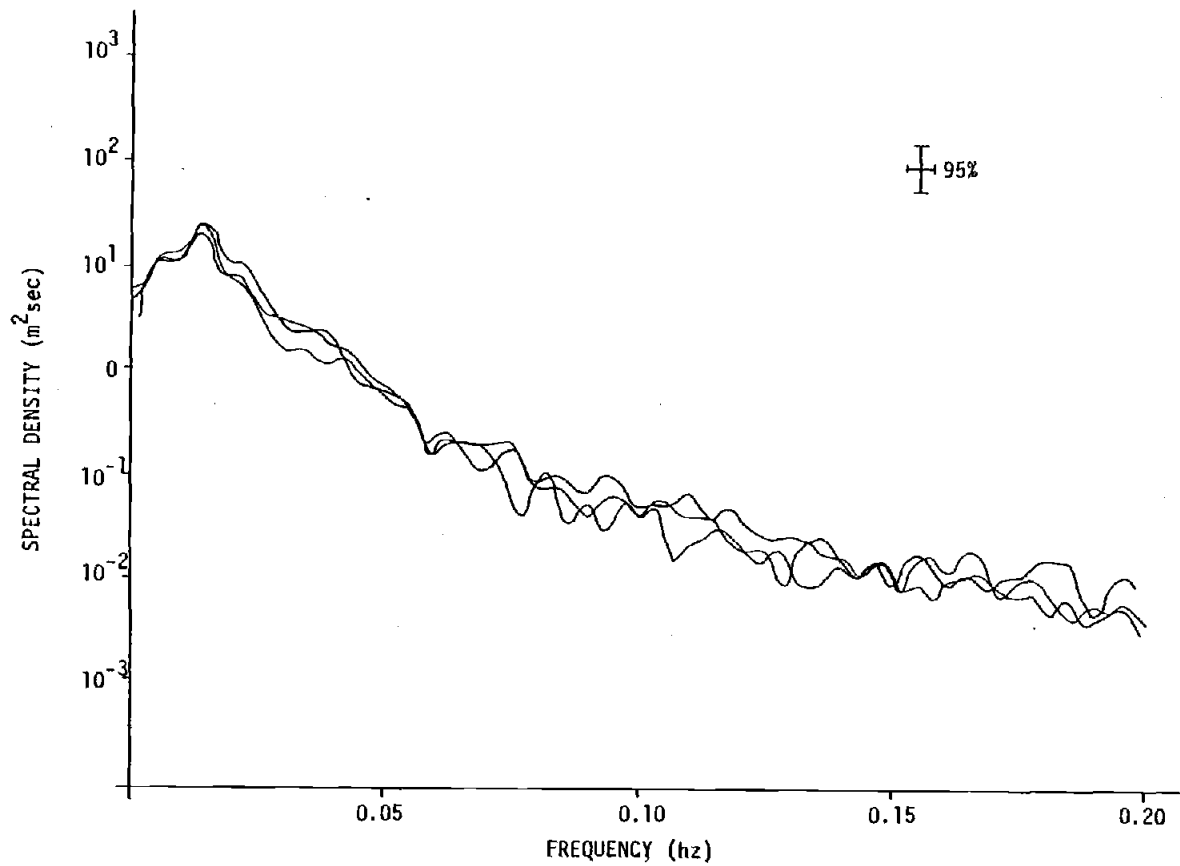


Figure 32. Spectra from multiple digitizations of film run 11 by three operators.

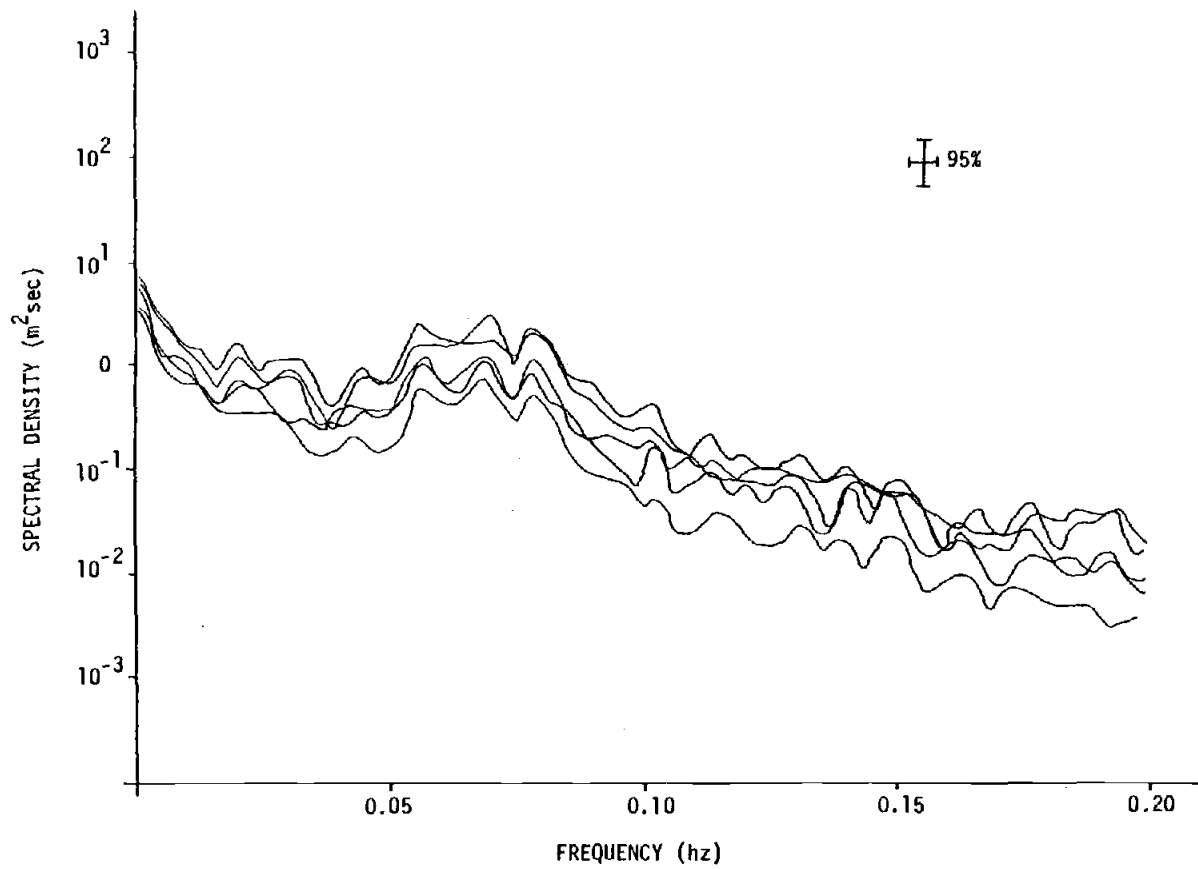


Figure 33. Spectra from multiple digitizations of film run 13 by three operators.

operator. The absolute errors on the variance are consistently no greater than 0.01 m . As one might expect this value is considerably less than the absolute error between operators. There does not appear to be any relationship between the variance, and hence magnitude of the swash excursions, and the average deviation from the mean variance for replicates by the same operator, as was noted for replicates by different operators. A total of thirty-four time series were produced for analysis.

#### Run-up and Incident Waves

Film data allow the determination of representative statistics of run-up, set-up and swash. Few field studies have been done to study and evaluate the relationships among these and incident wave parameters. Run-up,  $R_T^V$ , is defined as the variations in foreshore water level about the still water tidal level and has two components, the set-up and the swash. Run-up time series,  $R_V(t)$ , are determined from the films. Set-up  $\bar{\eta}$ , is the super elevation of the water level at the shoreline. It results from a sloping water surface acting to balance the excess momentum flux of breaking waves (Longuet-Higgins and Stewart, 1963). Set-up should vary with incident wave conditions, increasing as incident waves break further offshore, and therefore as significant wave height increases. It is determined by finding the elevation of mean run-up,  $\bar{R}_V$ , and subtracting the tidal elevation,  $\bar{\eta}_t$ , as determined well offshore or at some other location unaffected by wave breaking. Swash is the

variation in foreshore water level about the its mean and is quantified by using significant swash height,  $R_{1/3}$ , defined by

$$R_{1/3} = 4 [\text{var}(R_V(t))]^{1/2} \quad (\text{eqn.12}).$$

$R_T^V$  then is the sum of set-up and half the significant swash height. Guza and Thornton (1981, 1982) present 11 estimates of set-up and swash from a natural beach with low-slope under incident wave heights of 0.6-1.6 m. The most complete data set of set-up and swash measurements in the field consists of 154 measurements obtained by Holman and Sallenger (in press) on a moderately steep beach under widely varying incident wave conditions. Their data showed the importance of the Irribaren surf similarity parameter

$$\xi_0 = \beta / (H_{1/3}/L)^{1/2} \quad (\text{eqn.13}).$$

to run-up processes. Note that  $\xi_0$  and  $\epsilon$  describe inverse relationships between similar variables.

No offshore tidal elevation data was available for this study, so the Newport tide guage data was used. To do this it was necessary to assume that this tide guage was relatively unaffected by set-up or harbor seiches. The validity of these assumptions is not known, but it will be shown that the data are in reasonable agreement with those of other investigators. The field site coordinate system was calibrated to the Newport sea level datum by assuming that set-up equaled 0.35 times the significant wave height under the lowest incident wave conditions (0.7 m) during which filming was done. The

figure of 0.35 was estimated from data presented by Holman and Sallenger (in press).

Figure 34 shows the Siletz data alone, while figure 35 shows the Siletz data combined with the data of Holman and Sallenger. In all cases the run-up, set-up and swash data are normalized by the significant incident wave height. The plot of non-dimensional set-up versus the Irribaren number looks somewhat scattered but closer examination reveals that this is largely a result of varying water elevations at the times of data collection. When broken down into very-high, high, mid and low water elevations the relationships within all categories other than low water look fairly linear. As noted by Holman and Sallenger (in press), this sorting according to tide is largely a result of using the foreshore slope in the calculation of  $\xi_0$  instead of a mean beach slope which would vary with tide. The data indicate that set-up will be relatively less important under spilling breakers (low  $\xi_0$ ) than under plunging (higher  $\xi_0$ ). The Siletz data plot reasonably well in comparison with that of Holman and Sallenger. The greater error in digitization of the Siletz films than in those analyzed by Holman and Sallenger could account for the greater scatter. The five points calculated from multiple digitizations of film run 13 are labelled.

The plot of normalized swash height versus the surf similarity parameter suggests a linear relationship between the variables, although there is substantial scatter. When plotted with Holman and Sallenger's data this scatter is put into the larger perspective of a greater range of values for both variables. The two

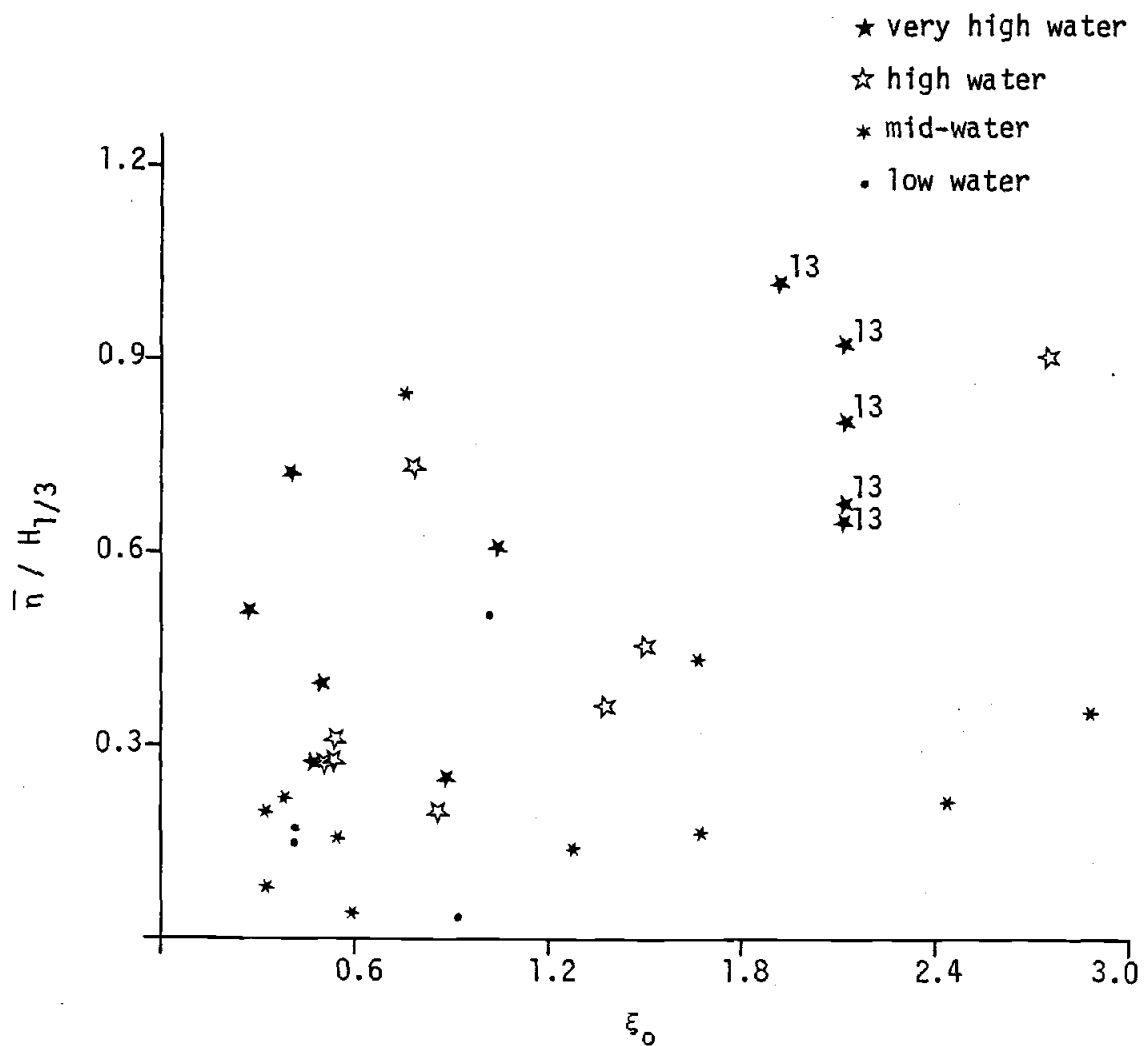


Figure 34. Plots of normalized run-up, set-up and swash versus the Irribaren number for the Siletz Spit data.

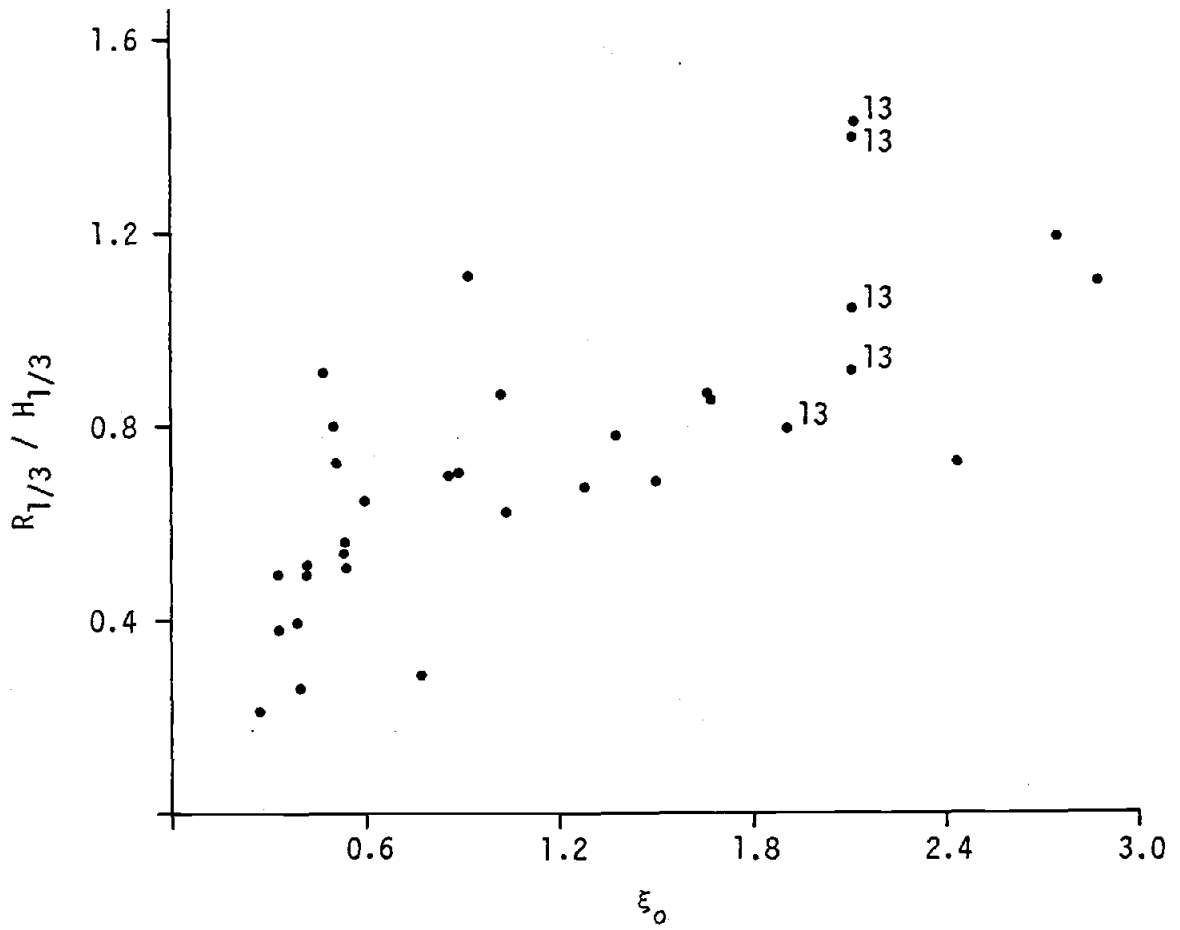


Figure 34 (cont.).

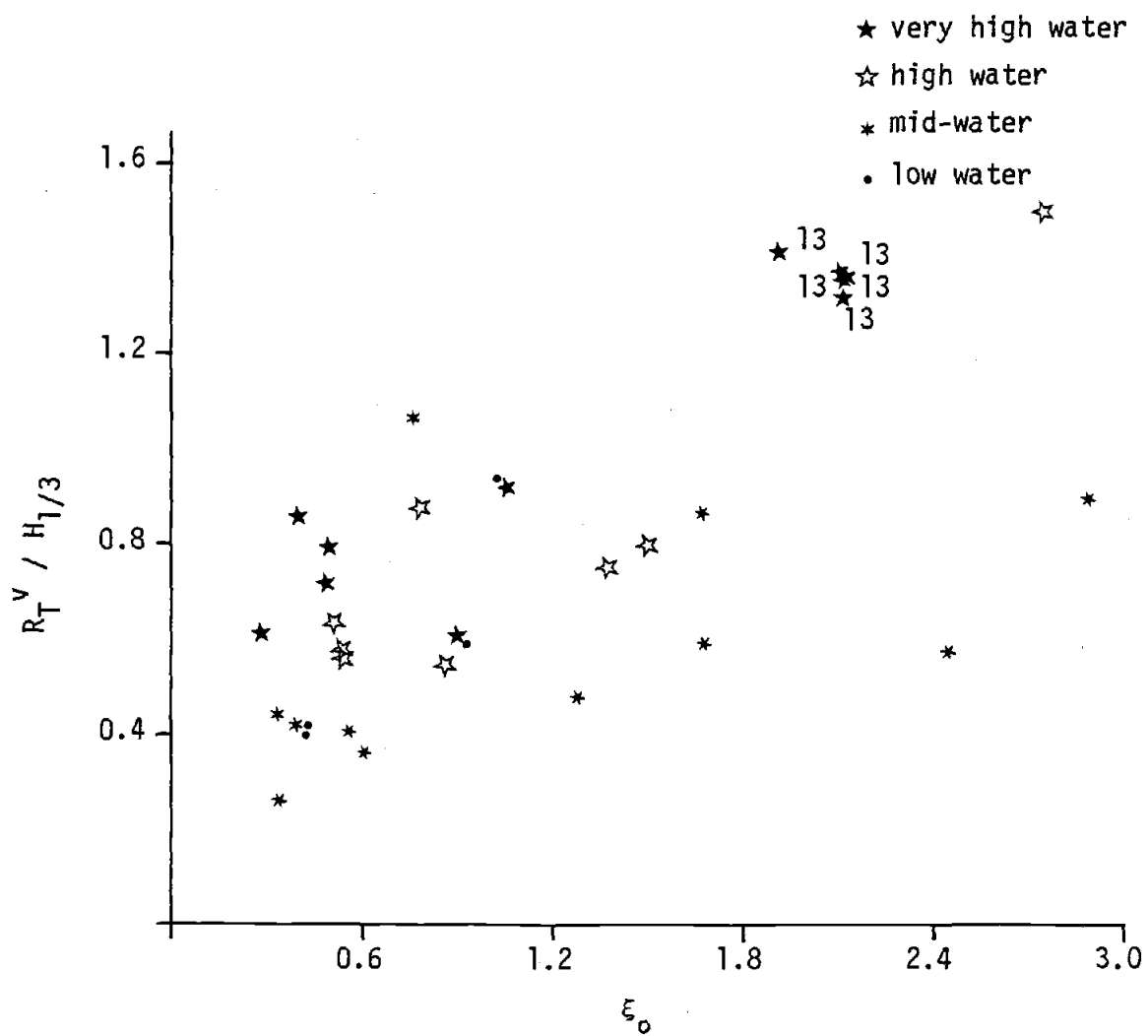


Figure 34 (cont.).

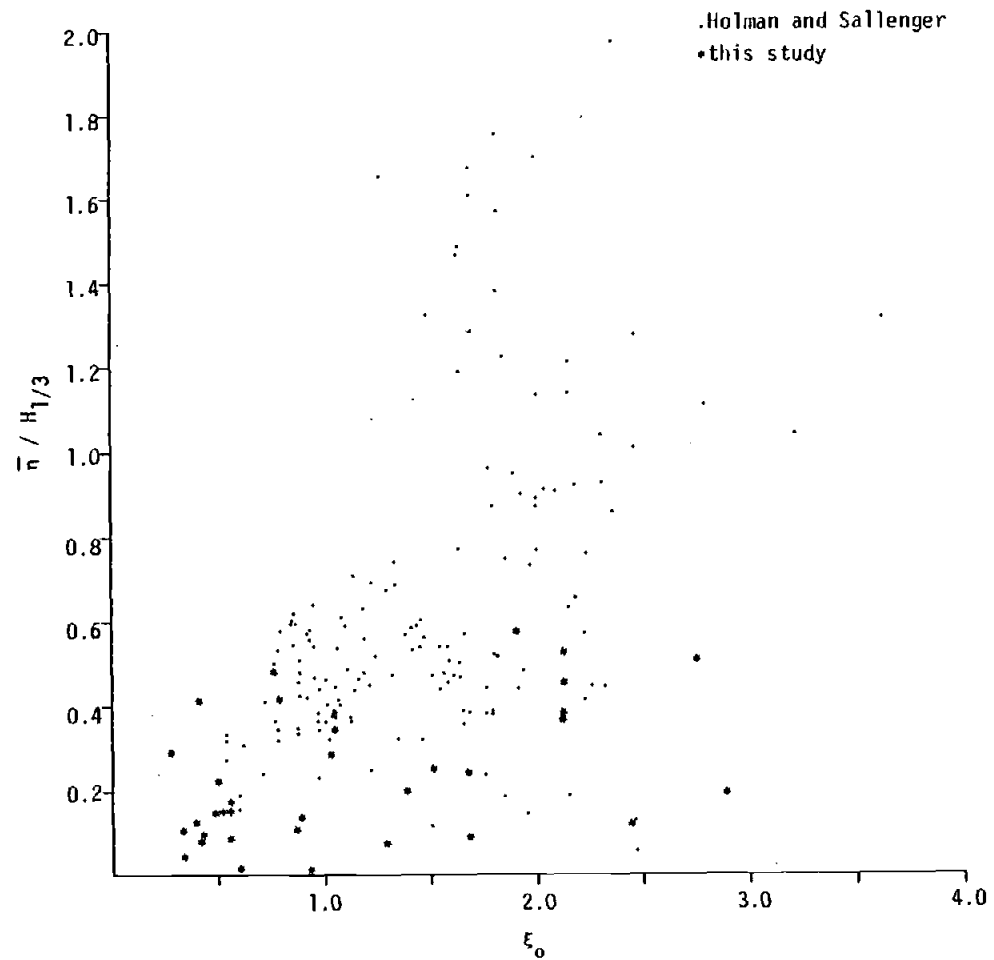


Figure 35. Plots of normalized run-up, set-up and swash versus the Iribarren number with data from Holman and Sallenger (in press) and this study.

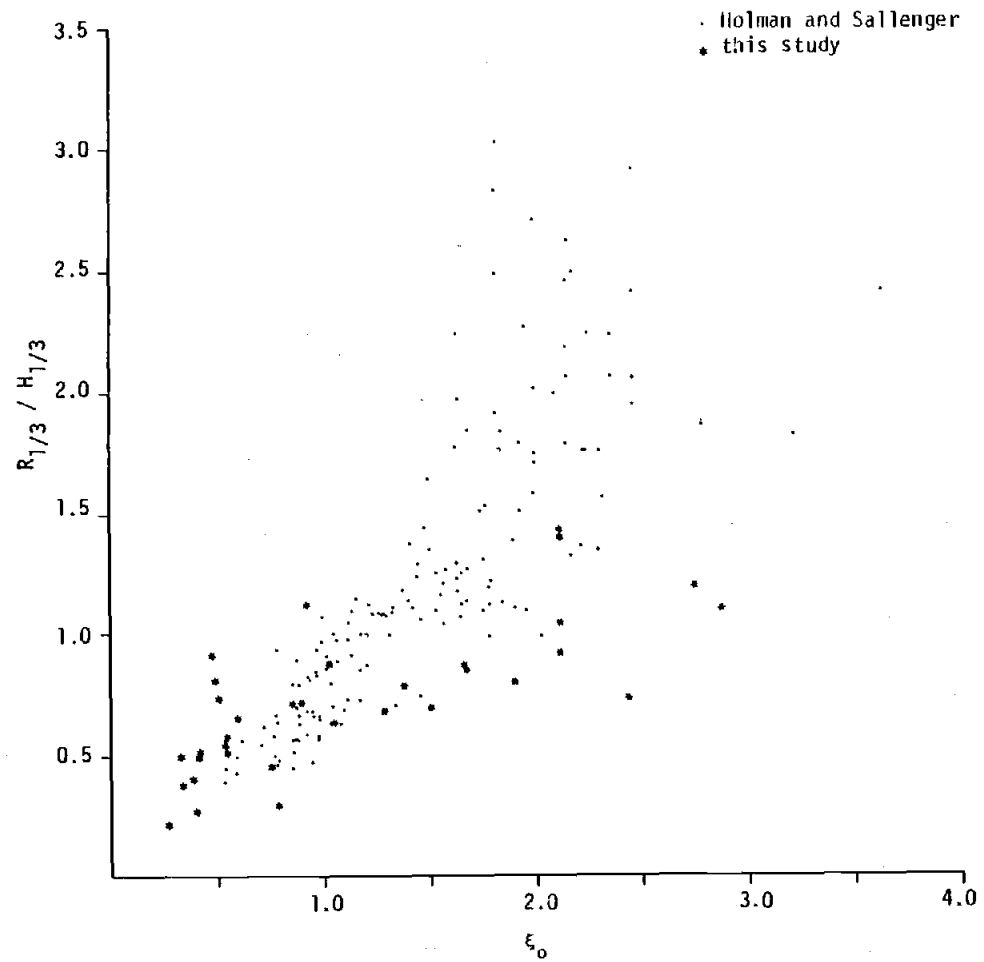


Figure 35 (cont.).

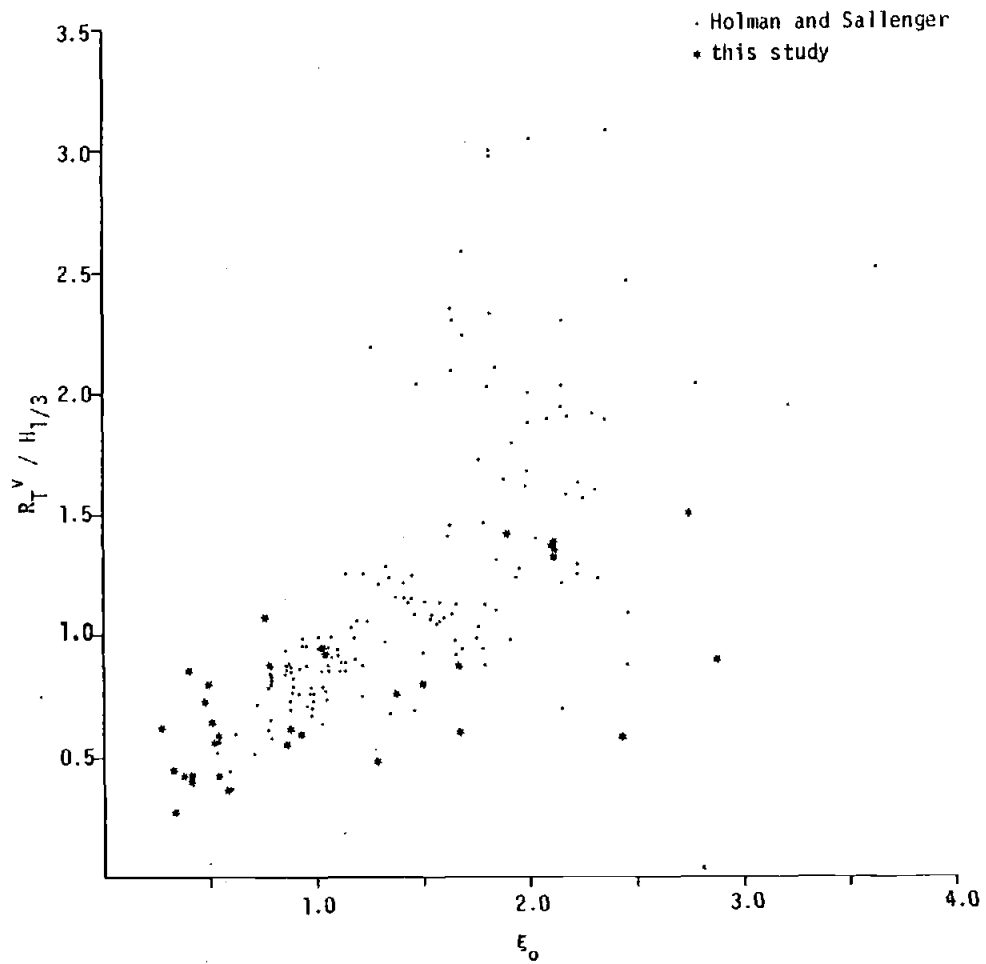


Figure 35 (cont.).

sets of data fit together quite well, the Siletz data providing an increased number of data points at low Irribaren numbers.

The relationship of normalized run-up to the Irribaren number also shows a linear trend. Scatter is reduced if water elevation at the time of filming is considered, as might be expected given the inclusion of set-up in the run-up values. The same five points identified on the plot of normalized set-up (run 13) are again indicated and show much less scatter on this plot. When plotted with the Holman and Sallenger data the Siletz data fits quite well and again extends the plot to lower Irribaren numbers.

Of particular interest is the conclusion in Holman and Sallenger that the infragravity band dominates the swash process at Irribaren numbers less than approximately 1.75. This was concluded by determining the regression lines relating normalized infragravity band swash and normalized incident band swash to the Irribaren number and determining the point of intercept below which the infragravity values were greater. A similar analysis for this data set suggests an infragravity band dominated swash process at  $\xi_0 < 3.54$ . This value is high by comparison and probably results from the greater errors in digitization and the considerable scatter in the relationship between normalized infragravity swash and  $\xi_0$  ( $r^2=0.59$ ).

#### Spectral Characteristics Of Run-up

All spectral plots are summarized in figure 36 which shows the spectral energy distribution. As comparison of the spectral shapes of replicates suggested there is little error in the

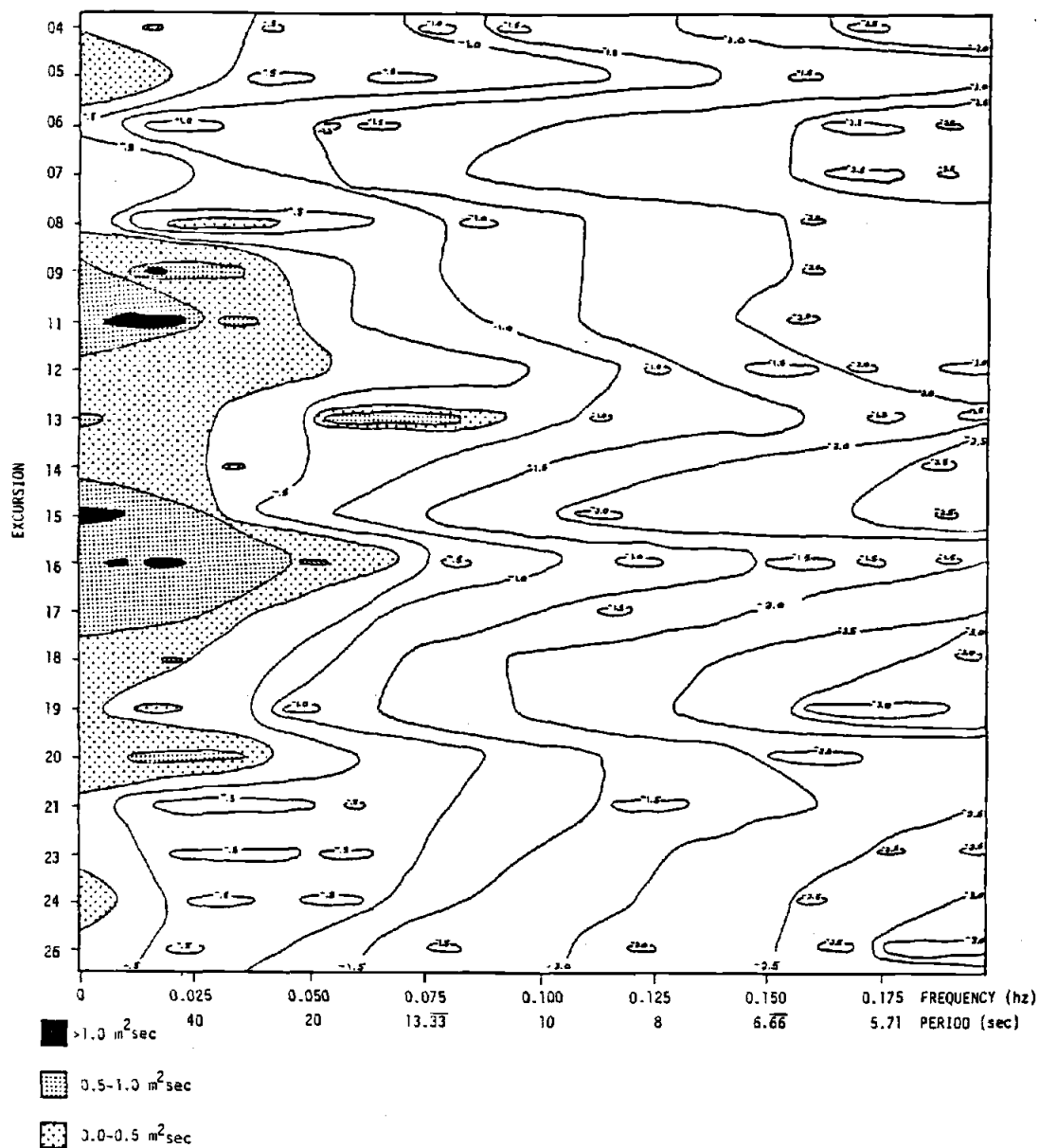


Figure 36. Summary plot of all film spectra. The contours are of spectral density values (contour interval =  $0.5 \text{ m}^2/\text{sec}$ ;  $v = 24$ ). Note the high energies in the low frequencies and the low frequency energy concentrations in the  $0.015\text{--}0.025 \text{ hz}$  band.

identification of spectral peaks and their associated frequencies . Low frequency peaks typically lie in the band 0.015-0.025 hz, many of these being rather broad. Thirteen of the twenty films have peaks of greater than 80% confidence in this range with 10 films having peaks which exceed 95% confidence. In two other films, where two ranges 35 m apart were digitized, one of the two time series also showed low frequency peaks.

From this range of low frequency energy peaks and the edge wave dispersion relation the possible offshore modes,  $n$ , of existent edge waves can be evaluated. For an estimated beach slope of 0.024 and an edge wave length of 1800 m modes of 5 through 16 are possible. Steeper estimates of beach slope, 0.03 and 0.05, result in predictions of lower modes, 4 through 13 and 2 through 7 respectively. Edge waves with modes higher than 4 have not yet been identified on natural beaches. Thus, the presence of edge waves with offshore modes in the range of 3 to 7 is likely, though the presence of higher mode edge waves (up to =16) is possible. The percentage of low frequency energy present during each filming is summarized in table 9. This calculation integrates the area under the energy spectrum curve and reflects the large errors in the digitization process. In all digitizations of films there is a very large percentage of energy in the low frequency range, the minimum being around 50%. Many of the spectra that have no energy peaks are nonetheless quite red. Two good examples of this are films 11 and 15, both photographed on days with 4.6 m significant wave heights and having 97-99% of the foreshore energy in the infragravity band. It is generally thought that infragravity motions are forced by the

FILM(EXCURSION NO)	RANGE	DIGITIZATION	PERCENT LOW FREQUENCY
04	1	A	82%
04	5	A	81%
05	1	A	74%
06	1	A	73%
07	1	A	94%
08	1	A	57%
08	5	A	76%
09	1	A	96%
09	5	A	96%
11	1	A	97%
11	1	B	97%
12	1	A	66%
12	5	A	74%
13	1	A	50%
13	1	B	53%
13	1	C	43%
13	1	D	50%
13	1	E	61%
14	5	A	87%
15	5	A	99%
15	5	B	99%
16	1	A	89%
17	1	A	94%
17	5	A	96%
18	5	A	97%
19	1	A	95%
20	5	A	93%
21	5	A	62%
23	1	A	69%
23	5	A	73%
24	1	A	81%
24	5	A	75%
24	5	B	49%
26	5	A	88%

TABLE 9. Percentage of low frequency (<0.05 hz) energy on the foreshore for all film digitizations.

incident wave field, though the forcing mechanisms are not well understood. Thus, a dominance of low frequency motions is consistent with a high energy incident wave climate. Furthermore, the characteristics of the incident wave field are thought to govern the frequency selection of the infragravity energy. Little is known about the actual relationship, but it is likely that an incoherent incident wave field would produce a very broad band forcing of infragravity motions. The two storms sampled by films 11 and 15 were of local origin and therefore the incident wave spectrum was not coherent and resulted in a dominance of broad banded low frequency energy.

It can be concluded from evaluation of the run-up spectra that low frequency energy was dominant on the foreshore during the field study. Furthermore there is evidence for a frequent, dominant energy peak in the 0.015-0.025 hz range. The predominance of low frequency energy and the characteristics of the beach topography previously analyzed suggests: 1) the frequent presence of infragravity edge waves with considerable energy probably modes  $n=3,4,5,6$  or 7; and 2) their importance in determining shoreline morphology.

## DISCUSSION

It is desirable to identify the process(es) responsible for the formation of large scale rhythmic topography on Siletz Spit. Three characteristic properties of the rhythmicity are identified in the preceding analyses and must be accounted for by any model seeking to explain its topographic development. These three properties are:

- 1) Localization of the rhythmicity to the 3 or 4 kilometers south of the Siletz River. Though less clear there may be a decrease in amplitude of the rhythmicity from north to south in this area. Even less clear but suggested by qualitative evaluation of air photographs is the recurrence of the rhythmic pattern within one to two km north of Government Point.
- 2) Non-stationarity of rhythmic features within those areas where they occur.
- 3) A longshore wavelength of 800-1000 m.

Models

Consideration of both the field and air photo data suggests that the rhythmic pattern initially develops with the 800-1000 m length scale and a very small amplitude, as occurred in 1982-83. Then, under appropriate conditions the amplitude may increase and the longshore position of the features may stabilize. There is no evidence that small perturbations of the inshore topography (Sonu, 1972) initiate the development of the large scale rhythmic topography

on this beach. Such a model may be attractive to explain the localization of rhythmicity and the nonstationarity of topographic features but it is unable to account for the consistent longshore wavelength.

Dalrymple's (1975) suggestion of intersecting wave trains producing alongshore variations in set-up does not explain the consistent longshore wavelength of the rhythmic features. Furthermore, though it can account for lengthscales greater than 600-650 m the topographic lengthscale on Siletz Spit is clearly independent of incident wave climate. Hino's (1975) hydrodynamic instability theory is also not supported by the independence of topographic wavelength and incident wave conditions.

The remaining models for the formation of rhythmic topography all depend on the presence of edge waves in the nearshore zone. The presence of such waves has been hypothesized based on the large amounts of low frequency energy commonly present during field experiments. There are a number of proposed and well documented hypotheses for the way edge waves can affect change in topography.

One proposed model for the development of cusped topography is the synchronous edge wave mechanism. This model requires that the edge wave and the incident wave be of the same period and predicts a topographic wavelength equal to the edge wavelength. Such a combination of waves produces longshore variations in set-up which drives near shore circulation cells whose rip currents erode embayments. Recalling the dispersion relation and assuming the longest probable incident wave period to be 20 sec then the maximum wavelength rhythmic topography that can possibly be generated by this

mechanism is 625 m. The synchronous mechanism then, can not produce rhythmic shoreline morphologies with wavelengths of 800-1000 m and can not account for the rhythmic shoreline morphology on this beach.

Other possible models depend on the presence of a standing edge wave or a combination of edge waves. These models account for erosion and deposition of nearshore and foreshore sands by the drift velocities just above the bottom boundary layer.

The velocity field induced by wave motions can be considered to have two components: the orbital velocity and the drift velocity fields. The orbital motions, given by the gradients of the velocity potential,

$$u(x,y,t) = \partial\phi/\partial x \quad (\text{eqn.14})$$

$$v(x,y,t) = \partial\phi/\partial y \quad (\text{eqn.15})$$

are perfectly symmetrical and therefore produce no net motions. Of greater interest are the net drift velocities, particularly those at the edge of the bottom boundary layer. Hunt and Johns (1963) derived a general expression for these velocities for the case of a wave propogating in two horizontal directions. When solved for the case of a unidirectional wave the equations correspond to those of Longuet-Higgins (1953).

The time averaged drift velocities for a standing wave are given by

$$\langle u \rangle(x,y) = \frac{-1}{2\sigma} (\langle 3u \partial u / \partial x \rangle + \langle v \partial u / \partial y \rangle + \langle 2u \partial v / \partial y \rangle) \quad (\text{eqn.16})$$

$$\langle v \rangle(x,y) = \frac{-1}{2\sigma} (\langle 3v \partial v / \partial x \rangle + \langle u \partial v / \partial x \rangle + \langle 2v \partial u / \partial x \rangle) \quad (\text{eqn.17})$$

where  $u$  is on/offshore velocity,  $v$  is alongshore velocity and  $\langle \rangle$  signifies time averaged values. Substituting for  $u$  and  $v$  gives

$$\langle v \rangle(x,y) = \frac{g^2 a_n^2 \lambda^2}{-4\sigma^3} u_* ((3 \partial u_* / \partial x + 2\lambda v_*) \cos^2 \lambda y - \lambda v_* \sin^2 \lambda y) \quad (\text{eqn.18})$$

(eqn.19)

$$\langle v \rangle(x,y) = \frac{g^2 a_n^2 \lambda^2}{-4\sigma^3} (3\lambda v_*^2 + u_* \partial v_* / \partial x + 2v_* \partial u_* / \partial x) \sin \lambda y \cos \lambda y$$

where

$$u_* = u_*(x) = -\frac{\partial}{\partial(\lambda x)} (L_n(2\lambda x) e^{-\lambda x}) \quad (\text{eqn.20})$$

and

$$v_* = v_*(x) = L_n(2\lambda x) e^{-\lambda x} \quad (\text{eqn.21})$$

To investigate the origin of cusped topography we can restrict our study to the beach foreshore and hence simplify the equations by considering them at  $x=0$  giving,

$$\langle u \rangle(0,y) = Au - Au' \cos(2\lambda y) \quad (\text{eqn.22})$$

and

$$\langle v \rangle(0,y) = Av' \sin(2\lambda y) \quad (\text{eqn.23})$$

where  $Au$ ,  $Au'$ , and  $Av'$  represent terms that are constant alongshore. Embayments are expected where  $\langle u \rangle$  values are greatest and cusps are expected where  $\langle u \rangle$  values equal zero.

It is clear from these equations that, for a single standing edge wave, the foreshore topography would be cusped with a topographic wavelength,  $L_t$ , one half that of the edge wavelength,  $L$ . For the Siletz study area possible reflectors are Government Point, the Siletz River Inlet and Cascade Head. Edge wave wavelengths of 1600 to 2000 m would be required to fit the observed topography. The nonstationarity of rhythmic features could be explained by small changes in  $L$  and, if the wave is standing between two reflectors, concurrent changes in  $m$ , the number of edge wave half wavelengths between the reflectors (where  $m$  must be an integer). The model of a single edge wave standing between two reflectors cannot account for the localization of rhythmicity to the 3 or 4 km south of the Siletz River. A model of an edge wave standing against the Siletz River Inlet and decaying to the south is also unlikely. First, it is questionable whether the delta would be a satisfactory reflector and it is not clear why only 1600 to 2000 m edge waves would be forced. Furthermore, changes in  $L$  from 1600 to 2000 m would result in variations of longshore position of 200 m for the northernmost embayment. The position of embayments located further south varying

by 400 m, 600 m, etc. successively. There is no indication in the data that the northernmost embayment is any more stable than those that form to the south.

Consideration of the three characteristic properties of shoreline rhythmicity at this site suggest a model of the superposition of two standing edge waves of slightly different wavelengths. Examination of the air photographs showing the Government Point area revealed that Boiler Bay and Fogarty Creek Bay have longshore lengths of 1000 and 1100 m respectively. This observation suggested the possible origin of the regular spacing of rhythmic features to the north. A model of two edgewaves, of wavelength 2000 and 2200 m, generated in these bays, and standing against their shared reflector and extending northward is evaluated below. It is concluded that this model explains all of the available data and is likely to describe the cause of shoreline rhythmicity in the study area.

The drift velocities for two waves beating together are given by,

$$\langle u_{12} \rangle = \langle u_1 \rangle + \langle u_2 \rangle = Au_1 - Au_1' \cos 2(\lambda_1 y + \theta) + Au_2 - Au_2' \cos 2(\lambda_2 y) \quad (\text{eqn.24})$$

and

$$\langle v_{12} \rangle = \langle v_1 \rangle + \langle v_2 \rangle = Av_1' \sin 2(\lambda_1 y) + Av_2' \sin 2(\lambda_2 y) \quad (\text{eqn.25})$$

Assuming that  $\langle u_1 \rangle \geq \langle u_2 \rangle$  and that  $\langle v_1 \rangle \geq \langle v_2 \rangle$

(eqn.26)

$$\langle u_{12} \rangle = Au^* - \{2Au_2' \cos[(\lambda_1 + \lambda_2)y + \theta] \cos[(\lambda_1 - \lambda_2)y + \theta]\}$$

and

(eqn.27)

$$\langle v_{12} \rangle = Av^* + \{2Av_2' \sin[(\lambda_1 + \lambda_2)y + \theta] \cos[(\lambda_1 - \lambda_2)y + \theta]\}$$

where

$$Au^* = Au_1 + Au_2 - (Au_1' - Au_2') \cos 2(\lambda_1 y + \theta) \quad (\text{eqn.28})$$

and

$$Av^* = (Av_1' - Av_2') \sin 2(\lambda_1 y + \theta) \quad (\text{eqn.29})$$

The terms given as  $Au^*$  and  $Av^*$  are associated with the preferential forcing of wave 1 with respect to wave 2. Though sinusoidal alongshore their magnitudes (amplitudes) will remain constant. As the forcing of infragravity edgewaves is not well understood at present the magnitudes of these terms cannot be evaluated. The last parts of these equations are of greatest interest here as they define both the expected local rhythmic topography wavelength,  $L_t = (2\pi/\lambda_1 + \lambda_2)$ , and the wavelength of modulation  $(2\pi/\lambda_1 - \lambda_2)$ . This modulation wavelength is reflected in the localization of rhythmic features.

From the dispersion relation we know that if the beach slope changes alongshore then  $\lambda_1$  and  $\lambda_2$  will also vary. Rewriting the

expressions  $(\lambda_1 + \lambda_2)$  and  $(\lambda_1 - \lambda_2)$  as functions of  $\lambda_{10}$ ,  $\lambda_{20}$ ,  $\beta_0$  and  $\beta'$ , where the 0 sub-script represents conditions in the southern bays and where  $\beta'$  ( $d\beta/dy$ ) is the rate of change in beach slope alongshore gives:

$$\lambda_1 + \lambda_2 = \frac{(\lambda_{10} + \lambda_{20})}{1 + (\beta' / \beta_0)y} = \frac{2\pi}{L_T} \quad (\text{eqn.30})$$

and

$$\lambda_1 - \lambda_2 = \frac{\lambda_{10} - \lambda_{20}}{1 + (\beta' / \beta_0)y} \quad (\text{eqn.31})$$

Substituting sensible values ( $y=9000$  m,  $\beta_0=0.03$ ,  $L_t=850$  m,  $\lambda_{10}=3.14 \cdot E-03$ , and  $\lambda_{20}=2.86 \cdot E-03$ ) into equation 30 and solving gives  $\beta'=-6.288 \cdot E-07$ . This predicts that  $\beta$  decreases to the north and equals 0.024 at  $y=9000$  m, a very reasonable estimate.

The modulation term from equation 26,

$$\cos[(\lambda_1 - \lambda_2)y + \theta] = k' \pi \quad (\text{eqn.32})$$

allows us to estimate the longshore locations of extrema ( $k'=n'$ , where  $n'$  is an integer), representing expected longshore locations of maximum amplitude rhythmicity, and of minima ( $k'=(2n'+1)/2$ , where  $n'$  is an integer), representing longshore locations of minimum amplitude rhythmicity. As this expression contains continuously varying wavenumbers it must be evaluated using the WKB approximation. This

model predicts that the southernmost amplitude maximum is at 1075 m, an amplitude minimum is near 5800 m and another amplitude maximum at approximately 9700 m (figure 37). This is in excellent agreement with the observed longshore topography.

This model imposes no constraints on edgewave mode,  $n$ , or angular frequency,  $\sigma$ , other than that they must satisfy the dispersion relation. Their relative values do not effect the characteristics of foreshore rhythmic topography. Longshore non-stationarity of topography features can be explained by small variations in  $\beta'$  ( $\pm 3.075 \times 10^{-7}$ ). Such variation would be reflected in small ( $\pm 100\text{m}$ ) changes in  $L_t$  with a cumulative longshore effect acting to shift the position of an embayment by up to 1700 m on the northern part of Siletz Spit. The observed migrations of approximately 400 m and the non-stationarity demonstrated by statistical analysis (requiring a minimum migration of 400 to 500 m) are thus easily accounted for.

Consideration of the relationship between the position of the mean shoreline and the longshore position of the rhythmic pattern allows us to test a prediction made by this model. First, it must be assumed that coarser grained beaches experience a greater decrease in beach slope than do finer grained beaches under the same increase in wave energy conditions. Aquilar-Tufion (1977) showed that beach volume changes are much greater on coarse grained beaches than on fine grained beaches under the same incident wave conditions. Thus, this assumption seems to be well supported. Mean grain size in the study area varies from 0.3  $\phi$  at Fogarty Creek to 0.92  $\phi$  two to three km north of the Creek to approximately 1.7-1.75  $\phi$  from Gleneden Beach

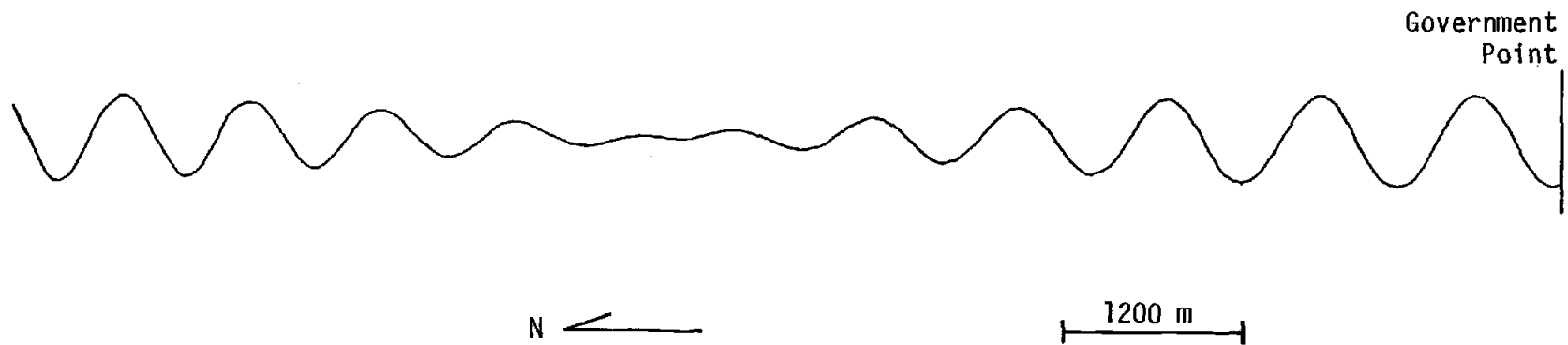


Figure 37. The predicted shoreline pattern from the proposed model of two topographically constrained edge waves extending northward together from Government Point.

north along Siletz Spit (Peterson, pers. comm.). One would, therefore, predict that  $\beta'$  would be more negative during the summer (or swell) season than during the winter (or storm) season. For this change in general beach morphology the model predicts northward migration of rhythmic features (slope changes of 0.03 to 0.02 at Government Point and of 0.024 to 0.017 at Siletz Spit can account for 850 m of topographic migration at the field site). Figure 38 shows the data from this study and is in agreement with the predicted relationship. Some of the variations shown by excursions twelve through nineteen may be due to the exaggeration of noise by the normalization of relatively low amplitude data sequences. Thus, there was northward migration (as noted earlier) during the fall as the beach slope on Siletz presumably decreased less than the beach slope near Government Point and there was southward migration in the late winter as the mean shoreline position moved offshore and the beach slope on Siletz should have increased less than the beach slope to the south. Rea (1976) also documented 300 meters of northward migration of rhythmic features in February and March of 1974, followed later by southward migration. He, however, explains the migration as a result of predominantly southwest winds through March and winds later shifting to the northwest. Survey data from this same time show overall accretion between early February and early May. Unfortunately this data is not broken down into smaller time periods so evaluation of beach slope changes cannot be made. Wave energy flux from early February through mid-March was greater than from mid-March through April. It would seem possible, then, that most beach accretion occurred during the latter time period. An alternate

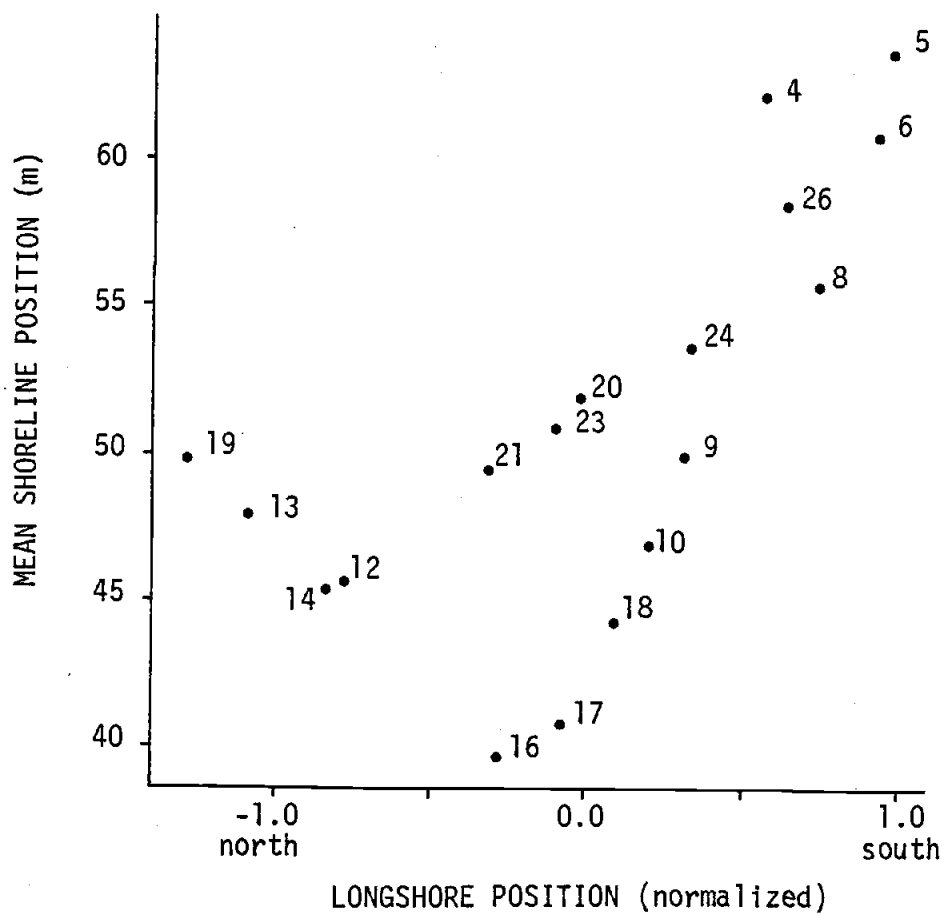


Figure 38. The mean shoreline position versus longshore position (normalized) of the rhythmic pattern. Northward migration of rhythmic features accompanied shoreline erosion.

scenario is that the southwest winds were associated with higher wave energies which caused a greater change in beach volume on the coarse grained beach than on the fine grained beach and thus, a greater decrease in beach slope near Government Point than on Siletz Spit. This change would produce northward migration of topographic features as observed . By early April, winds were predominantly from the northwest and were associated with lower energies, causing a greater increase in beach volume and beach slope to the south than to the north and therefore, southward migration of topographic forms.

Figure 39 is a schematic illustration , based on equations 26 and 27, of the predicted drift velocities and directions for both the on/offshore and alongshore flows associated with the local rhythmic topography. A particularly interesting feature is the divergence in  $\langle v \rangle$  at the topographic embayment which would act to decrease overall (rip current) flow velocities in the nearshore circulation cell. Thus, aside from the effects of refracting incident waves on the existing topography, rip currents should be most strongly developed under conditions where  $\langle u \rangle \gg \langle v \rangle$ , for instance when higher mode edge waves are present . An increase in amplitude of the rhythmic pattern, could then be a result of either changes in edge wave forcing (that is, changes in  $\sigma$  and  $n$  affecting the relative values of  $\langle u \rangle$  and  $\langle v \rangle$ ) or the refraction of incident waves around the existing rhythmic features. Data is not available to evaluate such changes in the amplitude of rhythmicity through time.

As shown in this evaluation, a model of two standing edgewaves of similar wavelengths generated in small bays to the south and beating in and out of phase as they extend north accounts for the

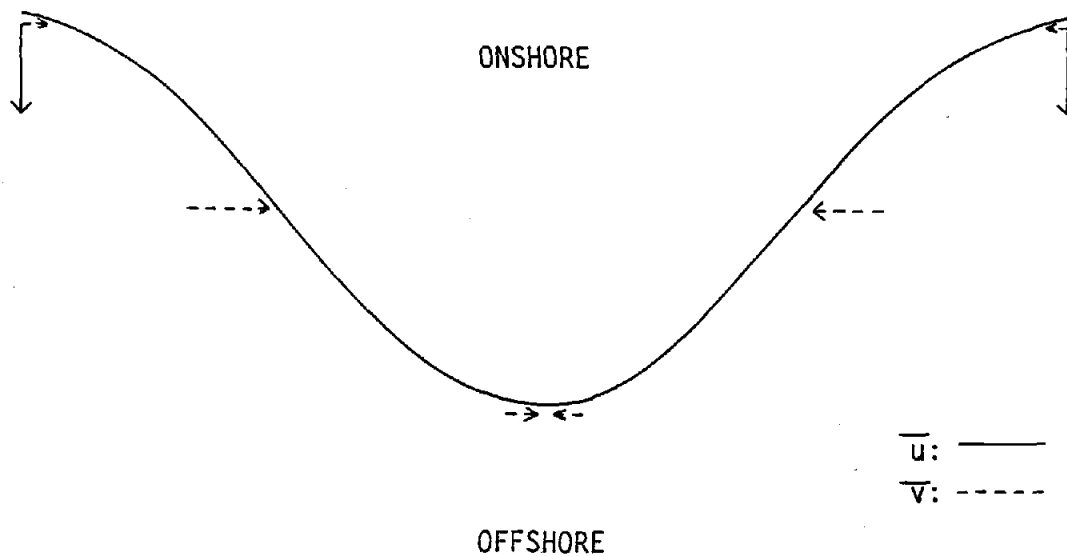


Figure 39. A schematic illustration of the time averaged drift velocities on the foreshore as predicted by the proposed model of two topographically constrained edge waves of slightly different wavelengths extending northward from Government Point.

three characteristics of rhythmic topography observed in this area. It is proposed that the drift velocities produced by these wave motions govern the longshore distribution of sand on the beach foreshore and result in the cusped topography commonly observed on Siletz Spit.

In the more general context of the origins and development of rhythmic topography this model simply suggests another edge wave selection mechanism. It is similar to the simpler model of an edge wave standing between two reflectors in that the local geography governs the selection process in both cases. Also, it is similar to the models of two or more edge waves with different longshore components, discussed by Holman and Bowen (1982); the presence of more than one wave, each with a different longshore structure, leading to increasingly complex shoreline morphologies. Thus, in future studies of beach topography the local geography might be considered in a broader sense than it has in the past and beach morphologies which are not simple rhythmic patterns might be investigated with a hypothesis based on the presence of multiple edge waves.

An alternate hypothesis for the formation of rhythmic topography in the study area remains. It is possible that the topography forms by rip currents hollowing out embayments and leaving cusps between them. It has been observed (Komar and Rea, 1976) that rip currents commonly occupy embayments, particularly at times of greatest erosion. Though the growth of this rhythmic shoreline to large amplitudes seems clearly related to the presence of rip currents, the role of rip currents in its initial development remains

unstudied. Nonetheless, any model based on this hypothesis would be constrained by the three characteristic properties of the rhythmicity at this site: localization, non-stationarity and a longshore wavelength of 800-1000 m.

### Waves, Tides, Weather and Topography

Relationships between parameters which represent important characteristics of shoreline morphology and between these parameters and wave, tide or weather conditions allow us to: 1) improve our understanding of what variables are important in producing rhythmic topography, 2) make some estimates of the response times for the beach morphology components, and 3) learn something about the way in which rhythmic topography forms. Regression analysis between the available topographic and environmental variables confirms some well established trends but also provides some new insights and surprises. The values used to represent the wave, tide and weather conditions in this investigation are the means for the time periods between surveys.

Though the linear correlation between mean significant wave height and the position of the mean shoreline is not high ( $-0.720$ ) the expected relationship exists. As significant wave height increases the mean shoreline position moves onshore (decreases) as a result of beach erosion. It is suggested that the correlation is as low as it is due to the rather slow response time of the mean shoreline to changes in incident wave conditions (Figure 40). Although the bi-weekly sampling precludes comments on very rapid

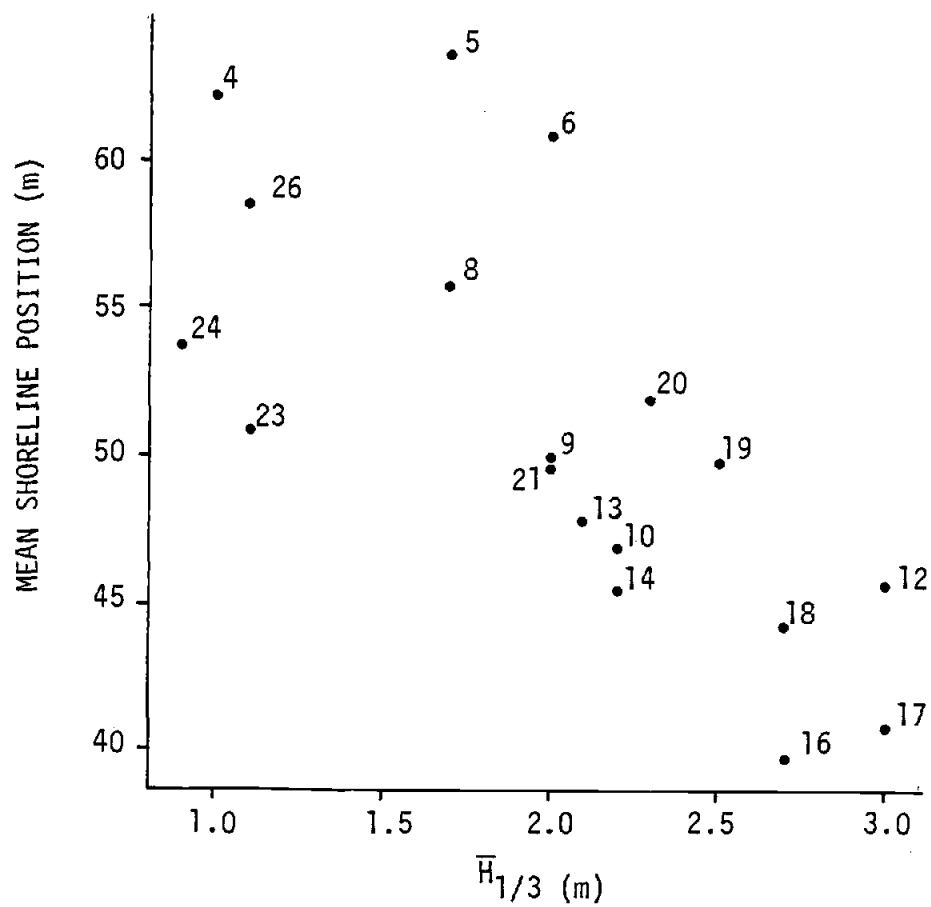


Figure 40. Mean significant wave height versus mean shoreline position showing a negative correlation between these variables.

responses, the mean shoreline position changed, at most, five meters between surveys.

More interestingly, the amplitude of the rhythmicity also shows a negative correlation (-0.614) with mean significant wave height. This is opposite to the relationship observed previously during major episodes of erosion on Siletz Spit. At those times erosion resulted from embayments impinging on the foredune during storms with incident wave heights exceeding 6 or 7 meters (Rea, 1975; Komar and Rea, 1976; McKinney, 1976). The spectral analyses of the high water lines indicate that this was due to an increased amplitude of the rhythmicity.

In the section on general observations it was shown that the winter of 1982/83 was characterized by anomalous weather and tide conditions. Consideration of three well documented periods of significant dune erosion on Siletz during the 1970's (McKinney, 1976) reveals fundamental differences in conditions between those periods and the 1982/83 winter. First, incident wave conditions do not vary appreciably. Incident wave periods during the three major erosive storms varied from 9 to 17 sec and significant wave heights ranged from 6 to 7 m. However, barometric pressures in the winter of 1982/83 were anomalously low. Monthly mean barometric pressures for January through April were the lowest since sometime before 1971 (Huyer et al., 1983). This difference reflects that storm centers were closer to the Oregon coast in 1982/83, being located off the central California coast, than during the periods of major erosion when they were located in the North Pacific just south of the Aleutian Islands, in the Gulf of Alaska (McKinney, 1977). It seems

to be a reasonable hypothesis then, that incident wave characteristics related to the proximity of a storm center are important in determining the amplitude of rhythmic topography on Siletz Spit. Interestingly, the amplitude of the rhythmicity in the 1982/83 winter showed larger responses to incident wave conditions than did the mean shoreline position (Figure 41). Up to 10 m of change occurred during any two week period.

The relationship between mean shoreline position and rhythmicity amplitude can reveal whether the rhythmic topography is erosional or depositional in origin. The correlation between these two morphology components is +0.841, indicating that amplitude increased as the shoreline prograded (Figure 42). From the winter of 1982/83 data alone it would appear that rhythmic topography forms under depositional conditions. The spectral analyses of the high water lines suggest a possible negative correlation between these same two variables. The photographs showing significant spectral peaks were taken during August, September, October, February and April. The high spectral energy found on the fall and mid-winter photographs indicate that rhythmic topography may also form under erosional conditions. Thus, it is concluded that rhythmic topography can develop under either depositional or erosional conditions. It is therefore, likely that the development of rhythmicity is independent of changes in the mean shoreline position.

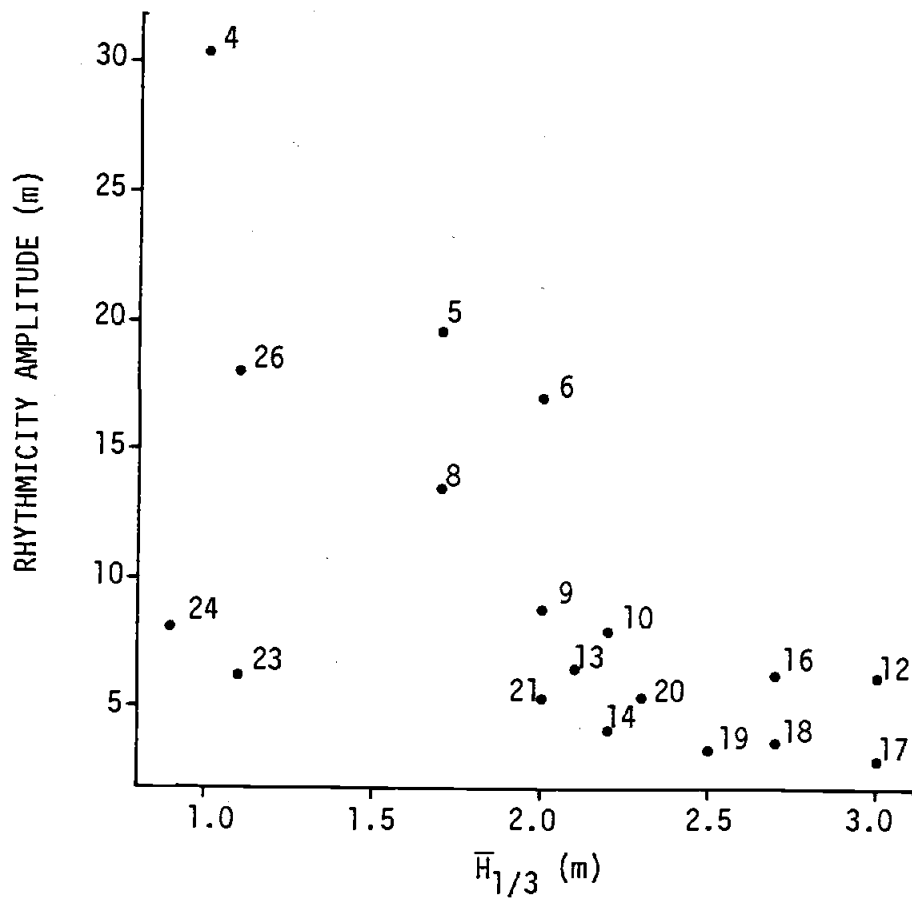


Figure 41. Mean significant wave height versus rhythmicity amplitude. The negative correlation between these variables differs from a positive correlation observed during major erosional episodes of the 1970's.

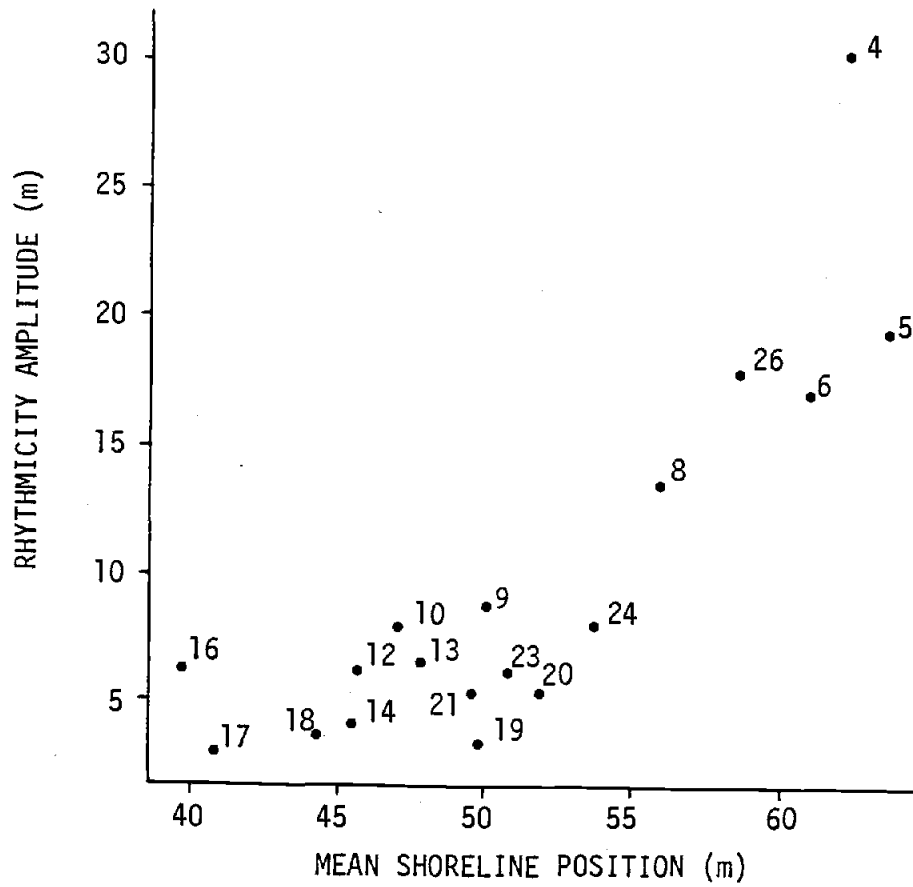


Figure 42. Mean shoreline position versus rhythmicity amplitude. The positive correlation indicates rhythmic topography was of a depositional origin during the time of this study.

## CONCLUSIONS

- 1) When shoreline rhythmicity is present between Government Point and the Siletz River Inlet, it occurs predominantly within the 3 to 4 kms south of the inlet.
- 2) It appears that rhythmicity amplitude within this section may decrease to the south.
- 3) It also appears that shoreline rhythmicity occurs within the 1 to 2 kms north of Government Point, though it seems less common here than to the north.
- 4) There is a definite non-stationarity of rhythmic features within the areas where they develop.
- 5) When the shoreline on this beach is rhythmic it is characterized by a wavelength of 800-1000 meters.
- 6) A model of two topographically constrained edge waves beating together accounts for the three characteristic properties of shoreline rhythmicity in the study area. The waves are generated in two bays at the southern end of the beach and have wavelengths of approximately 2000 and 2200 meters at this location. The modulation wavelength is on the order of 10,000 meters and local rhythmic topography wavelengths on the order of 900 meters are predicted. Small changes in the longshore variation of beach slope account for the non-stationarity of rhythmic features.

## REFERENCES

- Aguilar-Tuñon, N.A. and P.D. Komar (1978). The annual cycle of profile changes of two Oregon beaches. *The Ore. Bin.*, 40, no.2: 25-40.
- Ball, F.K. (1967). Edge waves in an ocean of finite depth. *Deep-Sea Res.*, 14: 79-88.
- Bowen, A.J. (1969). Rip currents, 1: theoretical investigations. *J. Geophys. Res.*, 74, no.23: 5467-5478.
- Bowen, A.J. (1972). Edge waves and the littoral environment. *Proc. 13th Conf. Coast. Eng.*, pp.1313-1320.
- Bowen, A.J. (1980). Simple models of nearshore sedimentation; beach profiles and longshore bars. In *The Coastline of Canada*, ed. by S.B. McCann, pp.1-11, Geological Survey of Canada, Paper 80-10.
- Bowen, A.J. and R.T. Guza (1978). Edge waves and surf beat. *J. Geophys. Res.*, 83, no. C4: 1913-1920.
- Bowen, A.J. and D.L. Inman (1969). Rip currents, 2: laboratory and field observations. *J. Geophys. Res.*, 74, no.23: 5479-5490.
- Bowen, A.J. and D.L. Inman (1971). Edge waves and crescentic bars. *J. Geophys. Res.*, 76, no.36: 8662-8671.
- Creech, H.C. (1981). Nearshore wave climatology Yaquina Bay, Oregon. Sea Grant College Program, ORESU-T-81-002.
- Dalrymple, R.A. (1975). A mechanism for rip current generation on an open coast. *J. Geophys. Res.*, 80, no.24: 3485-3487.
- Davis, J.C. (1973). *Statistics and Data Analysis In Geology*. Wiley and Sons, New York, 550pp.
- Davis, R.A. (1976). Coastal changes, Eastern Lake Michigan, 1970-73. U.S. Army Corps of Engrs., Coastal Engineering Research Paper No.76-16, 64pp.
- Dolan, R., B. Hayden, and W. Felder (1979). Shoreline periodicities and edge waves. *Jour. Geol.*, 87: 175-185.
- Dolan, R. and B. Hayden (1981). Storms and shoreline configuration. *J. Sediment. Petrol.*, 51, no.3: 737-744.
- Dolan, R. and B. Hayden (1983). Patterns and prediction of shoreline change. In *the CRC Handbook of Coastal Processes and Erosion*, Ed. P.D. Komar, CRC Press, Boca Raton, pp.123-150.

- Eckart, C. (1951). Surface waves in water of variable depth. Univ. of California, Scripps Inst. of Oceanography, Wave Report no.100, SIO Ref. 51-12, LaJolla, 99pp.
- Emery, K.O. (1961). A simple method of measuring beach profiles. *Limnology and Oceanography*, 6, no.1: 90-93
- Enfield, D.D. and J.S. Allen (1980). On the structure and dynamics of monthly sea level anomalies along the Pacific coast of North and South America. *J. Phys. Oceanogr.*, no.10: 557-578.
- Gallagher, B. (1971). Generation of surf beat by non-linear wave interactions. *J. Fluid Mech.*, 40, 1: 1-20.
- Guza, R.T. and A.J. Bowen (1981). On the amplitude of beach cusps. *J. Geophys. Res.*, 86, no.C5: 4125-4132.
- Guza, R.T. and R.E. Davis (1974). Excitation of edge waves by waves incident on a beach. *J. Geophys. Res.*, 79, no.9: 1285-1291.
- Guza, R.T. and D.L. Inman (1975). Edge waves and beach cusps. *J. Geophys. Res.*, 80, no.21: 2997-3012.
- Guza, R.T. and E.B. Thornton (1981). Wave set-up on a natural beach. *J. Geophys. Res.*, 86, no.C5: 4133-4137.
- Guza, R.T. and E.B. Thornton (1982). Swash oscillations on a natural beach. *J. Geophys. Res.*, 87, no.C1: 483-491.
- Hino, M. (1975). Theory on formation of rip current and cuspidal coast. *Proc. 14th Conf. Coast. Eng.* pp.901-919.
- Holman, R.A. and A.J. Bowen (1979). Edge waves on complex beach profiles. *J. Geophys. Res.*, 84, no.C10: 6339-6346.
- Holman, R.A. and A.J. Bowen (1982). Bars, bumps and holes: models for the generation of complex beach topography. *J. Geophys. Res.*, 87, no.C1: 457-468.
- Holman, R.A. and A.J. Bowen (in press). Longshore structure of infragravity wave motions.
- Holman, R.A. and R.T. Guza (in press). Measuring run-up on a natural beach.
- Holman, R.A., D.A. Huntley, and A.J. Bowen (1978). Infragravity waves in storm conditions. *Proc. 16th Conf. Coast. Eng.*, pp.268-284.
- Holman, R.A. and A.H. Sallenger, Jr. (in press). Set-up and swash on a natural beach.
- Hunt, J.N. and B. Johns (1963). Currents induced by tides and gravity waves, *Tellus*, 15, no.4: 343-351.

- Huntley, D.A. (1976). Long-period waves on a natural beach. *J. Geophys. Res.*, 81, no.36: 6441-6449.
- Huntley, D.A. and A.J. Bowen (1975). Field observations of edge waves and their effect on beach material. *Jour. Geol. Soc. Lond.*, 131: 69-81.
- Huntley, D.A., R.T. Guza, and E.B. Thornton (1981). Field observations of surf beat, 1: progressive edge waves. *J. Geophys. Res.*, 86, no.C7: 6451-6466.
- Huyer, A., W.E. Gilbert and H.L. Pittcock (1983). Anomalous sea levels at Newport, Oregon, during the 1982-83 El Nino. *Coastal Oceanography and Climatology News*, 5, no.4.
- Katoh, K. (1981). Analysis of edge waves by means of empirical eigenfunctions. Report Of the Port and Harbour Research Institute, 20, no.3: 3-51.
- Komar, P.D. (1973). Observations of beach cusps at Mono Lake, California. *Geol. Soc. Am. Bull.*, 84: 3593-3600.
- Komar, P.D. (1978). Wave conditions on the Oregon coast during the winter of 1977-78 and the resulting erosion of Nestucca Spit. *Shore and Beach*, 46, no.4: 3-8.
- Komar, P.D. (1983). Rhythmic shoreline features and their origins. In *Mega-Geomorphology*, Ed. R. Gardner and H. Scoging, Clarendon Press, Oxford, pp.92-112.
- Komar, P.D., W. Quinn, C. Creech, C.C. Rea, and J.R. Lizarrage-Arciniega (1976). Wave conditions and beach erosion on the Oregon coast. *The Ore. Bin.*, 38, no.7: 103-112.
- Komar, P.D. and C.C. Rea (1976). Erosion of Siletz Spit, Oregon. *Shore and Beach*, 44, no.1: 9-15.
- Lillesand, T.M. and R.W. Kiefer (1979). *Remote Sensing and Image Interpretation*. Wiley, New York, 612pp.
- Longuet-Higgins, M.S. (1953). Mass transport in water waves. *Phil. Trans. Roy Soc. (London)*, series A, 245: 535-581.
- Longuet-Higgins, M.S. and R.W. Stewart (1964). Radiation stresses in water waves; a physical discussion, with applications. *Deep-Sea Res.*, 11, no.4: 529-563.
- McKinney, B.A. (1977). The spring 1976 erosion of Siletz Spit, Oregon, with an analysis of causative wave and tide conditions: Oregon State Univ. master's thesis, 66pp.
- Munk, W.H. (1949). Surf beats. *Trans. Am. Geophys. Union*, 30: 849-854.

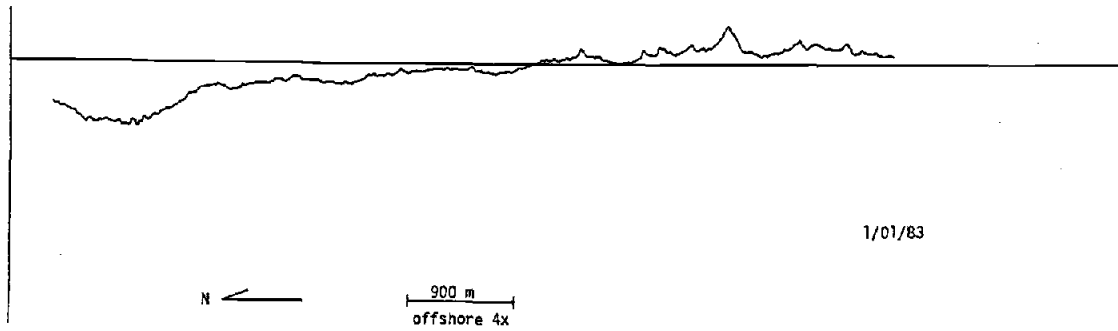
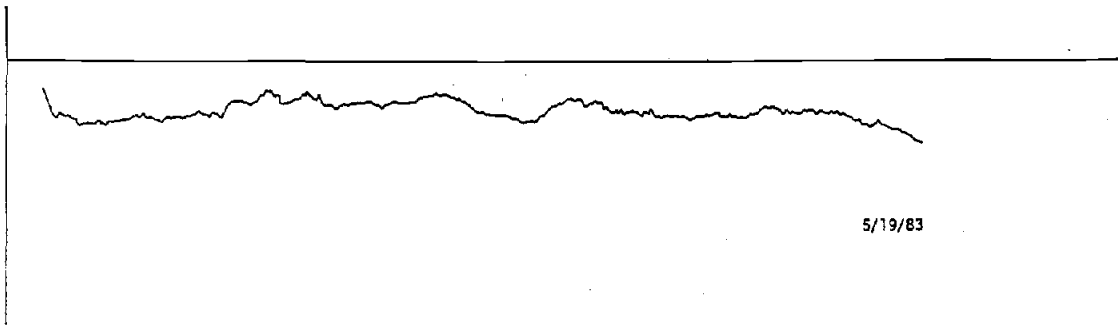
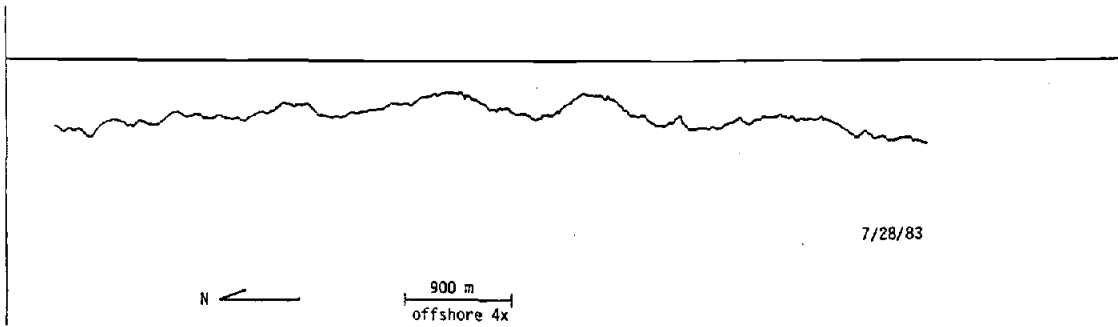
- Quinn, W.H., H.C. Creech and D.E. Zopf (1974). Coastal wave observations via seismometer. *Mariners Weather Log*, v.18, pp.367-369.
- Rea, C.C. (1975). The erosion of Siletz Spit, Oregon. Oregon State Univ. master's thesis, 105pp.
- Sasaki, T., K. Horikawa and S. Hotta (1976). Nearshore currents on a gently sloping beach. *Proc. 15th Conf. of Coast. Eng.*, pp.626-644.
- Sonu, C.J. (1972). Field observations of nearshore circulation and meandering currents. *J. Geophys. Res.*, 77, no.18: 3232-3247.
- Terich, T.A. and P.D. Komar (1974). Bayocean Spit, Oregon: history of development and erosional destruction. *Shore and Beach*, 42, no.2: 3-10.
- Tucker, M.J. (1950). Surf beats: sea waves of 1 to 5 minutes' period. *Proc. Roy. Soc. A*, 202: 565-573.
- Ursell, F. (1952). Edge waves on a sloping beach. *Proc. Roy. Soc. (London)*, series A, 214: 79-97.
- Wright, L.D., J. Chappell, B.G. Thom, M.P. Bradshaw and P. Cowell (1979). Morphodynamics of reflective and dissipative beach and inshore systems: Southeastern Australia. *Mar. Geol.*, 32: 105-140.
- Wright, L.D. and A.D. Short (1983). Morphodynamics of beaches and surf zones in Australia. In the *CRC Handbook of Coastal Processes and Erosion*, Ed. P.D. Komar, CRC Press, Boca Raton, pp.35-64.

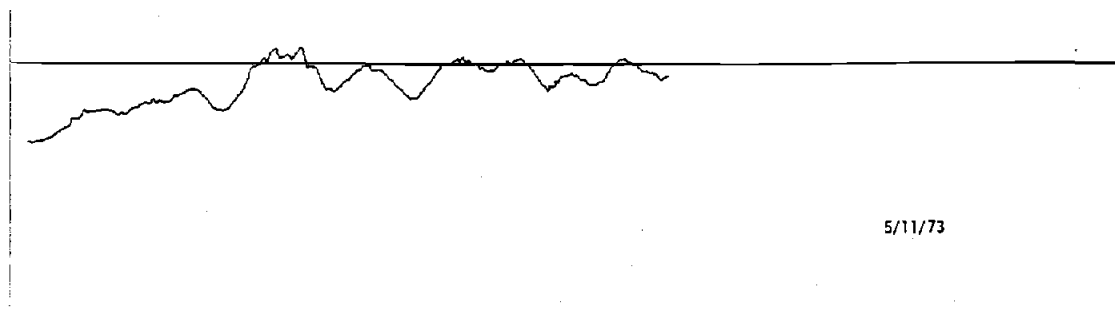
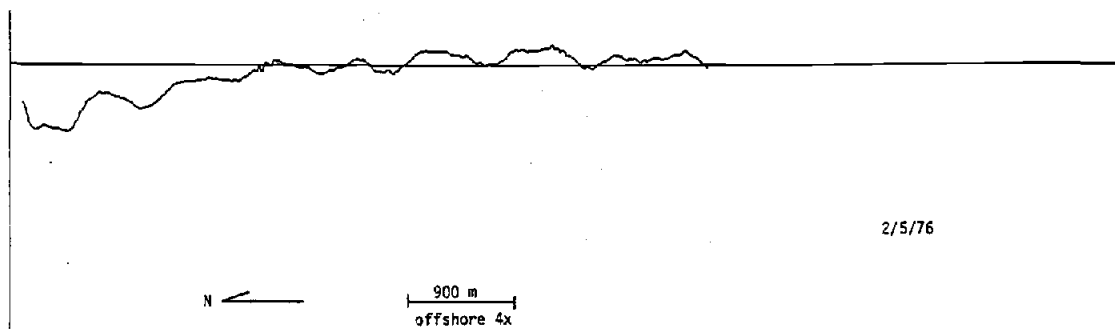
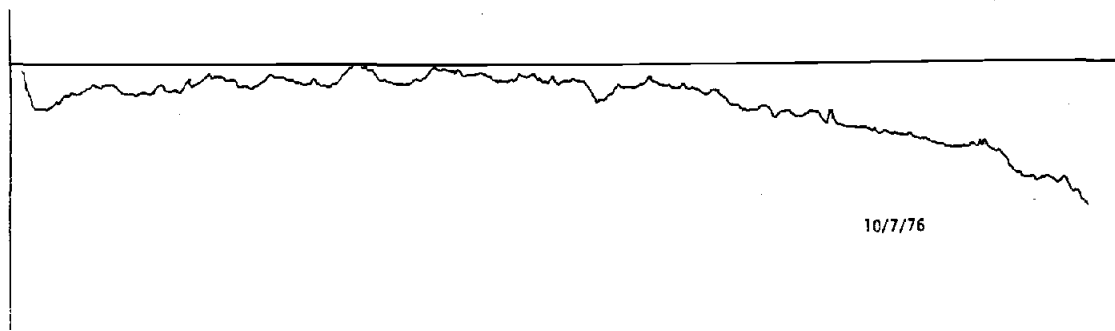
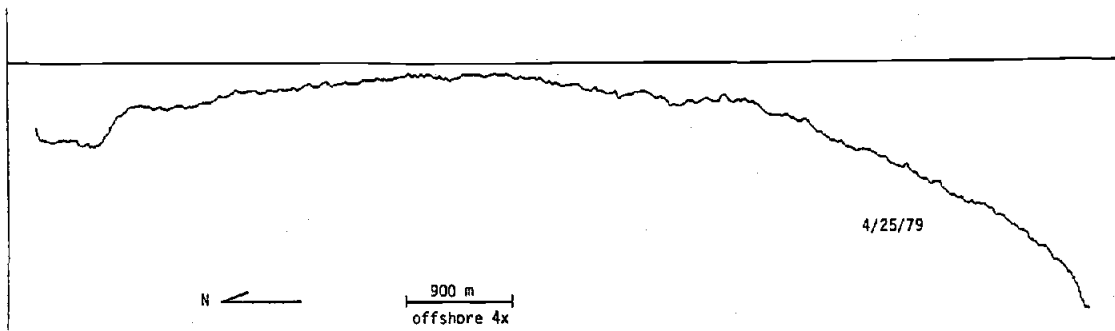
APPENDICES

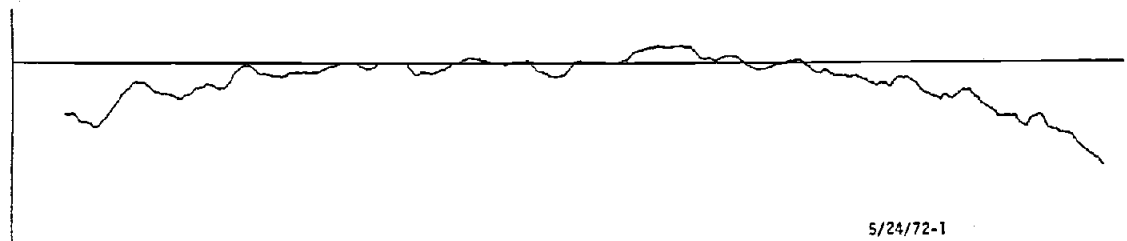
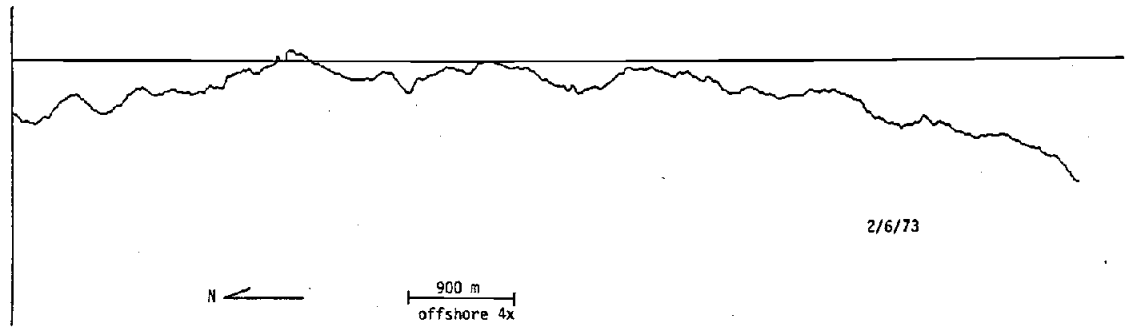
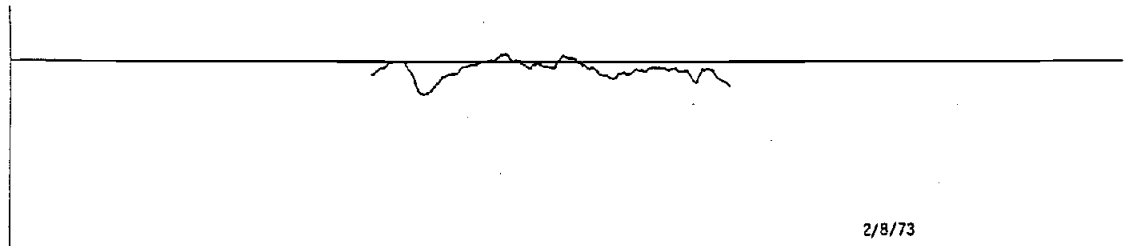
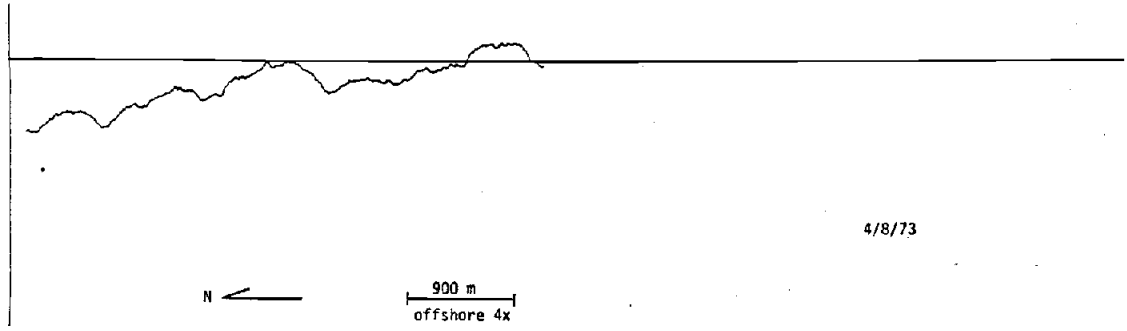
## APPENDIX 1

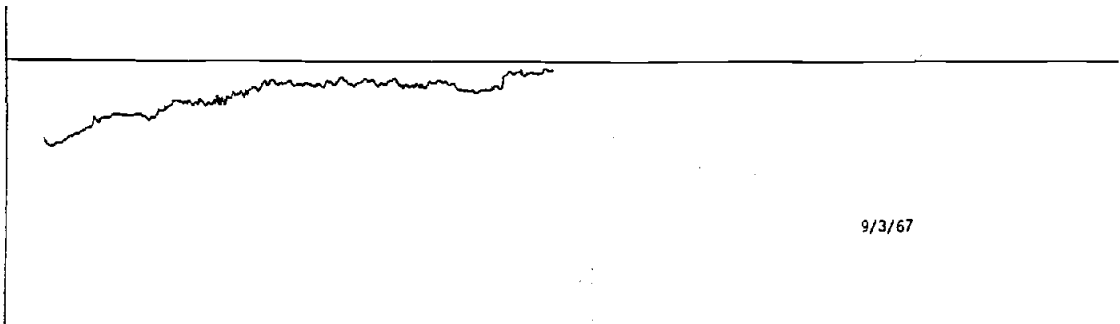
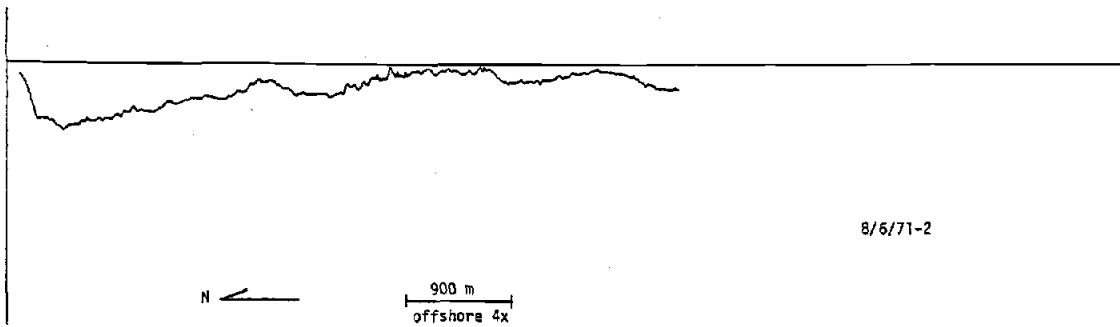
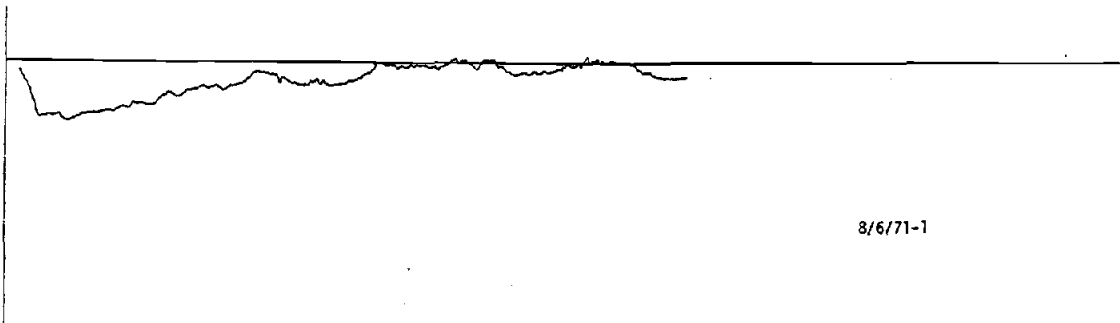
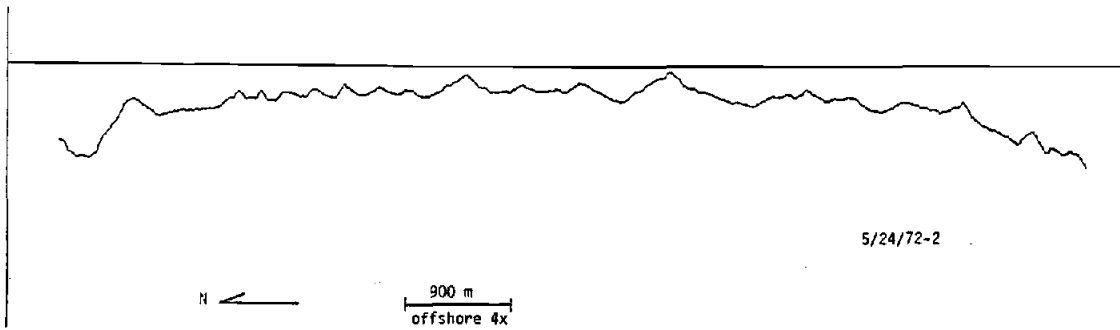
## High Water Lines From Air Photo Mosaics

The position of the axes remains in a fixed geographic position on all diagrams. The portion of the water line shown on a particular mosaic is plotted in its correct geographic location with respect to these axes.

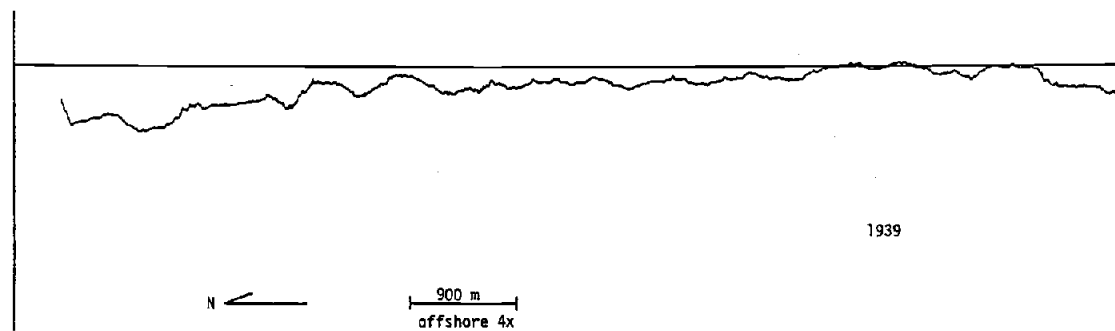
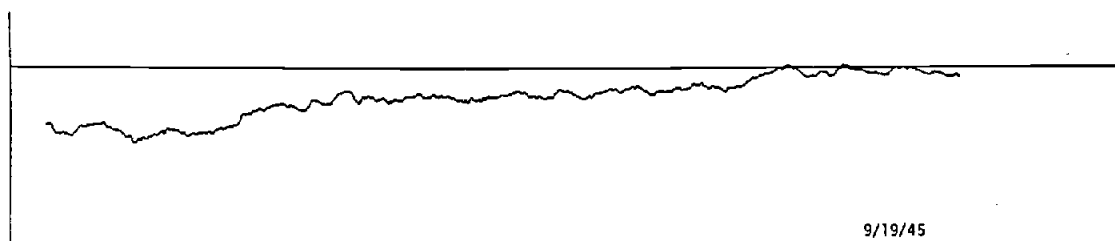
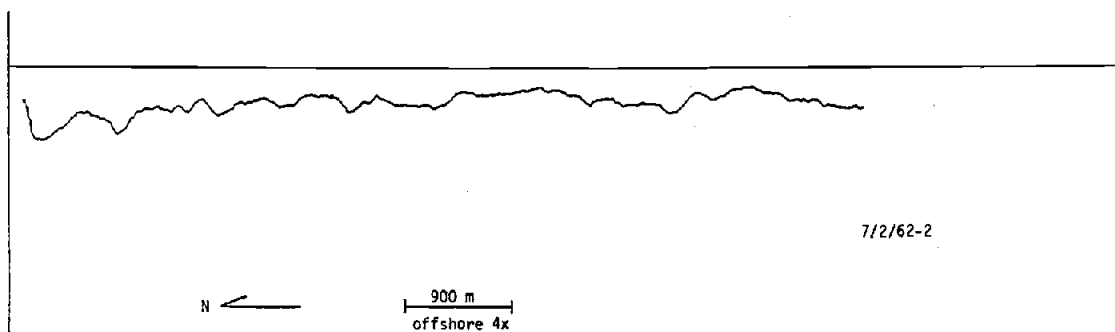










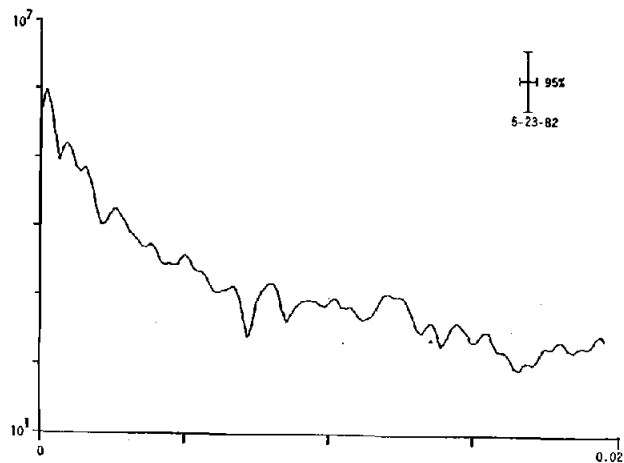
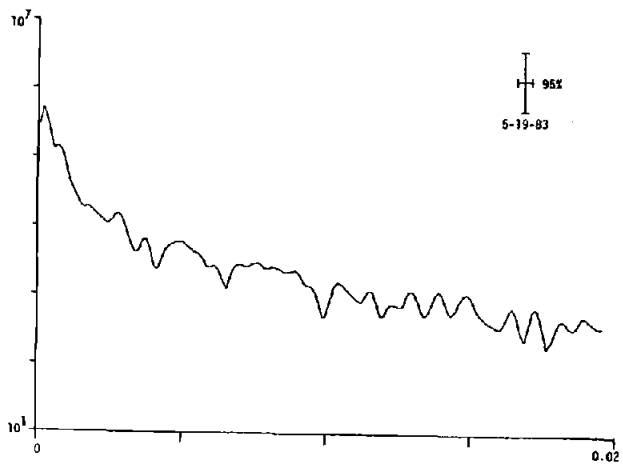
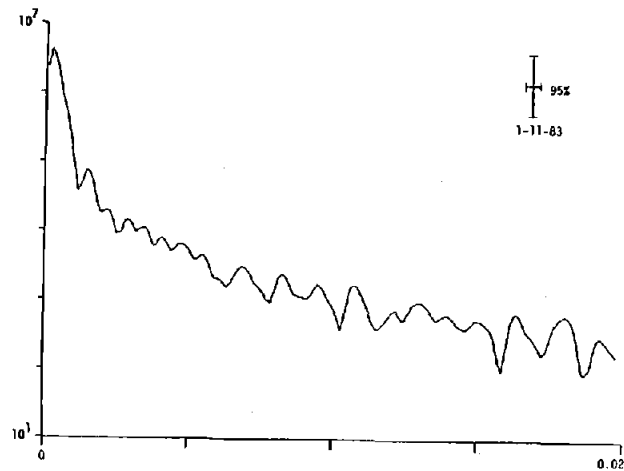
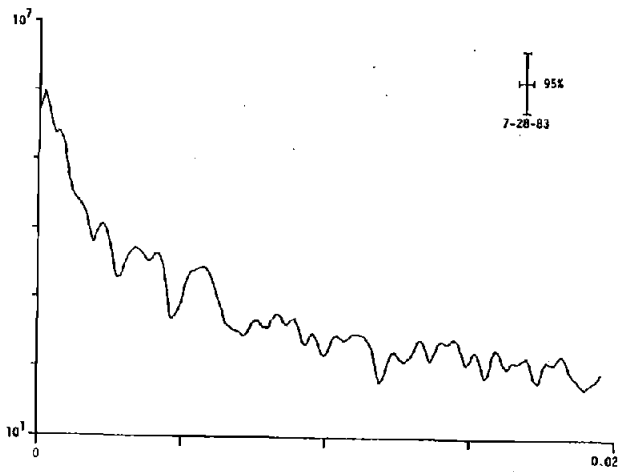


APPENDIX 2

Spectra Of High Water Lines

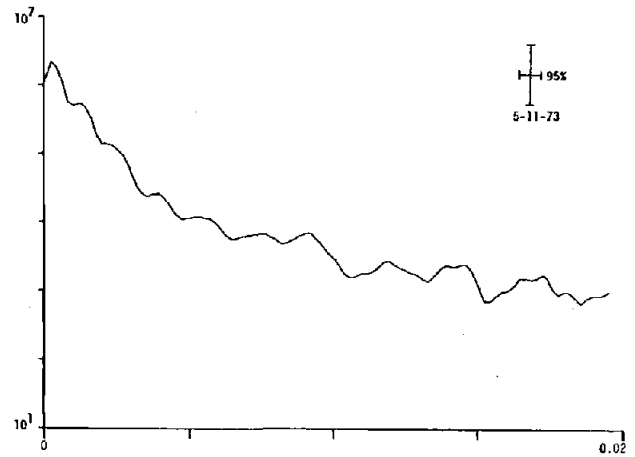
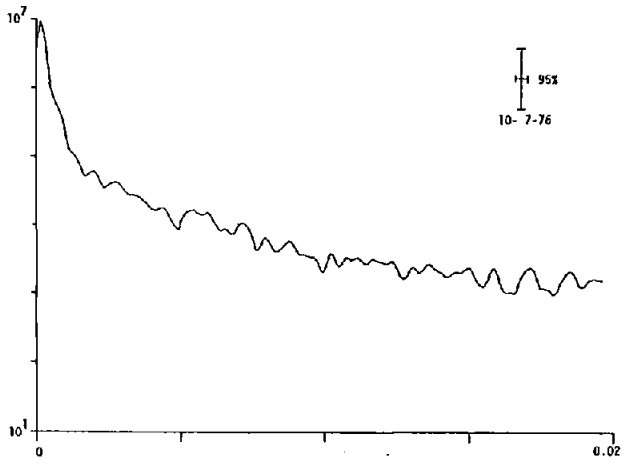
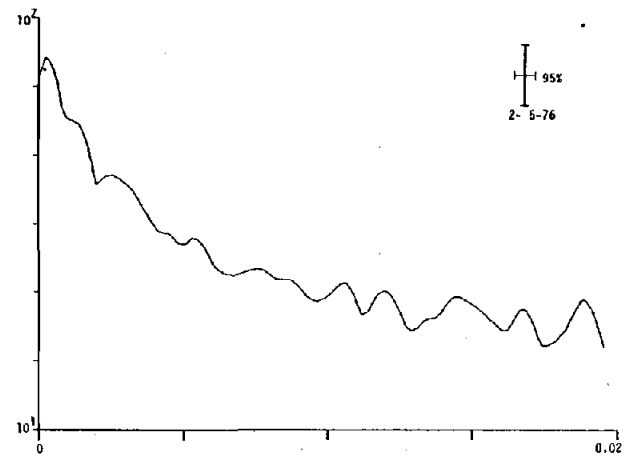
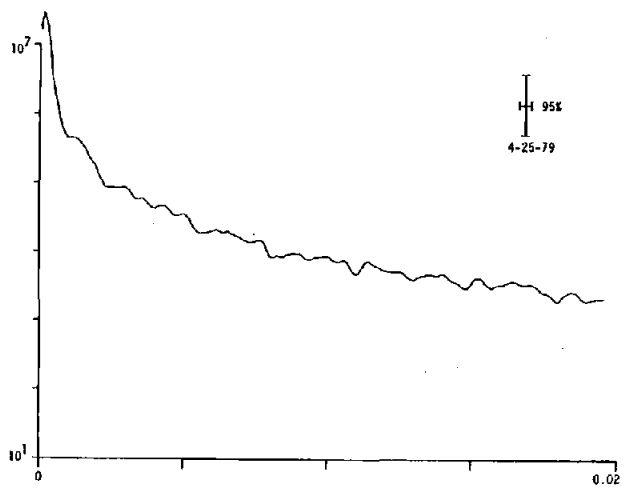
(discussed on p.32)

SPECTRAL DENSITY ( $m^2/m$ )



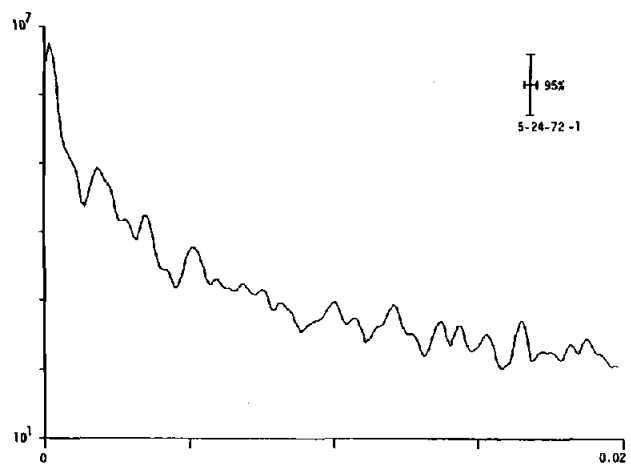
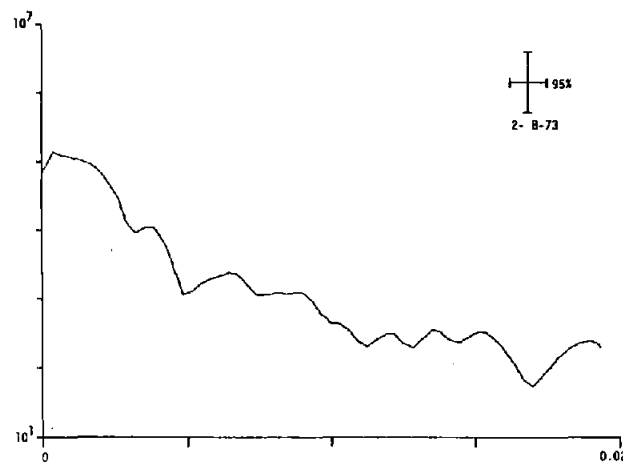
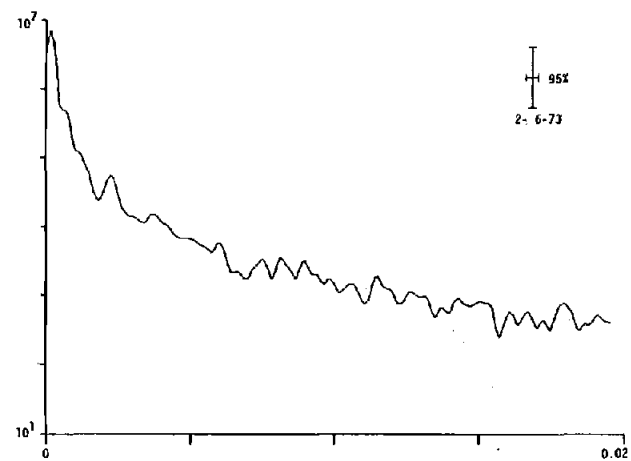
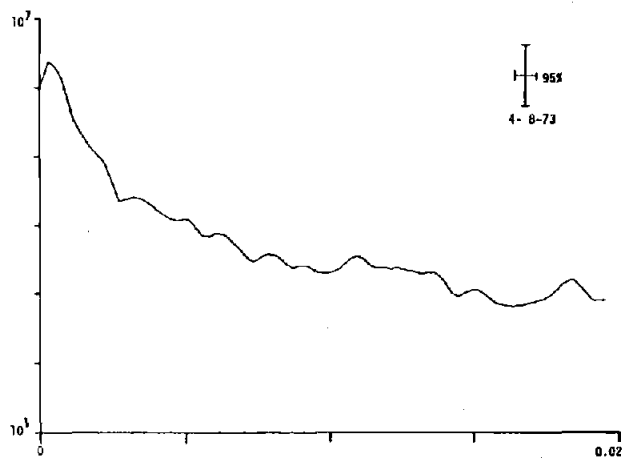
WAVENUMBER  $\kappa = 1/L$

SPECTRAL DENSITY ( $m^2m$ )

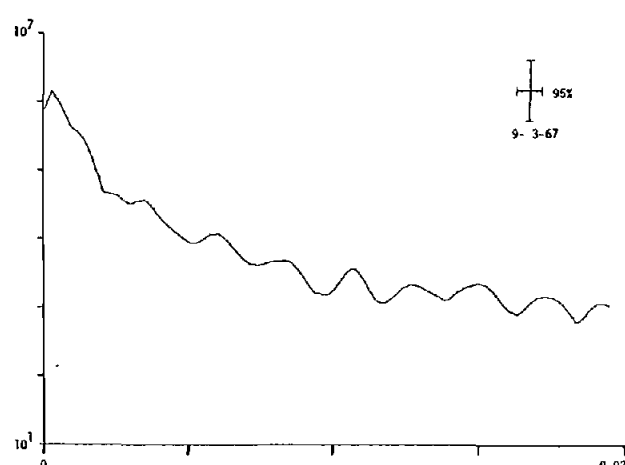
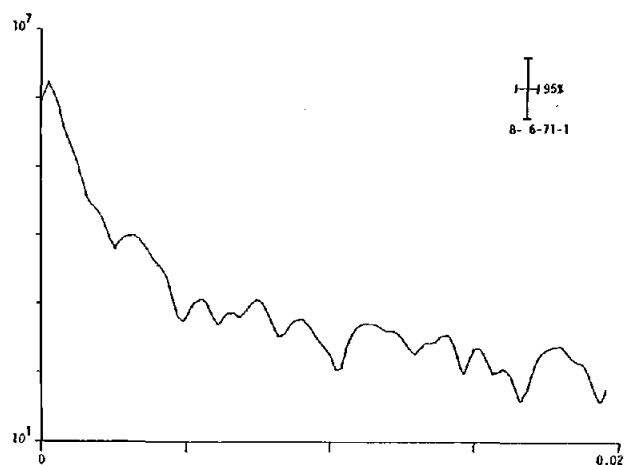
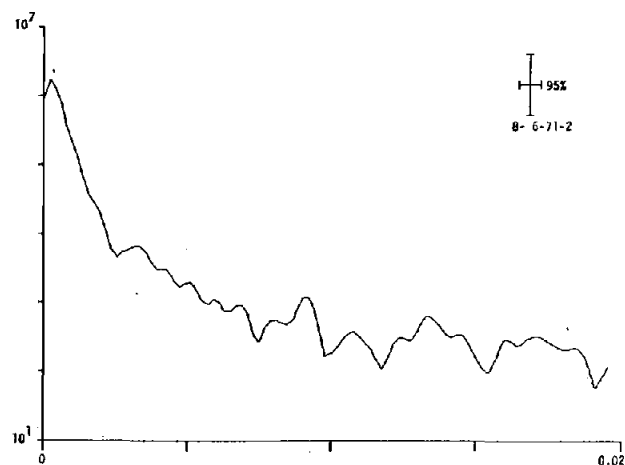
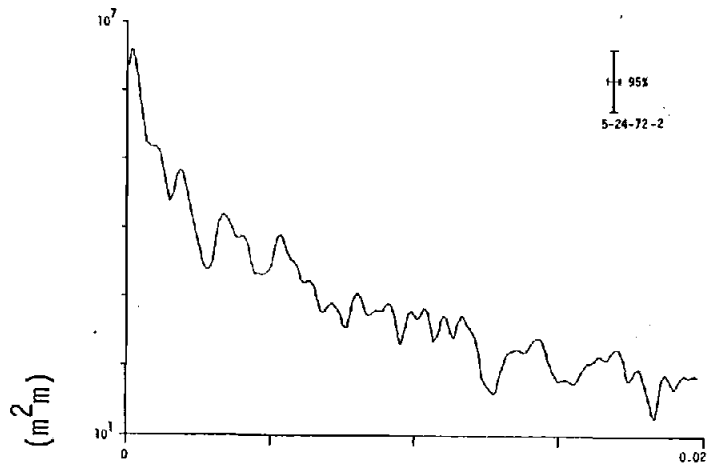


WAVENUMBER  $\kappa = 1/L$

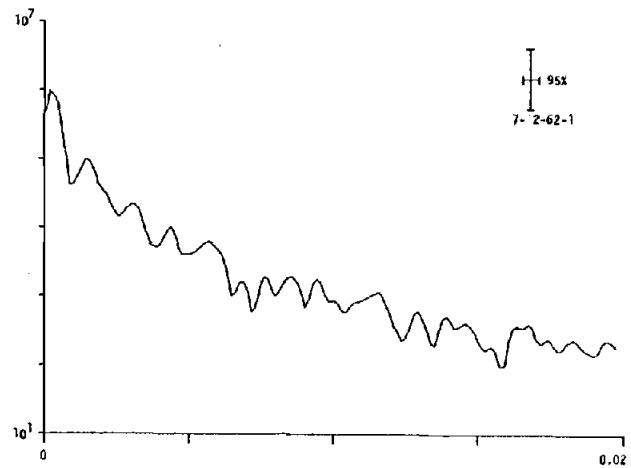
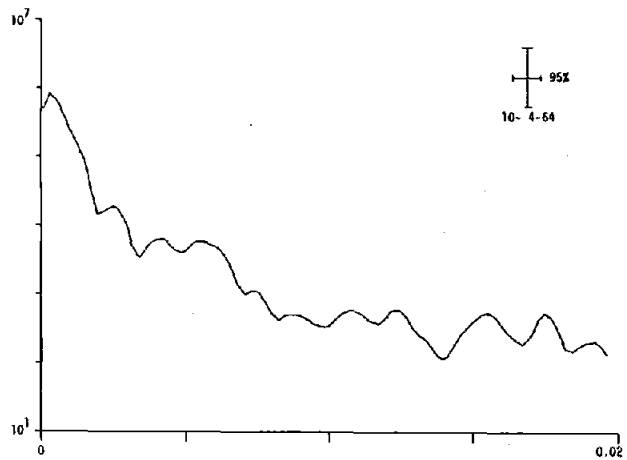
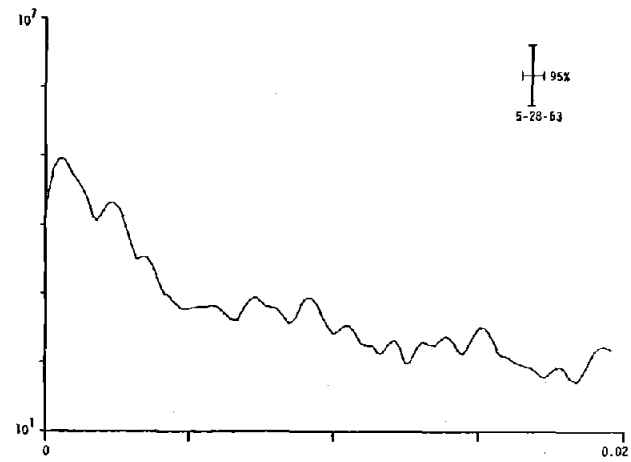
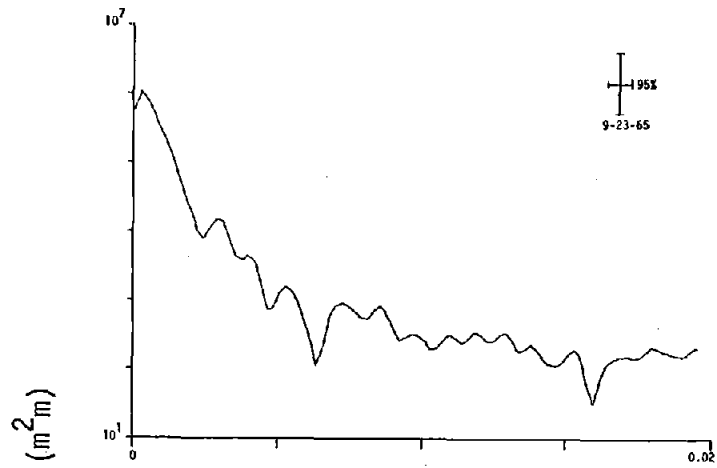
SPECTRAL DENSITY ( $m^2m$ )



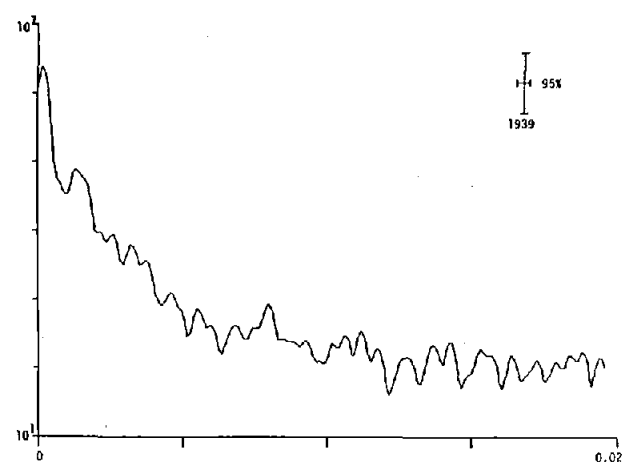
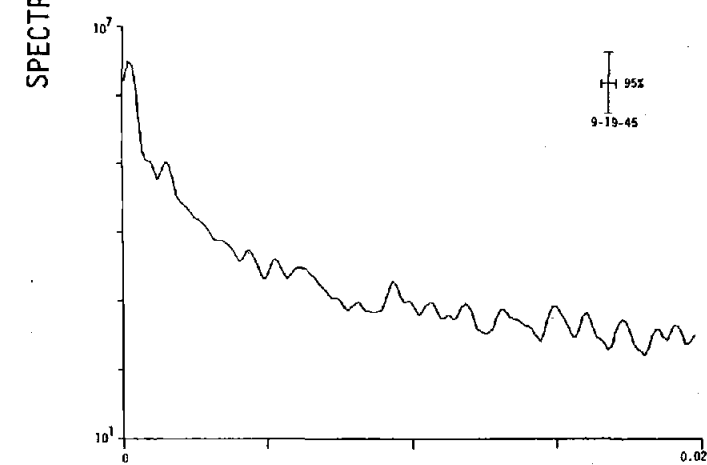
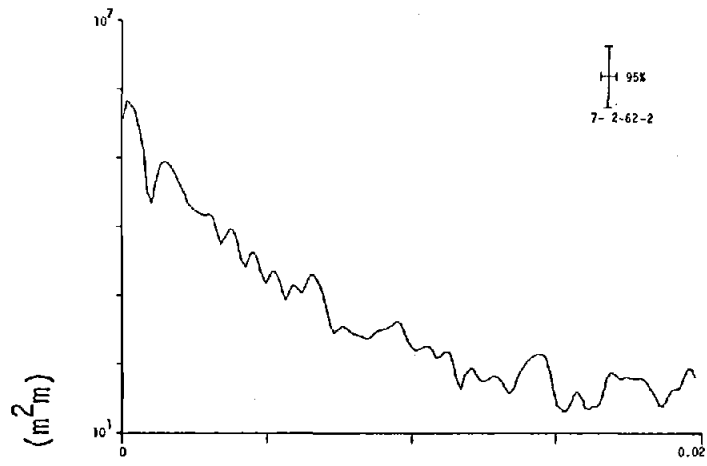
WAVENUMBER  $\kappa = 1/L$



WAVENUMBER  $\kappa = 1/L$



WAVENUMBER  $\kappa = 1/L$

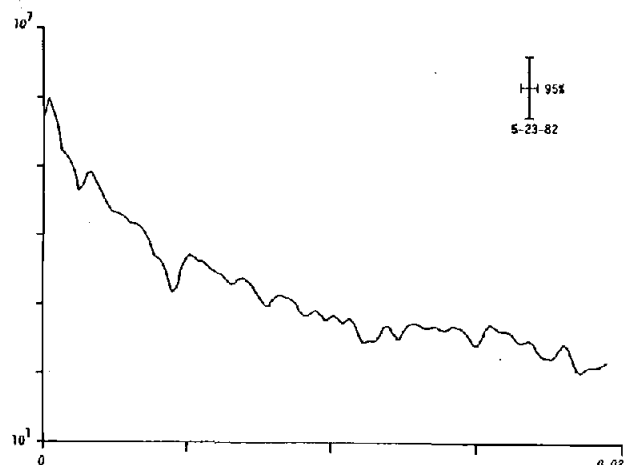
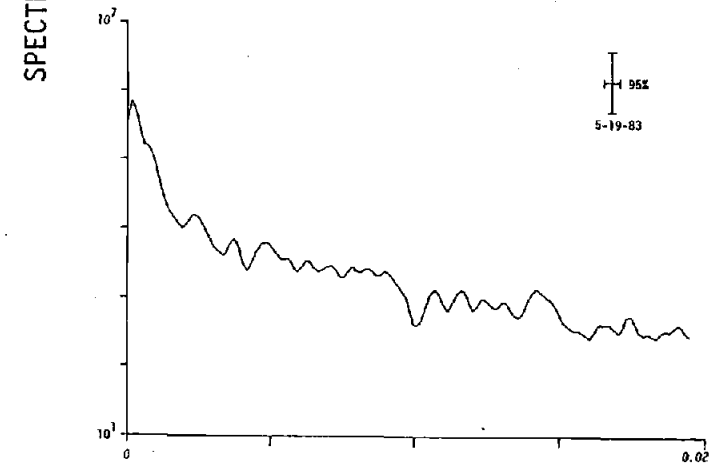
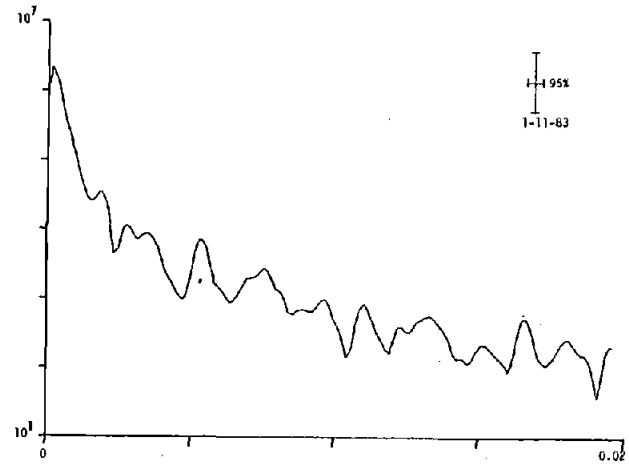
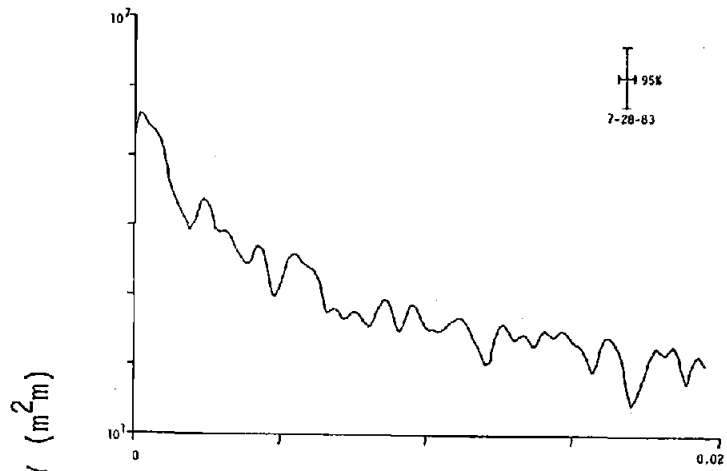


WAVENUMBER  $\kappa = 1/L$

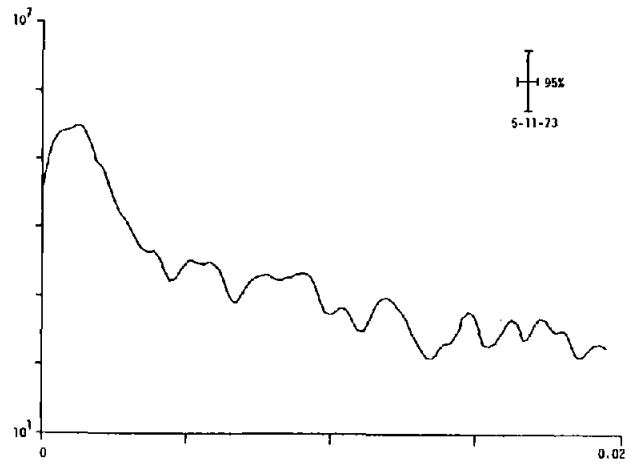
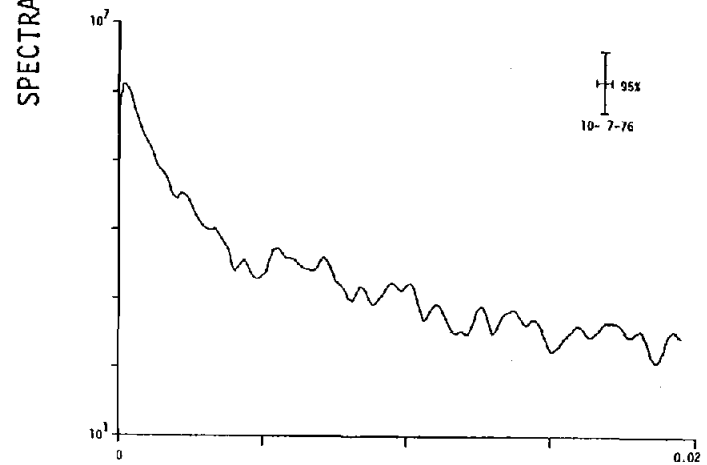
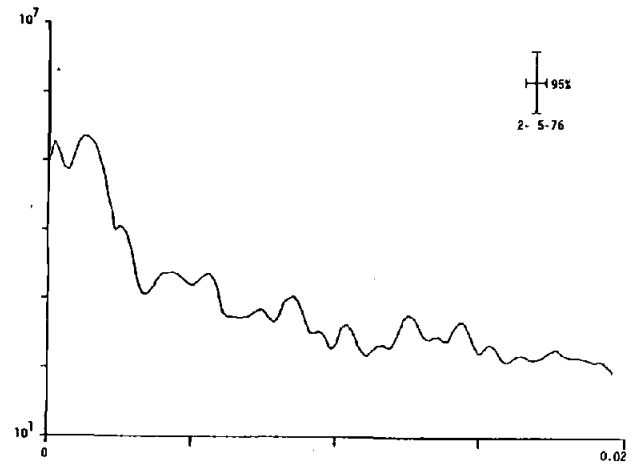
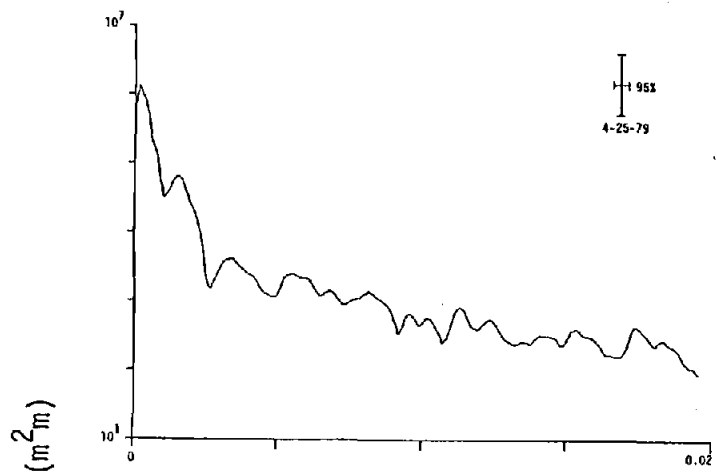
## APPENDIX 3

Spectra of 'Mean-subtracted' High Water Lines

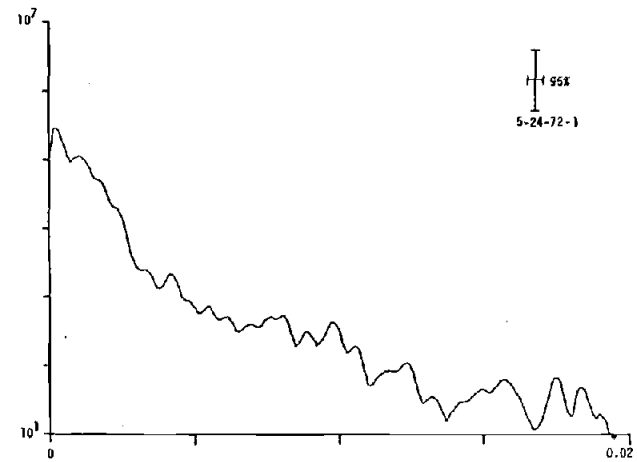
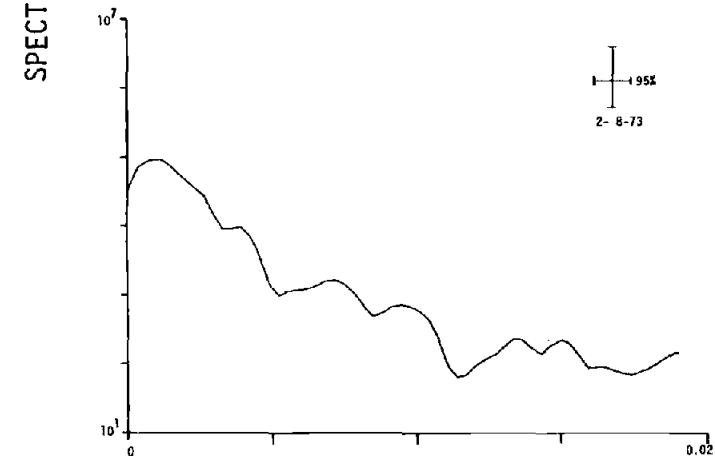
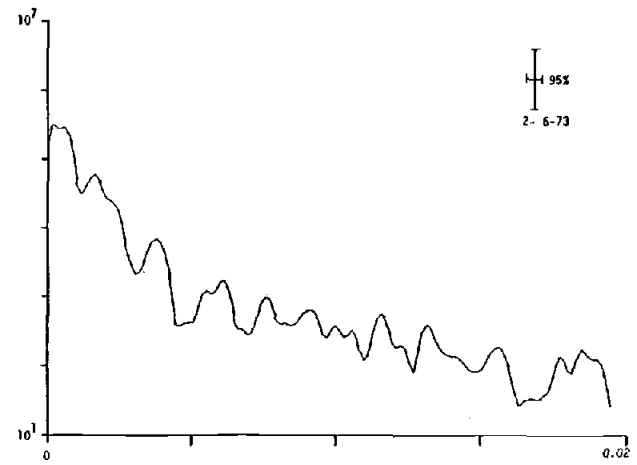
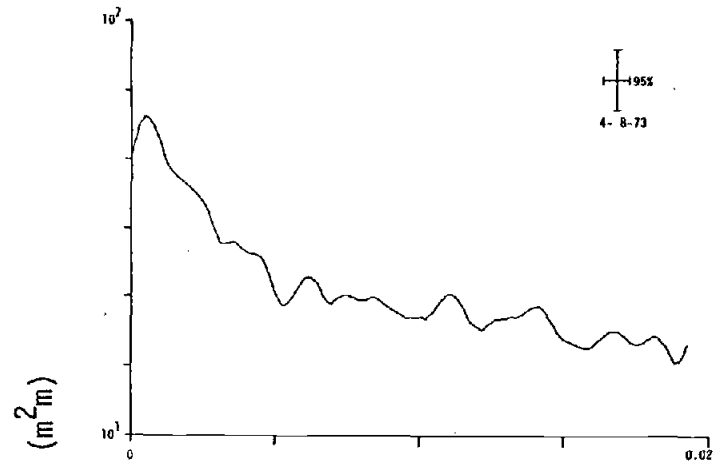
(discussed on p.36)



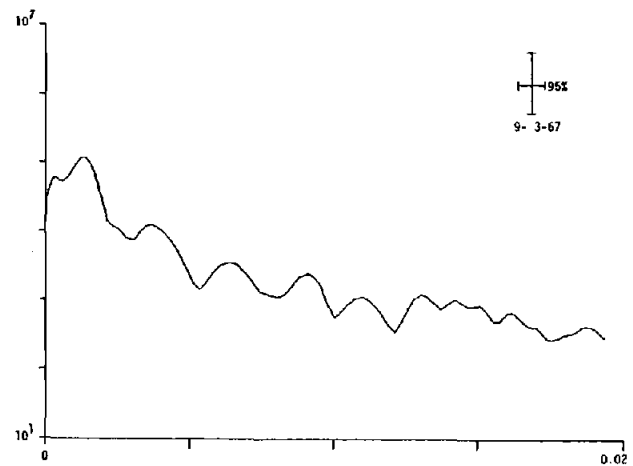
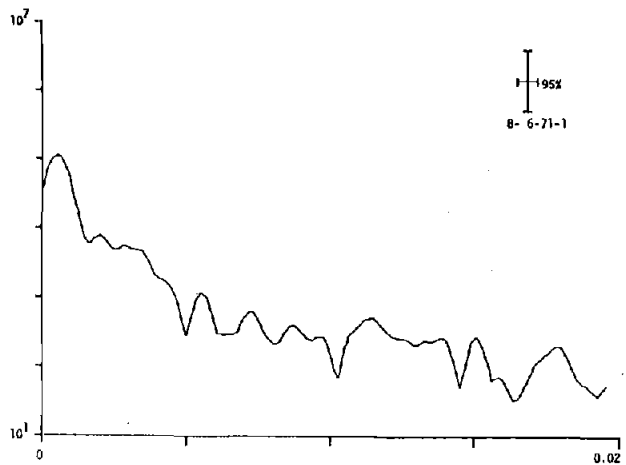
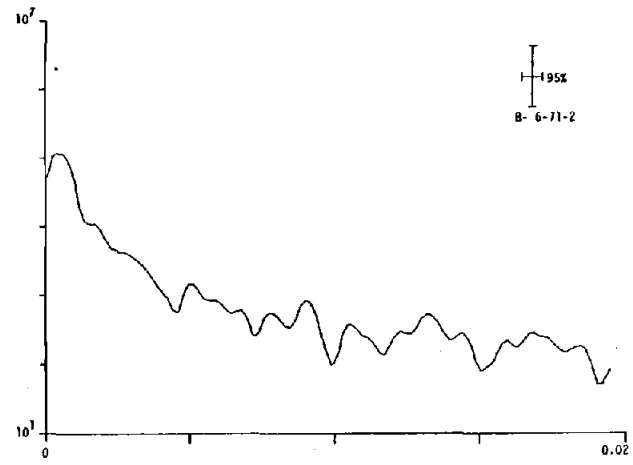
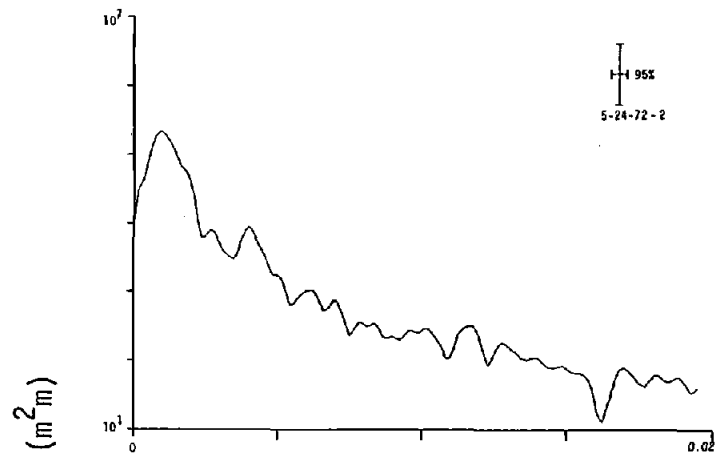
WAVENUMBER  $\kappa = 1/L$



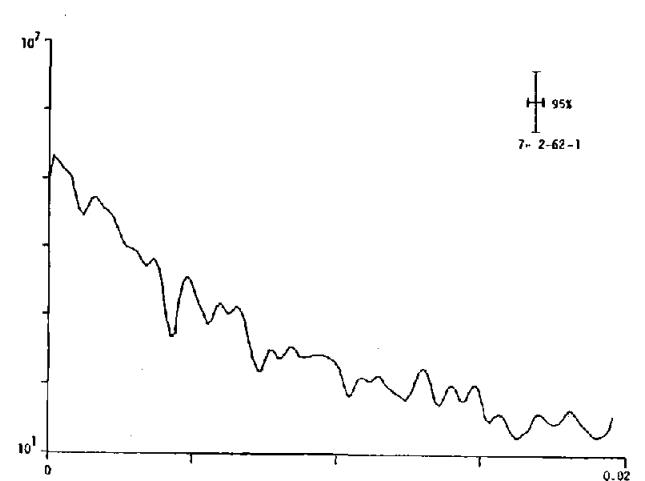
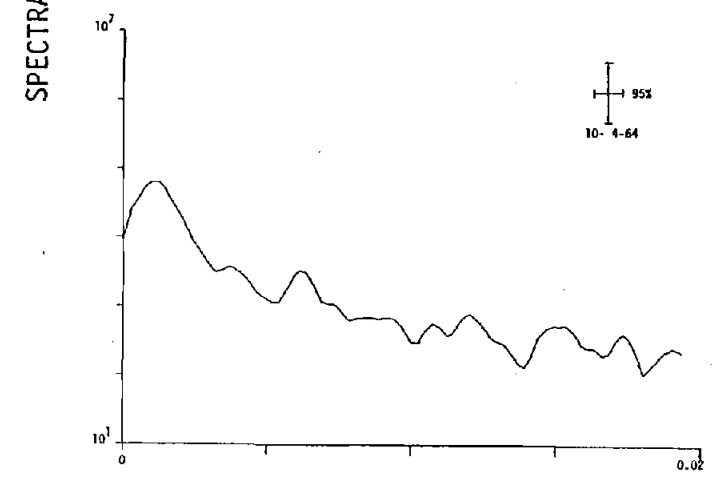
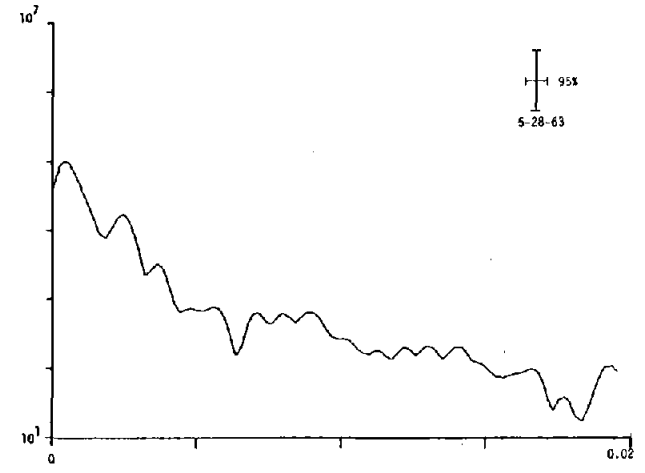
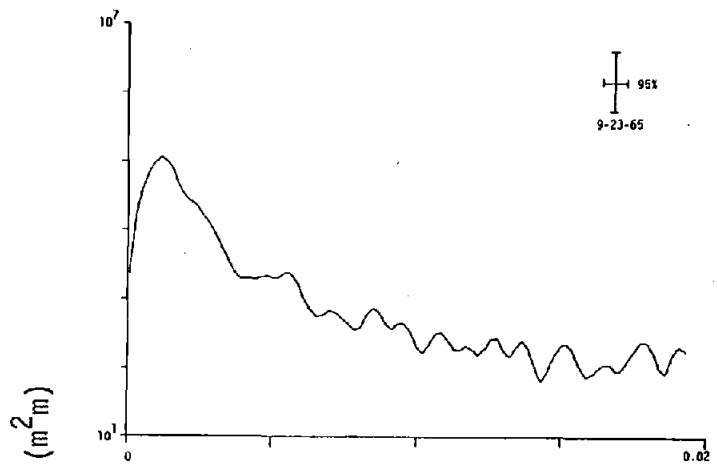
WAVENUMBER  $\kappa = 1/L$



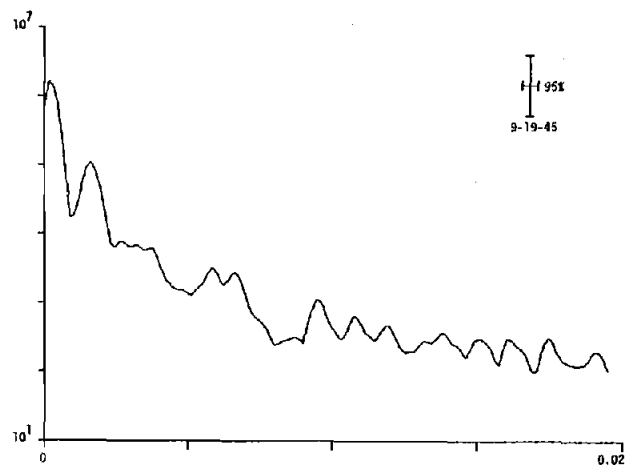
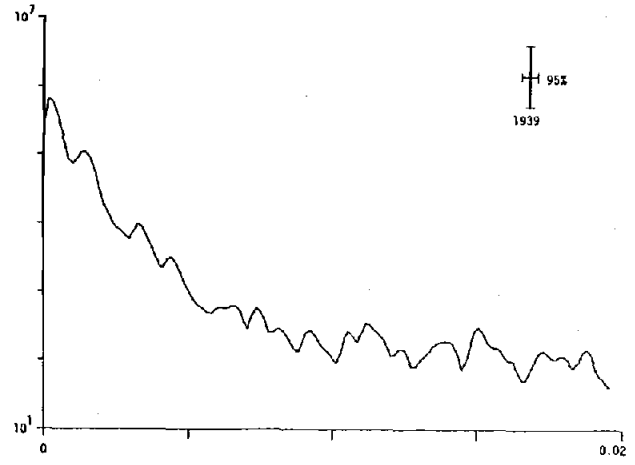
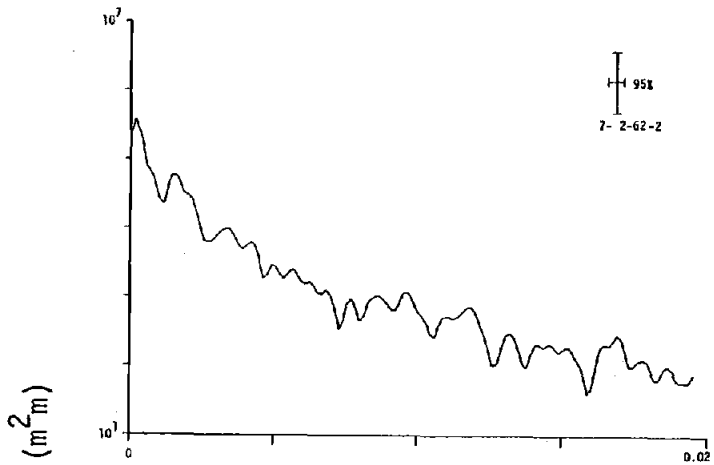
WAVENUMBER  $\kappa = 1/L$



WAVENUMBER  $\kappa = 1/L$



WAVENUMBER  $\kappa = 1/L$



WAVENUMBER  $\kappa = 1/L$

## APPENDIX 4

Topographic Maps Of The Study Site  
For Each Field Survey

(discussed on pp.60,65)

